

**Deciphering Catchment's Transit Time Distribution using Event
Isotopic Signatures**

**Dissertation
zur Erlangung des
Doktorgrades der Naturwissenschaften (Dr. rer. nat.)**

Der

Naturwissenschaftliche Fakultät III
Agrar- und Ernährungswissenschaften,
Geowissenschaften und Informatik

der Martin-Luther-Universität Halle-Wittenberg,

vorgelegt

von Frau Christina Franziska Radtke

Verteidigung der monografischen Dissertation
von Frau Christina Franziska Radtke
zum Thema

**Deciphering Catchment's Transit Time Distribution using Event
Isotopic Signatures**

Am 24. Juni 2024 um 17:00 Uhr
In Halle (Saale)

Die Prüfungskommission bestand aus:

- Apl. Prof. Dr. Wolfgang Goßel (Vorsitzender, Martin-Luther-Universität Halle)
- Prof. Dr. Ralf Merz (1. Gutachter, Helmholtz-Zentrum für Umweltforschung)
- Prof. Dr. Christine Stumpp (2. Gutachterin, BOKU Universität Wien)
- Prof. Dr. Christiane Stephan-Scherb (Martin-Luther-Universität Halle)
- Prof. Dr. Peter Bayer (Martin-Luther-Universität Halle)
- Prof. Dr. Boris Michel (Martin-Luther-Universität Halle)
- Prof. Dr. Christopher Conrad (Martin-Luther-Universität Halle)

Danksagung

Für die Betreuung meiner Arbeit und der Möglichkeit am Helmholtz-Zentrum für Umweltforschung zu promovieren möchte ich mich sowohl bei Prof. Dr. Kay Knöller als auch bei Prof. Dr. Ralf Merz bedanken. Ihre hilfreichen Ratschläge und zielführenden Feedbacks waren wertvolle Hilfestellungen zu meiner Arbeit. Ich bin besonders dankbar für die Erlebnisse, die ich als Doktorandin bei Konferenzen sammeln durfte, ebenso wie für die diversen neuen Erkenntnisse, die ich in der Zeit gelehrt bekommen habe. Für den vielfältigen wissenschaftlichen Input möchte ich mich außerdem bei Prof. Dr. Stefanie R. Lutz, Dr. Paolo Benettin, Dr. Jana von Freyberg, Dr. Tam Ngyuen, Prof. Dr. Xiaoqiang Yang, Dr. Larisa Tarasova und Dr. Christin Müller bedanken sowie allen weiteren Kollegen, mit denen ich zusammenarbeiten durfte. Für die Unterstützung im Labor möchte ich mich bedanken bei Dr. Stephan Weise, Stoyanka Schumann, Daniela Reichert, Lara Wegner, Hong Wei und Iman Sharifpour, sowie allen weiteren Kollegen mit denen ich im Labor zusammenarbeiten durfte. Es war mir stets eine Freude in diesem vielfältigen und freundlichen Team zu arbeiten.

Ein großer Dank geht außerdem an meinen Lebenspartner, meine Familie und an meine Freunde, die mir über die gesamte Zeit während der Promotion stets mit offenen Ohren zur Seite standen und mich sowohl in guten als auch schweren Zeiten unterstützt haben.

“In one drop of water are found all the secrets of all the oceans.”

Kahlil Gibran

Content

List of figures	III
List of tables	V
List of abbreviations	VI
Abstract	VIII
Zusammenfassung	X
1. Introduction	1
1.1. Water age in catchment studies	1
1.2. Data resolution	3
1.3. Approaches to derive water age metrics.....	4
1.4. The role of hydrological events on water age	6
1.5. Water age in relation to solutes	7
1.6. Nitrate: biogeochemical processes.....	10
1.7. Nitrate transport and nitrate age modelling	11
1.8. Aim of the study and research gap	11
2. Methods	14
2.1. Study Area	14
2.2. Sampling	20
2.3. Laboratory Analysis	21
2.4. Data preparation	22
2.5. Transit time modelling.....	24
2.5.1. Water age model.....	24
2.5.2. Nitrate age model	26
2.6. Model evaluation.....	31
2.6.1. Goodness of fit evaluation.....	31
2.6.2. Influence of sampling frequency.....	34

2.7.	Statistical analysis of model results	35
2.7.1.	Discharge sensitivity analysis of young water	35
2.7.2.	Event separation based on discharge	36
2.7.3.	Rayleigh plot analysis for denitrification indicators	37
3.	Results and discussion	38
3.1.	Monitored water samples	38
3.2.	Sampling frequency affects the model simulation	40
3.3.	Water age modelling	44
3.4.	Sensitivity of young water fractions to discharge.....	46
3.5.	The effect of hydrologically varying periods on discharge age distributions	50
3.6.	Catchment characteristics influence the discharge age distribution.....	54
3.7.	Evaluation of observed data in the Meisdorfer Sauerbach catchment.....	61
3.8.	Simulation results of the modified tran-SAS.....	69
3.8.1.	Water isotopic signatures and water age distributions in discharge.....	69
3.8.2.	Nitrate isotopic signatures and TTDs gained from the nitrate isotope model....	70
3.8.3.	Potential impact of conceptual simplifications on the nitrate isotope model performance	77
4.	Conclusion	79
	References.....	83
	List of publications related to this thesis	91
	Curriculum vitae	92
	Eidesstattliche Erklärung / Declaration under Oath.....	95

List of figures

- Figure 1: Study area with the sub-catchments, located in the Harz mountains, Central Germany.15
- Figure 2: The Meisdorfer Sauerbach catchment with an area about 11.5 km² is located at the north-eastern border of the Harz mountains of Germany (top left map of Germany). The red dot is the location of the autosampler for stream chemistry as well as the discharge measurement station. The orange triangles are locations of soil samples and the white circles with the black dot are locations of ground water wells. Land-use data in panel A is provided by GeoBasis-DE / BKG (2018), and elevation data in panel B in 200m resolution is taken from GeoBasis-DE / BKG (2013).17
- Figure 3: Illustration of all six catchments investigated, considering their most meaningful catchment characteristics...19
- Figure 4: Conceptual nitrate isotope model with two storages and the processes (equations) that influence the isotopic signature of $\delta^{18}\text{O}-\text{NO}_3$27
- Figure 5: Collection of isotopic signatures of water for both, precipitation and discharge, in catchments 1-5. 39
- Figure 6: Model results (lines) and observed data (points and triangles) of different sampling frequencies and sampling techniques (composite samples = dots versus grab samples = triangles) in comparison for catchments 1 to 5.43
- Figure 7: Discharge with the different fractions of water age in light blue (water age up to 7 days), medium blue (water age up to 180 days) and dark blue (water age more than 180 days) for the five investigated catchments; the measured isotopic signature of discharge is shown as grey dots, while the simulated isotopic signature of discharge gained from the tran-SAS model is shown as black line; the range of simulated stream isotopic signature from the 10% best simulations is shown as red shading.45
- Figure 8: Relationship between discharge and the fraction of water with an age up to 60 days (Fyw60) with the median discharge (Q [mm/d]) from each percentile and the mean Fyw60 as well as its standard deviation from each Q-percentile for the whole time series; Fyw60 of discharge percentiles (P10-P100) are represented as coloured points with standard deviation, while the black line represents Equ. 14 to describe the discharge sensitivity (S_d) of the Fyw60; the coefficient of determination (R^2) describes the fit of Equ. 14 to the coloured dots.47

Figure 9: Relationship between discharge and the fraction of water with an age up to 7 days (Fyw7) with the median discharge (Q [mm/d]) from each percentile and the mean Fyw7 as well as its standard deviation from each Q-percentile from the whole time series; Fyw7 of discharge percentiles (P10-P100) are represented as coloured points with standard deviation, while the black line represents Equ. 9 to describe the discharge sensitivity (S_d) of the Fyw7; the coefficient of determination (R^2) describes the fit of Equ. 14 on the coloured dots.	49
Figure 10: The age metrics (TT50 and Fyw7-180) for each catchment during dry spells (red), the whole time series (green) and wet spells (blue).	51
Figure 11: Focusing on the Fyw7 (Fractions of young water up to 7 days), boxplots are plotted for dry spells (red), time series (green) and wet spells (blue) during the seasons (Spring, Summer, Autumn and Winter).	52
Figure 12: Focusing on the Fyw60 (Fractions of young water up to 60 days), boxplots are plotted for dry spells (red), time series (green) and wet spells (blue) during the seasons (Spring, Summer, Autumn and Winter).	53
Figure 13: Fyw7 for different catchment characteristics (land use share [%]: agriculture, forest, grassland and urban area) with boxplots representing dry spells (dots), the entire time series (blank) and wet spells (stripes).	55
Figure 14: Fyw7 for different catchment characteristics (maximum slope, flow path length, catchment area, baseflow index, mean elevation, gradient) with boxplots representing dry spells (dots), the entire time series (blank) and wet spells (stripes).	56
Figure 15: Fyw60 for different catchment characteristics (land use share [%]: agriculture, forest, grassland and urban area) with boxplots representing dry spells (dots), the entire time series (blank) and wet spells (stripes).	58
Figure 16: Fyw60 for different catchment characteristics (maximum slope, flow path length, catchment area, baseflow index, mean elevation, gradient) with boxplots representing dry spells (dots), the entire time series (blank) and wet spells (stripes).	59
Figure 17: Isotopic signatures of nitrate (A, B) as well as the concentration of $\text{NO}_3\text{-N}$ in stream water (C) and the discharge (Q) [mm/d] (D) for the observation period.	62
Figure 18: Isotopic signatures of nitrate in stream water in the Meisdorfer Sauerbach catchment, indicating different possible nitrate sources.	63
Figure 19: Monthly distribution of the isotopic signature (panel A) $\delta^{18}\text{O-NO}_3$, (panel B) $\delta^{15}\text{N-NO}_3$ and (panel C) nitrate-N concentration during the years 2017-2020.	65
Figure 20: Comparison of the measured range of $\delta^{18}\text{O-NO}_3$ in stream water with calculated ranges of $\delta^{18}\text{O-NO}_3$ based on the $\delta^{18}\text{O-H}_2\text{O}$ ranges observed in different compartments using Equ. 9.	67

Figure 21: a. Relationship between nitrate concentrations (normalized to the highest measured concentration) and b. dual isotope plot showing the correlation between measured nitrogen and oxygen isotope signatures.68

Figure 22: Precipitation [mm] (blue) and isotopic signature of $\delta^{18}\text{O}\text{-H}_2\text{O}$ in precipitation (grey: dots = measured, line = sinusoidal fitting line to precipitation isotopic signature) on top and discharge [mm] boxplots on the right side of the graph show the distribution of isotopic signature in precipitation (top) and streamflow (bottom).70

Figure 23: Panel A with the simulated nitrate concentrations [mg/l] of the mHM model of discharge in dark green and as leaching flux in light green. The black line in panel A shows the nitrate concentrations obtained from the nitrate isotope model. Panel B shows the isotopic signature of $\delta^{18}\text{O}\text{-NO}_3$ in stream: green dots= measured with measuring error 0.8 ‰, black line= simulated, orange area= 10% best simulation according to a small bias.73

Figure 24: Top panel: Median Transit Times (TT50) of water (black, solid line) and nitrate (green, dashed line) through the lower storage, and discharge bottom panel: monthly boxplots of difference between TT50 of water and of nitrate.74

Figure 25: Relation between the measured nitrate concentration in stream water and the simulated median transit time of nitrate.76

List of tables

Table 1: Catchment characteristics with TWI as topographic wetness index and BFI as baseflow index considering time series between 2010 and 2021.18

Table 2: Water isotope model parameter ranges of the 10% best simulations according to the KGE of the water isotopic signatures in stream.32

Table 3: Nitrate isotope model parameter ranges of the 10% best simulations according to the KGE of the water isotopic signatures in stream (amount simulations = 212).33

Table 4: KGE values of the different sampling frequencies and sampling techniques with minimum, maximum and the mean in brackets. 41

Table 5: Deviation between the simulated isotopic signature in a daily sampling frequency versus the respective sampling frequencies (weekly, fortnightly, monthly), values given as percent bias (%).42

Table 6: Values for F_0 and S_d and their standard deviation obtained from Gauss-Newton fitting algorithm using Equ. 14 for $F_{yw7}(Q)$ (water with an age up to 7 days) and $F_{yw60}(Q)$ (water with an age up to 60 days).46

Table 7: The number of wet spells in total and the mean duration [days] of wet spells during the years for the investigated catchments.50

List of abbreviations

%	percent
&	and
~	approximately
<	smaller than
>	higher than
±	plus, minus
°	Degree
°C	Degree Celsius
µm	micrometre
‰	permille
20x	20 times
avg.	average
BFI	Baseflow index
BKG	Bundesamt für Kartographie und Geodäsie
BUEK1000	Soil map
DWD	Deutscher Wetterdienst
e.g.	for example
Equ.	Equation
Fyw	Young water fraction after Kirchner (2016a, 2016b)
Fyw14	Fraction of water with an age up to 14 days
Fyw180	Fraction of water with an age up to 180 days
Fyw28	Fraction of water with an age up to 28 days
Fyw60	Fraction of water with an age up to 60 days
Fyw60(Q)	Fraction of discharge water with an age up to 60 days
Fyw7	Fraction of water with an age up to 7 days
Fyw7(Q)	Fraction of discharge water with an age up to 7 days
GLUE	Generalized likelihood uncertainty estimation
H	Deuterium
ha	hectare
HYPE	Hydrological Predictions for the Environment model
i.e.	the abbreviation for id est and means “in other words”
kf-value	coefficient of hydraulic conductivity
KGE	Kling-Gupta-Efficiency
km	kilometre
km ²	Square kilometre
m	meter
m a.s.l.	meter above sea level
mg/l	milligram per litre
mHM	Mesoscale hydrological Model
mHM-nitrate	Mesoscale hydrological Model - Nitrate
mm	millimetre

mm/d	millimetre per day
MTT	Mean transit time
N	Nitrogen
n and No.	number
NO ₃	Nitrate
NO ₃ -N	Nitrate-Nitrogen
NO _x	shorthand for nitric oxide (NO _x) and <i>nitrogen</i> dioxide (NO ₂)
O	Oxygen
P	Precipitation
p	the p-value] is the probability of obtaining test results at least as extreme as the result actually observed, under the assumption that the null hypothesis is correct
P10	10% percentile
P100	100% percentile
PET	Potential Evapotranspiration
Q	discharge
R ²	Coefficient of determination
SAS (function)	Storage Selection (function)
S _d	Discharge sensitivity
SLAP	Standard Light Antarctic Precipitation
TERENO	TER restrial EN vironmental O bservatoria
TT50	Median transit time
TTD	Transit time distributions
TWI	Topographic wetness index
vs.	versus
VSMOW	Vienna Standard Mean Ocean Water

Abstract

With more frequent high flows and droughts, it becomes inevitable to understand potentially altered catchment processes under changing climatic conditions. Water age metrics such as median transit times and young water fractions are useful variables to understand the process dynamics of catchments and the release of solutes to the streams. This study, based on extensive high-frequency stable isotope data covering daily and sub-daily isotope measurements, unravels the changing contribution of different water ages to stream water in five heterogeneous catchments, located in the Harz mountains and the adjacent northern lowlands in Central Germany. Moreover, to understand the transport and fate of nitrate in catchments and its potentially hazardous impact to ecosystems, knowledge about transit times and age of nitrate is needed. In order to add to that knowledge, an analysis of a 5-year low-frequency data set followed by a 3-year high-frequency data set of water and nitrate isotopic signatures was conducted in an 11.5 km² headwater catchment with mixed land-use within the Northern lowlands of the Harz mountains in Germany.

Fractions of water up to 7 days old (Fyw7), comparable with water from recent precipitation events, and fractions of water up to 60 days old (Fyw60) were simulated by the tran-SAS model. As Fyw7 and Fyw60 were sensitive to discharge, an integrated analysis of high and low flows was conducted. This revealed an increasing contribution of young water for increasing discharge, with larger contributions of young water during wet spells compared to dry spells. Considering seasonal variations, young water fractions increased in summer and autumn, which indicates higher contributions of young water during prolonged dry conditions. Moreover, the relationship between catchment characteristics and the water age metrics revealed an increasing amount of young water with increasing agricultural area, while the amount of young water decreased with increasing grassland proportion. This is most important for the application of nutrients and pesticides on agricultural fields. For the first time, a combination of water and nitrate isotope data was used to investigate nitrate age and transport and their relation to water transit times. To do so, the numerical model tran-SAS based on Storage Selection (SAS) functions was extended using biogeochemical equations describing nitrate turnover processes to model nitrification and denitrification dynamics along with the age composition of discharge fluxes. The analysis revealed a temporally varying offset between nitrate and water median transit times, with a larger

offset at the beginning of wet periods due to higher proportions of young nitrate that is released more quickly with increasing discharge, compared to water that consists of a mixture of young and old water. The findings of the varying offset between water and nitrate transit times underline the importance of high-frequency analyses of solute transport and transformation in the light of projected more frequent hydrological extremes (droughts and floods) under future climate conditions. Moreover, by combining transit time modelling with high-frequency isotopic signatures in contrasting sub-catchments in Central Germany, this study extends the understanding of hydrological processes under high and low flow conditions.

Zusammenfassung

Mit der zunehmenden Wahrscheinlichkeit von Hochwasserereignissen und Dürren, ist es unumgänglich, potenziell veränderte Einzugsgebietsprozesse unter veränderten klimatischen Bedingungen zu verstehen. Variablen zur Beschreibung des Wasseralters wie bspw. mittlere Verweilzeiten und Anteile jungen Wassers sind nützlich, um die Prozessdynamik von Einzugsgebieten und die Freisetzung gelöster Stoffe in die angrenzenden Wasserkörper zu verstehen. Diese Studie basiert auf hochfrequent aufgelösten Daten von stabilen Isotopen des Wassers in täglicher und sub-täglicher Auflösung, um die Quellen des Wassers anhand der Altersstrukturen im Fließgewässer zu entschlüsseln. Die Probennahme wurde in fünf heterogenen Einzugsgebieten im Harz und im angrenzenden nördlichen Tiefland in Mitteldeutschland durchgeführt. Um den Transport und den Verbleib von Nitrat in Einzugsgebieten sowie die möglichen gefährlichen Auswirkungen auf Ökosysteme zu verstehen, sind außerdem Kenntnisse über die Verweilzeiten und das Alter von Nitrat erforderlich. Um dieses Wissen zu erweitern, wurde ein Datensatz generiert, der in geringer Auflösung für die ersten 5 Jahre vorliegt, gefolgt von hochfrequenten Daten über 3 Jahre von Wasser- und Nitratisotopensignaturen aus einem 11,5 km² großen Quellwassereinzugsgebiet mit gemischter Landnutzung im nördlichen Tiefland des Harzes in Deutschland.

Mit dem tran-SAS-Modell wurden bis zu 7 Tage alte Wasseranteile (Fyw7), vergleichbar mit Wasser aus jüngsten Niederschlagsereignissen, und bis zu 60 Tage alte Wasseranteile (Fyw60) simuliert. Da Fyw7 und Fyw60 empfindlich auf den Abfluss im Fließgewässer reagierten, wurde eine integrierte Analyse von hohen und niedrigen Abflüssen durchgeführt. Dies zeigte einen zunehmenden Anteil von jungem Wasser bei höherem Abfluss, wobei der Anteil von jungem Wasser in nassen Perioden im Vergleich zu trockenen Perioden größer war. Unter Berücksichtigung saisonaler Schwankungen stiegen die Anteile des jungen Wassers im Sommer und Herbst an, was auf einen höheren Anteil von jungem Wasser bei längerer Trockenheit hindeutet. Darüber hinaus ergab die Beziehung zwischen Einzugsgebietseigenschaften und den Anteilen von jungem Wasser, dass die Menge an jungem Wasser mit zunehmender landwirtschaftlicher Fläche zunimmt, während die Menge an jungem Wasser mit zunehmendem Grünlandanteil abnimmt. Dies hat eine besondere Wichtigkeit für die Ausbringung von Nährstoffen und Pestiziden auf landwirtschaftlichen Flächen. Zum

ersten Mal wurde eine Kombination aus Wasser- und Nitratisotopendaten verwendet, um das Alter und den Transport von Nitrat sowie deren Zusammenhang mit den Verweilzeiten des Wassers zu untersuchen. Zu diesem Zweck wurde das auf Storage Selection (SAS)-Funktionen basierende numerische Modell tran-SAS um biogeochemische Gleichungen erweitert, die Nitratumsatzprozesse beschreiben, um die Nitrifikations- und Denitrifikationsdynamik sowie die Alterszusammensetzung der Abflüsse zu modellieren. Die Analyse ergab einen zeitlichen Versatz zwischen den mittleren Verweilzeiten von Nitrat und Wasser, mit einem größeren Versatz zu Beginn von nassen Perioden aufgrund höherer Anteile an jungem Nitrat, das mit zunehmendem Abfluss schneller freigesetzt wird, im Vergleich zu Wasser, das aus einer Mischung von jungem und altem Wasser besteht. Die Ergebnisse des zeitlichen Versatzes zwischen Wasser- und Nitratverweilzeiten unterstreichen die Bedeutung von hochfrequentiert erhobenen Isotopensignaturen sowie Daten des Transports und der Umwandlung gelöster Stoffe im Hinblick der prognostizierten zunehmenden hydrologischen Extreme (Dürren und Hochwässer) unter zukünftigen Klimabedingungen. Darüber hinaus erweitert diese Studie durch die Kombination von Verweilzeitmodellierung mit hochfrequenten Isotopensignaturen in verschiedenen Teileinzugsgebieten in Mitteldeutschland das Verständnis hydrologischer Prozesse unter Hoch- und Niedrigwasserbedingungen.

1. Introduction

1.1. Water age in catchment studies

In the field of catchment hydrology, water pathways through river basins are investigated with tracer data to better understand the underlying processes. With water age metrics such as transit time distributions that describe how long water has travelled through the catchment since its entry via precipitation until it is released to the stream as discharge or via evaporation to the atmosphere, and the young water fraction, that describes the proportion of water with an age around two to three months in stream flow, one is able to get more information about underlying processes in river basins (Benettin et al., 2022). The water age metrics can be obtained by measured data for instance for the determination of young water fractions after Kirchner (2016a, 2016b) the observed isotopic signatures in stream and precipitation are used to fit sinusoidal curves while the ratio of the amplitudes of both curves results in a young water fraction for the whole time series. In comparison to that modelling approaches can be used to determine young water fractions in higher resolutions e.g. daily or even sub-daily. The higher resolution of modelling results that are calibrated on measured data are useful tools to get more insights about hydrological processes under short-term hydrological events (Benettin et al., 2022). For instance, the age distribution gives an overview of different water sources that contribute to the stream. With higher resolutions of water age metrics more knowledge about water sources during high and low flows can be gained. Water from deep storages such as the groundwater storage are much older than water from recent precipitation events that infiltrated into the soil and the corresponding subsurface storages. The proportion of different water sources differs depending on the flow conditions (Xia et al., 2023). Moreover, depending on the soil substrate, water can flow much easier through the soil zone e.g. with sandy soils and porous aquifers, or it can be damped for instance with loamy soils and aquifers with a low permeability. By knowing how long water has been transported through the catchment, one can also get more insights about the underlying geology and their corresponding processes. Catchments are characterized by many different aspects, for instance mountainous catchments that have elevated regions versus flat catchments that are in the lowlands and catchments dominated by agricultural area versus catchments that consist of diverse land use types such as forests, grassland, urban area and agricultural crop land. There are many more characteristics that influence the hydrological processes. So far, studies that investigated catchment

characteristics and their influence on catchment's water age distribution dealt with catchment area, elevation, slope, and land use characteristics. But there are other studies that investigated for individual catchments how precipitation events and different discharge conditions influence the age distribution in stream. So far there has not been evaluated on a broader scale how water transit times differ depending on flow conditions for multiple different catchments in relation to their catchment characteristics. There is an urgent need to gain more information about the underlying processes and sources of water during hydrologically varying periods to understand drought conditions and high flows (Wilusz et al., 2017). To unravel hydrological processes in catchments and factors that influence the hydrological processes, studies focused on the relation between water age and catchment characteristics such as catchment area, soil type, elevation, land use as well as hydrological indices such as rainfall intensity and discharge (Dimitrova-Petrova et al., 2020; Hrachowitz et al., 2009; Jasechko et al., 2016; Jutebring Sterte et al., 2021; Li et al., 2020; Lutz et al., 2018; Seeger & Weiler, 2014; Soulsby et al., 2006; Tetzlaff et al., 2009; von Freyberg et al., 2018a; Wilusz et al., 2017). Jasechko et al. (2016) analyzed young water fractions with an age around 60 to 90 days that have been estimated from the ratio between the amplitudes of the seasonal isotope cycles in stream water and precipitation, respectively (Kirchner, 2016a, 2016b) of 254 watersheds globally with regard to catchment characteristics. The analysis revealed high contributions of young water (30%) for most of the catchments with higher young water fractions for agriculturally dominated catchments. The higher proportion of young water in streams of agricultural dominated catchments has the risk to transport and release solutes and contaminants much faster to the stream. More knowledge is needed with regard to hydrological events such as floods and droughts as well as the transport of nutrients and contaminants to prevent the biodiversity from high loads of harmful substances and to understand better the hydrological processes that occur under varying hydrological conditions.

1.2. Data resolution

Monitored data for time series of several years are often in coarse resolutions such as monthly records (Birkel et al., 2010; Timbe et al., 2015) due to the high effort and high costs of water sampling and analysis. The low-frequency tracer data in timesteps of monthly or even fortnightly data can be used to get general information about hydrological processes in catchments that occur throughout the year without acknowledging specific hydrological events. Studies that used monthly data are for instance Lutz et al. (2018) and Borriero et al. (2023). Lutz et al. (2018) investigated several catchments in the Bode watershed, in central Germany with the focus on estimating fractions of young water with monthly isotopic signatures of water to improve transit time distribution estimates. They found that mean ages of river water range between 9.6 months and 5.6 years depending on catchment characteristics. The results of Lutz et al. (2018) are interesting impressions about the region and the individual catchments, but to get more information about hydrological processes that vary under high and low flows as well as during droughts and floods, higher resolutions of data are needed. However, one limitation of the application of low-frequency (i.e. weekly or monthly) tracer data is the insufficient representation of the short-term dynamics such as high flow events and their corresponding hydrological processes (Stockinger et al., 2016; von Freyberg et al., 2018a). As shown by von Freyberg et al. (2017) and von Freyberg et al. (2018a), sampling frequencies of daily and sub-daily resolutions can provide more detailed information about short-term hydrological processes such as storm runoff events. The studies von Freyberg et al. (2017) and von Freyberg et al. (2018a) estimated fractions of young water in several Swiss catchments in a daily to sub-daily resolution of monitored tracer data to investigate relationships between young water fractions and catchment characteristics as well as climatic conditions such as storm runoff. They were able to reveal insights of the diverse hydrological behaviour of different catchments under changing flow conditions. Few studies have analyzed the water age in catchments with high resolution isotope data sets, such as sub-daily to daily sampling schemes, during hydrologically varying periods (e.g., Soulsby et al., 2015; von Freyberg et al., 2017, von Freyberg et al., 2018a). Knapp et al. (2019) showed in their analysis of new water fractions and transit time distributions at the Plynlimon experimental catchments in mid-Wales that estimates of water age metrics are affected by sampling frequency. Stream flow isotopic signatures are more damped with a lower sampling frequency, which causes

a strong difference between water age estimates derived from 7-hour and weekly tracer data (Knapp et al., 2019). Especially, for the analysis of water from previous precipitation events, von Freyberg et al. (2017) showed the relevance of high-resolution isotopic signatures for water age estimates. The study of von Freyberg et al. (2017) took water samples in a sampling interval of 30 minutes, to analyse stream water isotopic signatures with the aim to estimate event water for eight storm events, which demonstrated the high variability during different storm events as well as a more precise estimation of event water with high-frequency isotope data compared with aggregated isotope data for lower sampling resolutions (von Freyberg et al., 2017). This highlights the potential of high-frequency tracer data applications to understand hydrological processes and their variability during varying climatic conditions such as high and low flows and furthermore implies that more research is needed in this field of science. Due to the high effort and high costs of monitoring campaigns the duration of high frequency water sampling is in many studies limited to short-term periods, therefore modelling approaches can be used to produce data in high resolutions to be able to gain deeper insights of hydrological processes during time series of years and decades. The models are usually set up with hydrological data of the catchments and are calibrated on tracer data of stream water to estimate water age metrics such as transit time distributions and fractions of young water. The computed water age metrics in higher resolutions can help to understand the variations during different flow conditions or in general during varying climatic conditions. With this knowledge, the predictions of water release of different catchments under droughts and floods can be improved and by this the prevention of human beings and biodiversity can be improved considerably.

1.3. Approaches to derive water age metrics

Thanks to the use of tracer data such as isotopic signatures of water to unravel the water age (e.g. median transit time and fraction of young water), the understanding of hydrological processes and the contribution of different water sources and their respective water ages has been improved (Benettin et al., 2022). Water age metrics such as median transit times and fractions of young water are widely used tools to understand the hydrological pathways of catchments of different sizes. Knowledge of hydrological pathways is an inevitable prerequisite to understand and predict water

and pollutant fluxes and pollutant legacies. The composition of different water ages can be simulated by models (Benettin & Bertuzzo, 2018; Harman, 2015; Hrachowitz et al., 2016; Hrachowitz et al., 2009; Kim & Troch, 2020; Kuppel et al., 2018; Soulsby et al., 2015) or purely derived from tracer data (Jasechko et al., 2016; Kirchner, 2018; Kirchner, 2016a, 2016b; Lutz et al., 2018). For instance, Kirchner (2016a, 2016b) developed a straightforward approach to determine young water fractions with an age between 60 and 90 days (Fyw). Measured and weighted isotopic signatures of precipitation water and stream water are used separately to fit a sinusoidal curve to the observed values. The ratio of the amplitudes of both sinusoidal curves, from precipitation and from stream water are further used to derive the young water fraction of the whole time series of the observed data. The benefit of this approach is the straightforward implementation of measured and weighted isotopic signature data without the need of any additional data. But the disadvantage is the dampening of the isotopic signatures due to the fitted sinusoidal curves that approximate the measured isotopic signatures and besides, the value of Fyw is one value for the whole time series. The dampening of the isotopic signature results in a higher uncertainty of the final result, because the high variability of the isotopic signature has not been adequately mirrored by the sinusoidal curve. This is especially crucial for short-term studies such as in the study of Wang et al. (2023), where the young water fraction as well as the mean transit time has been determined with measured data from a headwater catchment of the Tibetan region. In the study of Wang et al. (2023) the data was collected during the summer months, because of frozen water sources during winter time. Therefore, Wang et al. (2023) were restricted to the short-term period for the estimation of young water fractions and mean transit times. Considering the short-term data base of the study in concert with the dampening of the isotopic signature using the approach after (Kirchner, 2016a, 2016b) increases the uncertainty of the study results. In case of missing data due to climatic conditions in the regions or due to device problems, models are useful tools to simulate processes in a catchment. With models such as the tran-SAS (Benettin & Bertuzzo, 2018) much finer resolutions such as sub-daily and daily (depending on the input data frequency) fractions of different young water thresholds can be determined with the measured isotopic signatures and additional hydrological data such as discharge, precipitation and evapotranspiration. The ability of determining higher resolutions of water age metrics gives the opportunity to investigate short-term events such as heavy rainfall events as well as events with

longer durations, for instance, droughts. For instance, models are calibrated on stream water isotopic signatures to obtain water age metrics. So far studies used different approaches to derive water age metrics, one of the most straightforward approaches are storage selection (SAS) functions. Commonly used storage selection functions are gamma distribution, power-law and beta distribution. Using storage selection functions is a straightforward approach to statistically summarize the transport behaviour of a hydrological system (Benettin et al., 2022). They are defined to represent how a catchment storage releases water of different ages to the outflow (e.g. as discharge or evapotranspiration) and therefore, storage selection functions are regulating the chemical composition of the out-fluxes (Rinaldo et al., 2015). The parametrization of the SAS functions can be estimated a priori (Kim and Troch, 2020) or can be estimated using a calibration routine to fit the model simulation to observed data (Benettin et al., 2022). In the case of measured tracer data in a catchment with lower resolutions such as monthly or fortnightly data, a SAS model can easily be calibrated on these low-resolution tracer data with the ability to simulate tracer concentrations during the data gaps as well as to determine water age metrics in an appropriate time scale. By setting up a SAS model with high-resolution tracer data, as done in this study, the determination of daily variations of water age metrics can be done. Moreover, using a model gives the opportunity to derive not only young water fractions in a daily or sub-daily timestep, but especially one of the biggest benefits is to be able to determine fractions of water ages with specific thresholds such as seven days, two weeks and other. The lower threshold of young water fraction can help to separate the water sources in water from previous precipitation events, which can improve the understanding of hydrological processes during events.

1.4. The role of hydrological events on water age

Hydrological events are often described as time periods with intense rainfall, high discharge and oversaturated soils and water storages, but events can also be time periods without rainfall or discharge such as droughts where high temperatures and intense solar radiation cause the soils and water storages to dry out. There are event classification approaches that classify events based on precipitation or discharge (Lang et al., 1999; Merz et al., 2006; Sikorska et al., 2015; Soulsby et al., 2015) and there are approaches that classify events based on both, precipitation and discharge

(Giani et al., 2022). In this study, events are classified as wet and dry spells based on the discharge volume. By this the whole time series is separated in multiple wet and dry spells, while the further analysis focuses on the overall categories (wet vs. dry spells) to evaluate the results of the water age modelling. Understanding the hydrological processes during wet and dry spells as well as the age composition of water and its transit time has gained an increasing importance during the past decade which is reflected by several studies dealing with water age estimates under varying discharge (e.g. Benettin et al., 2015; Soulsby et al., 2015; von Freyberg et al., 2017; Wilusz et al., 2017; von Freyberg et al., 2018a; von Freyberg et al., 2018b). Soulsby et al. (2015) analyzed with a high-resolution data set the variability of stream water age during wet and dry periods using a threshold on the discharge to classify the periods. The study of Soulsby et al. (2015) revealed the relevance of how transit times of water differ depending on the discharge volume, they pointed out that the water age rises during dry periods such as summer time when less precipitation occurs, instead the transit time is lowered during winter time with high precipitation. Even though the knowledge about how transit times differ during wet and dry periods is a valuable insight in hydrological processes, with the consideration of fractions of young water with diverse age thresholds, more information can be gained during the varying discharge and respective hydrological events. With focus on the fraction of young water of recent precipitation events (e.g. threshold of seven days), there is an opportunity to determine more precisely how discharge is sampled from the storages, which can help to understand better floods and their risk to human beings and biodiversity. By knowing how much water from previous precipitation events is released to the stream during high flow events, the prediction of floods can be improved and by this the warning system of floods can be improved as well.

1.5. Water age in relation to solutes

Soluble substances such as nutrients (e.g. nitrate and phosphate) are applied on crop land to supply the agricultural crops with necessary elements for growing and to support a big harvest at the harvest time of the culture. Pesticides such as fungicides, herbicides and others are applied on crop cultures to prevent the plant from fungi, weeds, bacteria, nematodes and in general crop disease. Even though with good management practices the loss and fate of nutrients and pesticides from the

agricultural field can be reduced, nevertheless there is a relevant amount of solutes that are released to the waterbody such as the river that flows between the agricultural fields but also the groundwater where infiltrating water transports the solutes, that has not been taken up by plants, to the deeper water storages. Solutes such as pesticides that are released to the water ecosystem are contaminating the habitat of various plant species, microbes, fishes and insects. Flora and fauna are harmed by the loads of contaminant mixture, whereby the ecosystem is damaged. Nutrients such as phosphate and nitrate that are released to the water bodies are causing eutrophication due to the increased growth of algae and the corresponding loss of oxygen in water. Due to the eutrophication, the diversity of fish species, microbes and insects is lost, because they die due to the oxygen loss. These circumstances show that more knowledge about the fate and transport of solutes in catchments of diverse land use types is necessary to optimize the application regulation of pesticides and nutrients to prevent the ecosystems from dying out. In this study the focus is on the nutrient nitrate. Due to conventional agricultural practice, the amount of nitrogen (N) applied on agricultural land very often significantly exceeds that of the actual plant uptake (Bijay & Craswell, 2021; Kirschke et al., 2019), resulting in a N surplus accumulating in soils and groundwater systems. Once organic soil nitrogen is transformed to nitrate, it is mobilized and transported by water fluxes, with the risk of contaminating receiving water bodies (Galloway et al., 2004) and fostering eutrophication in lakes and rivers that may trigger biodiversity loss.

A powerful avenue to decipher nitrate issues are transit time approaches, which estimate the time a water parcel or a solute has spent in a catchment since its entry via precipitation or field application and until it reaches the stream via discharge or releases the catchment via evapotranspiration (Hrachowitz et al., 2016; Lutz et al., 2018; Rinaldo et al., 2015; van der Velde et al., 2010). There is a considerable number of transit time studies that derive water age based on tracers (Benettin et al., 2020; Birkel et al., 2010; Dupas et al., 2020; Hrachowitz et al., 2016; Kleine et al., 2020; Lutz et al., 2018; Lutz et al., 2020; Molénat & Gascuel-Oudou, 2002; Nguyen et al., 2021; Rinaldo et al., 2015; Smith et al., 2020; van der Velde et al., 2010; van der Velde et al., 2012). The relevance of water transit times in relation to solute transport is pointed out in the study of van der Velde et al. (2010) who investigated nitrate export at the Hupsel brook catchment and discovered the relationship between the dynamics of contact times of water and soil and the observed nitrate concentrations in stream. Van der

Velde et al. (2010) revealed the relevance of nitrate removal in the Hupsel brook catchment in comparison to the water transit time and mentioned the relevance of water quality models to know the contributions of relatively young water to discharge than knowing the average catchment transit time. They state that stream water is a result of mixing different water sources with a higher proportion of old water, that transports a relatively constant nitrate concentration, with a discharge-dependent contribution of younger water that transports variable concentrations of nitrate. Therefore, more knowledge about the fractions of young water can reveal insights of nitrate transport. Moreover, being able to determine the exact nitrate age since its forming would be an improvement for the understanding of the fate and transport of nitrate in a catchment, which has not been done in other studies so far. Nitrate transport in relation to water age was discussed by other studies (van der Velde et al., 2012; Molénat & Gascuel-Oudou, 2002; Kaandorp et al., 2021; Nguyen et al., 2021; Yu et al., 2023). Nitrate removal in relation to water age was explicitly pointed out by Benettin, Fovet, & Li (2020) who estimated water age based on chloride as a tracer to analyze the relationship between water age and nitrate removal. Their findings revealed that nitrate removal and water age do not correlate throughout the whole year, but a relationship between nitrate removal and young water fractions was found during summer periods. They pointed out that during drier periods such as low flows during summer periods such as low flows during summer times. The old water contribution from deeper groundwater storages transports nitrate from a pool that underwent some extent of denitrification. Due to the latter fact, there is a negative correlation between young water fractions and nitrate removal, while nitrate removal decreases when young water fractions increase. The relation between water age and nitrate removal in riparian zones has been discussed in other studies as well (e.g. Lutz, et al., 2020). However, so far, there have been few investigations of age metrics of nitrate compared to age metrics of water. None of the studies attempted to estimate the explicit nitrate transit time, describing the time from its formation during nitrification in the soil until nitrate release to the stream by using isotopic signatures.

1.6. Nitrate: biogeochemical processes

Nitrate transit times can be largely different from those of water because of chemical reactions involving nitrate transport (Hrachowitz et al., 2016). The biogeochemical reactions affecting nitrate transit times are difficult to quantify, but they specifically impact oxygen isotopic signatures in nitrate which have the potential to reveal information on nitrate transit times. During nitrification, microbes are oxidizing ammonia to nitrite and from nitrite to nitrate. During these processes the oxygen atoms of nitrite and nitrate are exchanged with surrounding oxygen sources such as soil air and soil water. Nitrification of reduced inorganic nitrogen and the associated oxygen isotope exchange between reaction intermediates and ambient water was investigated in detail by Boshers et al. (2019), Buchwald and Casciotti (2010), Casciotti et al. (2011), Granger and Wankel (2016), Kendall et al. (2007) and Kool et al. (2011). Granger & Wankel (2016) established a precise overview of functions describing the exchange of isotopes during the processes nitrification and denitrification for both, oxygen isotopic signatures and nitrogen isotopic signatures. Even though the nitrogen isotopic signature of nitrate is used widely to describe the sources of nitrate and the extent of biogeochemical reactions (Granger & Wankel, 2016; Kendall et al., 2007), it cannot be readily used to track nitrate age because it is governed by the highly variable isotopic signature of the nitrogen compounds being transformed to nitrate such as ammonia or nitrite. In contrast, the oxygen isotopic signature of nitrate stems from surrounding water and soil air and is incorporated into nitrate during its formation via nitrification (Boshers et al., 2019; Griffiths et al., 2016; Kendall et al., 2007). While nitrification describes the forming of nitrate, denitrification describes the degradation of nitrate. More precisely, the denitrification describes the conversion of the bound nitrogen in nitrate to molecular nitrogen and nitric oxide by heterotrophic and autotrophic bacteria. With denitrification the amount of nitrate on its flow path is reduced and by this nitrate concentrations are lowered in the stream. Denitrification along the flow paths and within the storage system is associated with an isotope fractionation resulting in a shift of both nitrogen and oxygen isotope values in the remaining nitrate pool towards higher values with the characteristic ratio of $\Delta\delta^{18}\text{O} : \Delta\delta^{15}\text{N}$ between 0.5 and 1 (Kendall et al., 2007; Knöller et al., 2010; Mariotti et al., 1981). Hence, with longer transit times, the potential impact of denitrification on nitrate isotopes increases. With the isotopic signatures of water as tracer, one is able to track the age and transit time of nitrate since water is

incorporated during the nitrification until nitrate is released to the stream. This knowledge can improve the understanding of nitrate transport.

1.7. Nitrate transport and nitrate age modelling

While the age of water is determined by the moment when precipitation enters the soil surface, nitrification taking place in the upper soil can be considered as the initial process when the “nitrate clock” begins to tick. Naturally, there is a time lag between precipitation entering the soil and the mobilization of newly formed nitrate during nitrification. Sebiló et al. (2013) conducted experiments that showed that the temporal offset between nitrogen input to the soil and mobilization as nitrate can take up to decades. Once mobile though, nitrate can be considered to follow the same flow paths as the water. However, processes like biological nitrate uptake, denitrification and mixing may have a significant influence on the median age of the nitrate pool resulting in an apparent shift of the difference between the transit times of nitrate and of water. Unraveling the time lag between N input and nitrate mobilization and transport and the differences between water and nitrate transit times is a prerequisite to better understand a catchment’s capability to retain and mitigate nitrogen input for different seasons and hydrological conditions. While the time lag between input and mobilization has been addressed in previous studies (Sebiló et al., 2013; van der Velde et al., 2010), no studies have attempted to model nitrate transit times directly from the forming process until nitrate is released to the stream and the offset in water and nitrate ages is largely unknown. The novelty of this study is the usage of oxygen isotopic signatures to simulate the forming and the degradation of nitrate at the catchment scale and by this being able to estimate the age and transit time of nitrate more accurately.

1.8. Aim of the study and research gap

This study is focusing on water age metrics from six contrasting catchments in the Bode basin, Central Germany. Automatic samplers are set up to collect high-resolution data sets of isotopic signatures in water to derive water transit times and fractions of different young water ages during events that are classified as wet and dry spells. In one of those catchments, water samples have been analysed with regard to nitrate

concentrations and nitrate isotopic signatures with the aim to investigate the age of nitrate compared to the age of water.

While recent studies have investigated the overall relationship between the water age and catchment characteristics, there are very few studies focusing on the role of water age during varying hydrological conditions such as high and low flows in streams (Benettin et al., 2015; Soulsby et al., 2015; von Freyberg et al., 2017, von Freyberg et al., 2018a). Regarding varying discharge Benettin et al. (2015) analysed time-varying transit times as well as the transport and the biogeochemical processes of solutes in the Hubbard Brook watershed on a bi-weekly sampling frequency. By showing how transit times are changing due to storm events and drought periods (hydrological varying periods), Benettin et al. (2015) revealed that storm events cause more young water to be released to the stream, which is reflected by lowered transit times. In a comparison of 22 Swiss catchments von Freyberg et al. (2018a) were able to show the differences of catchments releasing young water depending on catchment characteristics and discharge by using the sinusoidal amplitude method after Kirchner (2016a, 2016b) to compute young water fractions based on monthly precipitation isotopic signatures and fortnightly stream water samples. These studies were able to show that transit times and young water fractions vary depending on discharge and catchment characteristics, but so far there is no study that was able to consider the daily variation of different fractions of young water such as water with an age up to 7 days (Fyw7) that represents water from recent precipitation events and in comparison to that the fraction of young water with an age up to 60 days (Fyw60) as metric to be compared to studies based on the young water fraction after Kirchner (2016a, 2016b). To overcome the blind spot on short term hydrological dynamics of previous studies linking water age distribution based on low-frequency data to climate and landscape features, this study uses high-frequency isotope data and transit time modelling to reveal the difference of age compositions during varying flow conditions in streams, investigating five of the six contrasting sub-catchments within the Bode watershed in Central Germany. This study aims to understand how fractions of young water are changing under varying discharge periods such as wet and dry spells and how this is controlled by catchment characteristics. On the basis of an exceptionally extensive high-frequency water stable isotope data set provided by an elaborate isotope monitoring program, the aim of the investigation is (i) to understand how different fractions of young water (Fyw7 from previous rainfall events, Fyw60 as young water

fraction comparable with Fyw from Kirchner (2016a, 2016b)) are influenced during high and low flows, (ii) to analyse the variation of fractions of young water across catchments and (iii) to analyse the sensitivity of different fractions of young water (Fyw7, Fyw60) against discharge variations. These analyses will help to inspect the relationship between water age distributions and landscape structures to support a better understanding of flow paths under varying hydrological conditions. Such understanding is of extreme relevance for the prediction of potential nutrient losses and of changed fluxes and legacies of anthropogenic pollutants that may harm the ecosystems.

With regard to nitrate age versus water age the objective of this study is to unravel the relationship between water age and nitrate age by hypothesizing that (iv) transit times of water and nitrate have a temporal offset in a mixed land-use headwater catchment and (v) transit times of water and nitrate are impacted by varying discharge. To test these hypotheses, high frequency data (needed to investigate transit time distributions (TTD) more precisely, Stockinger et al., 2016) of isotopic signatures of water and nitrate was collected in the Meisdorfer Sauerbach catchment, which is part of the intensively studied terrestrial environmental observatory TERENO (Lutz et al., 2018; Mueller et al., 2016; Wollschläger et al., 2016) and which is located within the Selke catchment where many studies have been conducted related to transit times of water and nitrate transport, albeit without the use of nitrate isotopes or model-based transit times (Ehrhardt et al., 2021; Lutz et al., 2020; Nguyen et al., 2021; Nguyen et al., 2022; Winter et al., 2021; Yang et al., 2021).

In addition to the conventional evaluation of the high frequency isotope data sets of water and nitrate, the transit time model tran-SAS v1.0 (Benettin & Bertuzzo, 2018) has been adopted to simulate nitrate transit times and nitrate age incorporating the simulation of oxygen isotope signatures and by considering dominant processes like nitrification and denitrification and the associated oxygen isotope fractionation effects. Besides high-frequency isotopic data, the model was fed with simulated hydrological data derived from the mesoscale hydrological Model-Nitrate (mHM-N: Yang et al., 2018, Yang & Rode, 2020). The simulated water and nitrate transit times obtained by the model were analyzed in order to better understand the storage and release of nitrate in mixed land-use headwater catchments.

2. Methods

2.1. Study Area

The selected catchments for the investigation of water transit times during hydrological events, are located within the intensively studied Bode catchment in the Harz mountains and the adjacent northern lowlands in Central Germany (Borriero et al., 2023; Lutz et al., 2018; Mueller et al., 2016; Nguyen et al., 2021; Wollschläger et al., 2016). The mesoscale Bode catchment is part of the Elbe river basin and ranges between 55 and 1100 m above sea level. Considering the landscape structure, a strong gradient from forested headwater catchments to intensively cultivated lowland catchment shapes the Bode basin and the included sub-catchments. A humid climate with a mean annual temperature about 9 °C and average annual rainfall about 660 mm, ranging spatially between 450 and 1600 mm is present in that area. Other studies dealing with water fluxes and water quality have been conducted in some broader catchments such as the Holtemme basin and the Selke basin (Borriero et al., 2023; Lutz et al., 2018; Nguyen et al., 2021; Wollschläger et al., 2016). In this study, six sub-catchments of various landscape pattern and catchment areas (Figure 1) were selected. To provide extensive high-frequency isotope data sets in daily and sub-daily resolutions an elaborate monitoring program was conducted with automatic samplers that are specifically designed and proven to collect water samples for isotope analysis with the consideration to avoid evaporation effects (Michelsen et al., 2019). Automatic samplers were set up at five catchment outlets to collect high-frequency stream water and precipitation samples. At the catchments No. 4 and No. 6, citizen scientists collected daily manual samples of stream water and precipitation. Catchment characteristics such as elevation, slope and topographic wetness index (TWI) were calculated using the Saga toolbox in QGIS version 3.18.1, while the land use shares are obtained by Corine Landcover data with a resolution about 5 ha (GeoBasis-DE / BKG, 2018). Soil type data was obtained by the Bundesanstalt für Geowissenschaften und Rohstoffe, using the BUEK1000. Annual average discharge and time series for the calibration of the hydrological models (mHM and mHM-nitrate) were obtained from discharge measuring stations provided by the Landesbetrieb für Hochwasserschutz und Wasserwirtschaft (Landesbetrieb für Hochwasserschutz und Wasserwirtschaft, 2022). The baseflow index (BFI) is calculated using the daily discharge datasets of the catchments, using the hydroEvents package in R, version 4.0.5 (<https://CRAN.R-project.org/package=hydroEvents>). From the Deutsche Wetterdienst (DWD, 2021),

annual average precipitation as well as precipitation time series as input for the models were used. Annual average evaporation was obtained from the hydrological model mHM (Kumar et al., 2013; Samaniego et al., 2010).

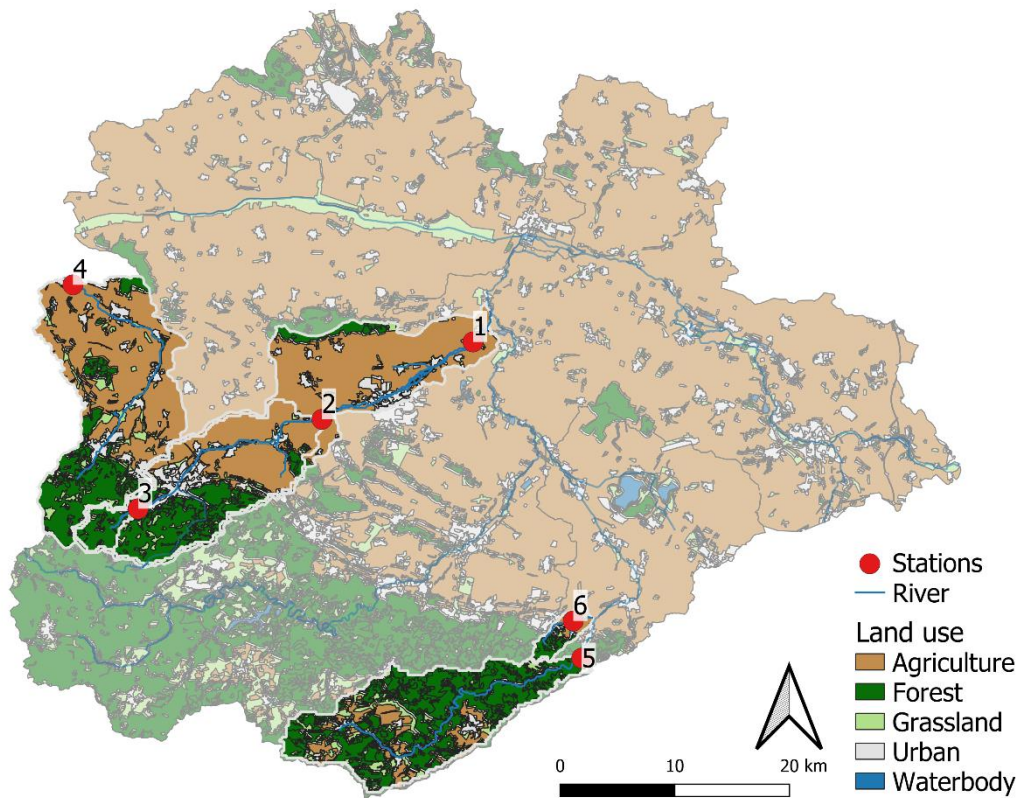


Figure 1: Study area with the sub-catchments, located in the Harz mountains, Central Germany.

The sub-catchments selected for high-frequency isotopic sampling cover a wide range of climate and landscape characteristics of the Bode river basin. The largest sub-catchment is a hilly anthropogenically impacted catchment (Nienhagen catchment, 282 km²) (Figure 3, catchment 1), showing the highest density of river network and including lowlands with intensive agriculture (18%) and urban area (25%). The Mahndorf catchment (142.86 km²) (Figure 3, catchment 2) is nested within the Nienhagen catchment and shows some anthropogenic impacts, such as urban area (24%) and agricultural crop land (13%). One of the smallest sub-catchments is Steinerne Renne (13.37 km²) (Figure 3, catchment 3), a typical German mid-elevation mountainous headwater catchment with dominant forest (33%) and grassland (67%) cover. The catchment may be seen as a pristine headwater catchment, as no agricultural fields and no urban areas are located within the catchment. With 529 mm

the discharge is highest in the Steinerne Renne catchment compared to the other catchments. The Steinere Renne is part of the Mahndorf catchment. The mountainous agriculturally dominated Ilse catchment (194 km²) (Figure 3, catchment 4) has the highest elevation range (ranging between 97 and 1138 m) with forest (22%) and grassland (40%) dominating the upper part of the catchment and a high density of agricultural area (19%) in the lowlands. Compared to the Steinerne Renne and Mahndorf catchment, the Ilse catchment shows less discharge (160 mm). With more forested (31%) and grassland (44%) area, the Selke catchment (157 km²) (Figure 3, catchment 5) shows less anthropogenic impacts than the Mahndorf catchment. The Selke catchment is located in the lower part of the Harz mountains, but is still hilly and mainly forested. A neighbouring catchment to the Selke is the Meisdorfer Sauerbach catchment (Figure 3, catchment 6). It is an agriculturally dominated headwater catchment in the lowlands of the Harz mountains. This catchment is the smallest (11.5 km²) of all investigated catchments and has the lowest annual average discharge (40 mm). The climate in the area is semi-humid with an annual precipitation of 474 mm and an annual mean temperature of 12 °C (years 2013-2020). While arable land accounts for 48% of the 11.5 km² catchment, around 46% of the catchment are covered with forest and grassland. The remaining 6 % are urban areas (GeoBasis-DE / BKG, 2018). Dominant soil types are brown earth and podzols with a higher proportion of clay as well as luvisols with pseudogleys from loess. Alluvial soils surround the surface water bodies in the catchment. The permeability of the underlying geological sequences mainly consisting of greywacke, red sandstones and shell limestones varies between moderate and low (hydraulic conductivity coefficient (kf-value) between 1E-12 and 1E-5). Aquitard sections are found throughout the catchment. Catchment 6 has been investigated more intensively with additional soil samples and groundwater samples (Figure 2).

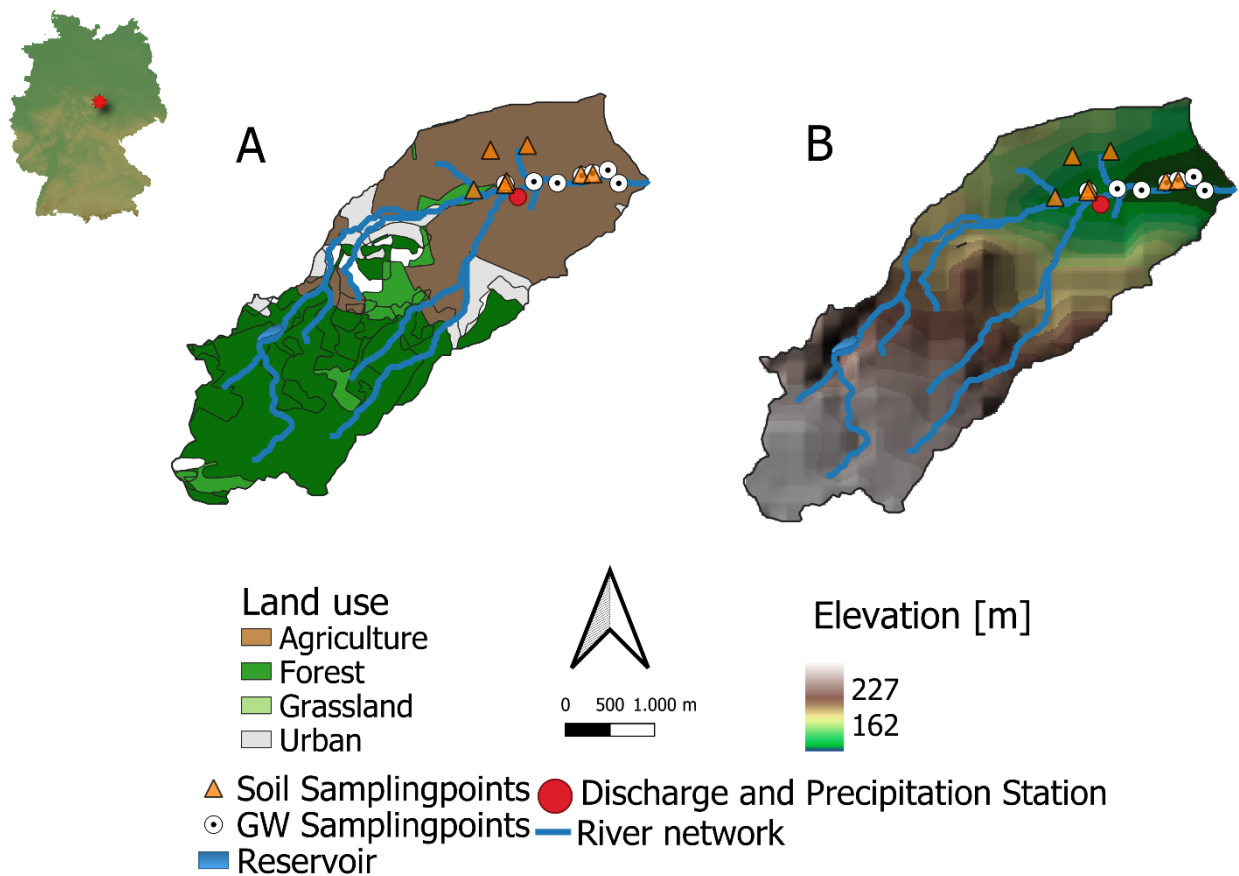
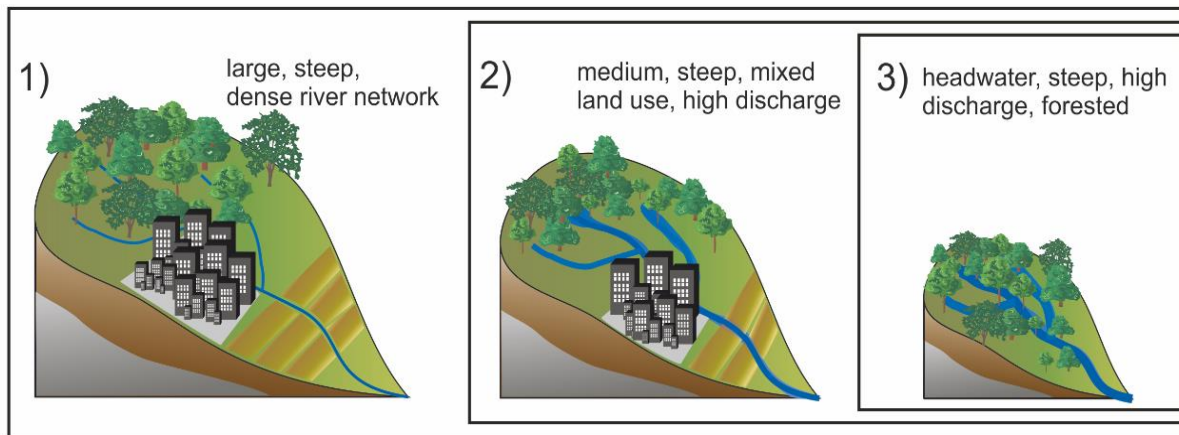


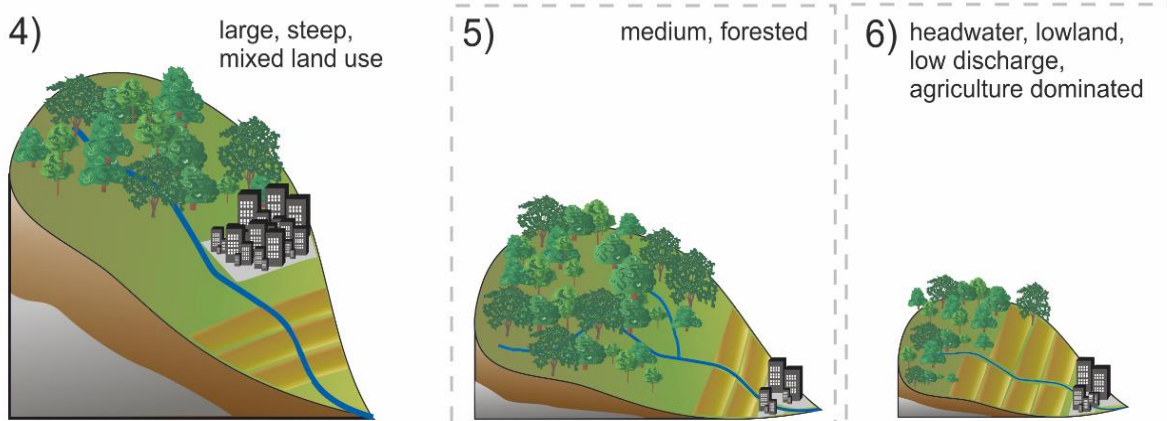
Figure 2: The Meisdorfer Sauerbach catchment with an area about 11.5 km² is located at the north-eastern border of the Harz mountains of Germany (top left map of Germany). The red dot is the location of the autosampler for stream chemistry as well as the discharge measurement station. The orange triangles are locations of soil samples and the white circles with the black dot are locations of ground water wells. Land-use data in panel A is provided by GeoBasis-DE / BKG (2018), and elevation data in panel B in 200m resolution is taken from GeoBasis-DE / BKG (2013).

Table 1: Catchment characteristics with TWI as topographic wetness index and BFI as baseflow index considering time series between 2010 and 2021.

Catchment characteristics	1 (Nienhagen)	2 (Mahndorf)	3 (Steinerne Renne)	4 (Ilse)	5 (Selke)	6 (Meisdorfer Sauerbach)
Area [km ²]	282	142.86	13.37	194	157	11.5
Elevation [m a.s.l.]	84-863	134-863	300-863	97-1138	193-576	170-353
Forest [%]	23	25	33	22	31	36
Grassland [%]	33	37	67	40	44	15
Agriculture [%]	18	13	0	19	13	27
Urban [%]	25	24	0	19	11	22
Soil type	Chernozem, brown earth, gley soils, podzols, luvisols	Brown earth, luvisols, chernozem sub-types, podzols	Brown earth podzol with mixtures of clay	Luvisols, gley soils, podzol-brown earth, chernozem, brown earth	Brown earth, luvisols	Brown earth, luvisols, gley soils
TWI (mean)	11-28 (16)	11-27 (15)	11-20 (15)	11-24 (16)	12-23 (15)	12-23 (15)
Slope [°] (mean)	0.01-21.29 (2.9)	0.01-21.29 (4.04)	0.39-20.87 (7.95)	0.01-25.82 (2.98)	0.16-17.55 (3.77)	0.03-6.55 (2.31)
Flow path length [km]	42.66	23.09	2.07	28.68	30.12	7.37
Annual avg. discharge [mm]	102	208	529	160	128	40
BFI	0.48	0.62	0.55	0.60	0.55	0.26
Annual avg. precipitation [mm]	424	465	576	538	547	548
Annual avg. evaporation [mm]	480	489	507	468	485	470



nested catchments



isolated catchment

neighbouring catchments

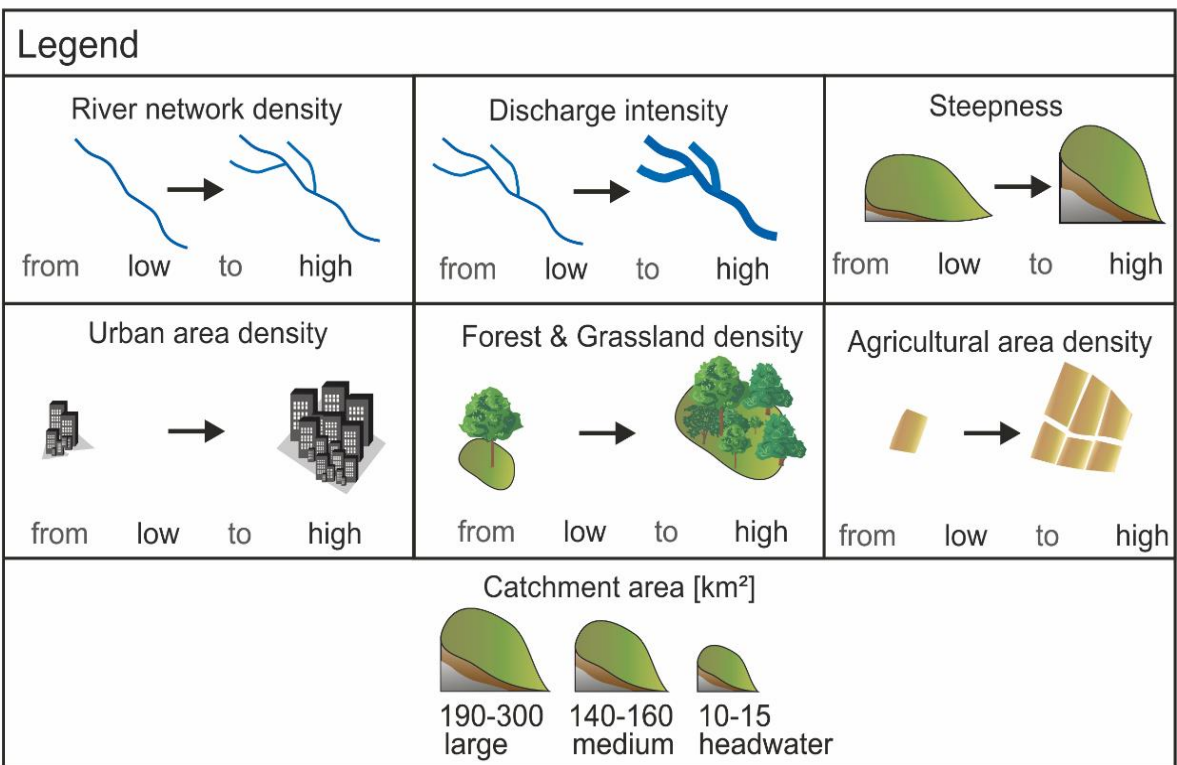


Figure 3: Illustration of all six catchments investigated, considering their most meaningful catchment characteristics.

2.2. Sampling

Water samples of precipitation were collected as composite samples in a monthly frequency from 2013 to 2017 for the catchment 5, while for catchments 1-3 monthly precipitation samples were taken from 2013 to 2019. Automatic samplers were set up in the catchments 1-3, 5 and 6 in 2020 to be able to collect daily and sub-daily samples of precipitation and stream water. Manual samples of research citizens were taken at the outlet of catchment 4 for stream water and precipitation since 2020. According to the public weather forecast, event water samples were taken in sub-daily timesteps (4 hours to 8 hours) with the autosamplers whenever heavy rainfall was predicted to occur. The stream water samples were taken via a pump as grab samples at specific time steps: daily samples were taken at 3 pm and sub-daily samples were taken every 4, 6 or 8 hours, depending on the chosen program for the event sampling scheme. A precipitation collector was used to sample precipitation water. The collector switches the position of the sampling bottle at each programmed time step: 24 hours during daily sampling and 4-, 6- or 8-hours during event sampling.

In catchment 6 nitrate concentrations, nitrate isotopic signatures ($\delta^{15}\text{N}$ and $\delta^{18}\text{O}$ values) and water isotopic signatures ($\delta^2\text{H}$ and $\delta^{18}\text{O}$ values) were measured in stream water close to the catchment outlet with varying temporal resolution. The stream water stable isotope samples were taken at fortnightly intervals from February 2017 to September 2018. Monthly samples were taken from October 2018 to April 2019. From May 2019 until March 2021, samples were generally taken as daily grab samples. During that period, sampling was changed from a daily to a sub-daily scheme with sampling intervals between 4 and 8 hours for selected precipitation events, whenever the weather forecast predicted precipitation events in the investigation areas.

Sampling schemes for nitrate concentrations and nitrate isotope signatures in stream water are in fortnightly timesteps from February 2017 to September 2018 and daily from May 2019 to March 2021. During October 2018 to April 2019, no samples were taken for the analysis of nitrate concentrations and nitrate isotopes.

Besides stream water samples, composite precipitation samples were collected on a monthly base between 2013 and 2017. Fortnightly composite precipitation samples were taken from February 2017 to September 2018. Daily composite precipitation samples and sub-daily precipitation samples for selected precipitation events were collected from May 2019 to March 2021. Depending on the volume of water that has

been sampled with the autosampler from stream water (less water during low flows), the amount of samples differ for nitrate concentrations, nitrate isotopic signatures and water isotopic signatures. Due to technical challenges related to the operation of the autosamplers (mainly temporary clogging of tubes and valves especially during low flow periods), only considerably reduced, variable sample volumes were collected at certain periods of times. As a consequence, a parallel analysis of nitrate isotope signatures and nitrate concentration could not be realized for all samples. In total there are 147 measurements of nitrate isotopic signatures and 161 measurements of nitrate concentrations, while only 71 measurements of both are overlapping (from the same sampling time). Measurements of water samples of stream water count in total 391 and for precipitation there are 535 measurements. In addition, seasonal groundwater (n=39) and soil moisture (n=127) samples for water isotope analysis were taken between February 2017 and September 2018 at seven different locations close to the stream in the agricultural land use section of the catchment (Figure 2).

2.3. Laboratory Analysis

Prior to the analysis of isotopic signatures and nitrate concentrations, water samples were filtered through a 0.45 μm filter. Nitrate concentrations were measured by ion chromatography with a Dionex ICS-2000 instrument combined with an AS50 autosampler. For determining the isotopic composition of dissolved nitrate, the denitrifier method with bacteria strains of *Pseudomonas chlororaphis* was applied (Casciotti & Ward, 2001; Sigman et al., 2001). With a combination of a GasBench II and a DELTA V Plus mass spectrometer (Thermo Scientific) the isotope measurements of the produced N_2O gas of the microbes were conducted. The analytical precision for nitrogen and oxygen isotope measurements of nitrate were 0.4 ‰ and 0.8 ‰, respectively. International standards (USGS32, USGS34, USGS35 and IAEA NO3) were applied for correction and calibration of the raw analytical data. For duplicate measurements of stable isotopic signatures of water, a liquid isotope analyser (Picarro L2120-I) was used. The samples were normalized to replicate (20x) analysis of internal standards that are calibrated to the Vienna Standard Mean Ocean Water (VSMOW) and Standard Light Antarctic Precipitation (SLAP) certified reference materials. The analytical uncertainty of $\delta^{18}\text{O}$ and $\delta^2\text{H}$ were ± 0.1 ‰ and ± 0.6 ‰

respectively. The isotopic ratios are expressed in delta notation relative to VSMOW for the oxygen and hydrogen isotope signatures of water:

$$\delta_{sample}[\text{‰}] = \left(\frac{R_{sample}}{R_{standard}} - 1 \right) \times 1000 \quad (1)$$

For water: with R_{sample} describing the isotopic ratio of the water sample and $R_{standard}$, describing the isotopic ratio of the VSMOW-standard.

Due to higher measurement precision and a correlation factor of 0.9 between $\delta^{18}\text{O}$ and $\delta^2\text{H}$, the isotopic signature of $\delta^{18}\text{O}$ of water is used for the following investigations. And for nitrate: with R_{sample} describing the isotopic ratio of nitrate in the water sample, and $R_{standard}$ describing the isotopic ratio of atmospheric nitrogen ($R_{standard} = 3.677 \times 10^{-3}$) and the VSMOW-standard ($R_{standard} = 2.0052 \times 10^{-3}$) for nitrogen and oxygen isotope measurements, respectively.

2.4. Data preparation

The transit time model tran-SAS (Benettin & Bertuzzo, 2018) that is used in this study to compute age distributions of water and nitrate requires continuous hydrological and tracer input data. Discharge observations have not been available at all locations in a continuous timescale and the actual evapotranspiration was not measured, therefore simulations of the Mesoscale Hydrological Model (mHM) (Kumar et al., 2013; Samaniego et al., 2010) were used. mHM is a process-based, well-established model at a 1 km spatial resolution which accounts for the sub grid variability of essential basin physical characteristics by using the Multiscale Parameter Regionalization scheme proposed by Samaniego et al. (2010) and further developed by Kumar et al. (2013). The model has been thoroughly evaluated and calibrated against observed discharge in the Bode basin in past studies (Lutz et al., 2018; Mueller et al., 2016; Zink et al., 2017). Specifically, the mHM set-up utilized in this study follows Mueller et al. (2016) – wherein the model was parameterized at a daily time-scale for the whole Bode River Basin at 1 km spatial resolution. Model evaluation across several discharge gauging stations in the Bode basin shows very satisfactory results (e.g., with an average NSE estimated over 30 gauging stations – including ones of this study - for an independent 20-year validation period was around 0.65; see Mueller et al., 2016 for more detail). In subsequent studies, mHM was also successfully evaluated for evapotranspiration and

soil moisture across a diverse range of measurement sites in Germany demonstrating its overall applicability for hydrologic simulations (see e.g. Boeing et al., 2022; Zink et al., 2017). Meteorological forcings such as precipitation and air temperature to drive the model were acquired from the German Weather Service, DWD (DWD, 2021). DWD provides point estimates of weather information across more than 5000 rainfall and weather stations. Gridded estimates of precipitation and temperature fields were estimated using the external drift kriging-based interpolation technique wherein the terrain elevation was used as an external drift (see Zink et al., 2017 for more details). The daily temperature fields of maximum, minimum and average daily estimates were then used to calculate potential evapotranspiration – one of the meteorological drivers of mHM - using the Hargreaves and Samani method. The PET fields are later adjusted within mHM to reflect the differences in the terrain aspect. For more information about the mHM processes and parameterization, the reader is referred to Samaniego et al. (2010) and Kumar et al. (2013) as well as to Mueller et al. (2016) for specific details.

For further investigation of nitrate concentrations and isotopic signatures, continuous datasets of nitrate concentrations that are transported with the water pathways were obtained using the mHM-nitrate model (Yang, Jomaa et al. 2018; Yang & Rode 2020), which is based on the mHM model, but is extended with biogeochemical equations to simulate nitrate transport and removal in catchments. mHM-nitrate was set up for the broader Selke catchment, including the upper and the lower Selke, where the Meisdorfer Sauerbach (catchment No. 6) is located, by Yang & Rode (2020). A detailed description of the model structure, conceptualization and calibration, which combines concepts of the mHM model and the Hydrological Predictions for the Environment (HYPE) model (Lindström et al., 2010), is provided by Yang & Rode (2020). The mHM-nitrate model is running at daily time steps, using precipitation and temperature data interpolated from observed data and calibrated against observed discharge as well as measured nitrate concentrations in the stream at three main stem stations of the larger Selke catchment (Yang et al., 2018; Yang & Rode, 2020), for which the catchment 6 is a tributary.

To cover the isotopic variation of precipitation over the different catchments and their elevation, the isotopic signatures of precipitation obtained by the different precipitation sampling stations were used to conduct an ordinary kriging with elevation as external drift, using the R package “automap” in R version 4.0.5 (see Lutz et al., 2018). The

spatial mean isotopic signature per day was extracted from each catchment for the following transit time modelling.

2.5. Transit time modelling

The numerical model tran-SAS (Benettin & Bertuzzo, 2018) was set up for the catchments 1-5 to model water age distributions. For the simulation of age distributions of both, water and nitrate, in catchment 6 a modified version of tran-SAS was used. In the following, the tran-SAS model that was used to compute water age distributions is described, following a description of the modified version to simulate nitrate age distributions.

2.5.1. Water age model

With tracer data such as isotopic signatures of water in combination with hydrological data (precipitation, discharge and evapotranspiration), the tran-SAS model computes age distributions by using storage age selection functions (SAS). From these age distributions, median transit times and fractions of different water ages can be derived. In general, SAS functions describe how a catchment releases water since its entry via precipitation until it is released e.g. as discharge to the stream or as evapotranspiration to the atmosphere. SAS functions have been used widely in various studies to compute transit times of water in catchments (Benettin et al., 2015; Benettin et al., 2017; Hrachowitz et al., 2016; Kim et al., 2016; Rinaldo et al., 2015). SAS functions that are commonly used and parameterized are power law (Asadollahi et al., 2020; Benettin et al., 2017), beta (Drever et al., 2017; van der Velde et al., 2012) and gamma distributions (Harman, 2015; Wilusz et al., 2017). So far, there is no general agreement on which SAS function should be used, because of the complexity and variability of hydrological processes across catchments. Therefore, a common approach is to rely on a specific function that represents the observed catchment behaviour and then to estimate its parameters (Harman, 2015). For the investigated catchments, the beta distribution function against the time-variant power law function has been evaluated, which yielded in equally acceptable results of both for catchments 1- 5. Therefore, the beta distribution function was used for following water transit time modelling. Instead in catchment 6, the results of both age distribution functions differed in their model

performance, therefore the time-variant power-law function was used due to a better catchment representation. In the tran-SAS model the conceptualization of each catchment is based on a single storage $S(t)$ with a water-age balance that can be expressed as follows (Benettin & Bertuzzo, 2018):

$$S(t) = S_0 + V(t) \quad (2)$$

$$\frac{\partial S_T(T, t)}{\partial t} + \frac{\partial S_T(T, t)}{\partial T} = P(t) - Q(t) * \Omega_Q(S_T, t) - ET(t) * \Omega_{ET}(S_T, t) \quad (3)$$

$$\text{Initial condition: } S_T(T, t = 0) = S_{T_0}(t) \quad (4)$$

$$\text{Boundary condition: } S_T(0, t) = 0 \quad (5)$$

Where S_0 is the initial storage, $V(t)$ (mm) are the storage variations, $P(t)$ is precipitation (mm/d), $Q(t)$ is discharge (mm/d) and $ET(t)$ is evapotranspiration (mm/d). $S_T(T, t)$ (mm) is the age-ranked storage with S_{T_0} (mm) as initial age-ranked storage. The cumulative SAS functions are described as $\Omega_Q(S_T, t)$ for discharge and $\Omega_{ET}(S_T, t)$ for evapotranspiration.

The SAS functions can be expressed as probability density functions with regard to the normalized age-ranked storage (P_S):

$$\omega(P_S(T, t), t) = k * (P_S(T, t))^{k-1} \quad (6)$$

$$\omega(P_S(T, t), t) = k(t) * (P_S(T, t))^{k(t)-1} \quad (7)$$

$$\omega(P_S(T, t), t) = \frac{(P_S(T, t))^{\alpha-1} * (1 - P_S(T, t))^{\beta-1}}{B(\alpha, \beta)} \quad (8)$$

Where the catchment's water age preference for outflow is described by the parameters k , α and β , while $B(\alpha, \beta)$ is the two-parameter beta function. The catchment has a preference to release young water if $k < 1$, $\alpha < 1$ and $\beta < 1$. In the case of $k > 1$, $\alpha > 1$ and $\beta > 1$, the catchment tends to discharge old water. No selection preference (i.e., random sampling) is described with $k=1$, $\alpha=1$ and $\beta=1$. For stream water in catchments 1 to 5, the beta distribution SAS function (Equ. 8) was applied, while for catchment 6 the time-variant power-law function (Equ. 7) was used in the modified nitrate isotope model. Since the focus of this study is not on the water age of evapotranspiration and

due to the lack of tracer data from evapotranspiration, the time invariant power law function (Equ. 6) was applied to evapotranspiration fluxes for the completeness of the model. By this, there are four parameters to be evaluated for the catchments 1 to 5 using the fit of modelled vs. observed streamflow isotope data, i.e., α and β for stream water, k for evapotranspiration and the initial storage parameter S_0 . A spin-up period was conducted as well while the parameters length of the dataset and time how often the dataset is repeated were determined by the GLUE approach, evaluated by the Kling-Gupta-Efficiency (Gupta et al., 2009). For further information about the model structure and the imbedded SAS functions, the reader is referred to Benettin & Bertuzzo (2018). As model output, transit times of water as well as water age fractions of up to 7, 14, 28, 60 and 180 days were extracted for further analysis.

2.5.2. Nitrate age model

The nitrate transit time model is based on the water transit time model tran-SAS, because nitrate is known to be transported by water. The tran-SAS model was modified by implementing a second storage and biogeochemical equations that describe both, nitrification and denitrification (Figure 4). By using a two-storage approach which conceptualizes the catchment, the model is able to estimate the nitrate transit time since its forming until it is released to the stream. The upper storage receives water as precipitation and releases water as evapotranspiration to the atmosphere and as leaching to the routing storage. The upper storage represents the upper soil layer where nitrification takes place and from which nitrate is released via leaching to the routing storage that represents deeper soil compartments where denitrification takes place. Water is released from the routing storage as evapotranspiration to the atmosphere and as discharge to the stream which transports the denitrified nitrate.

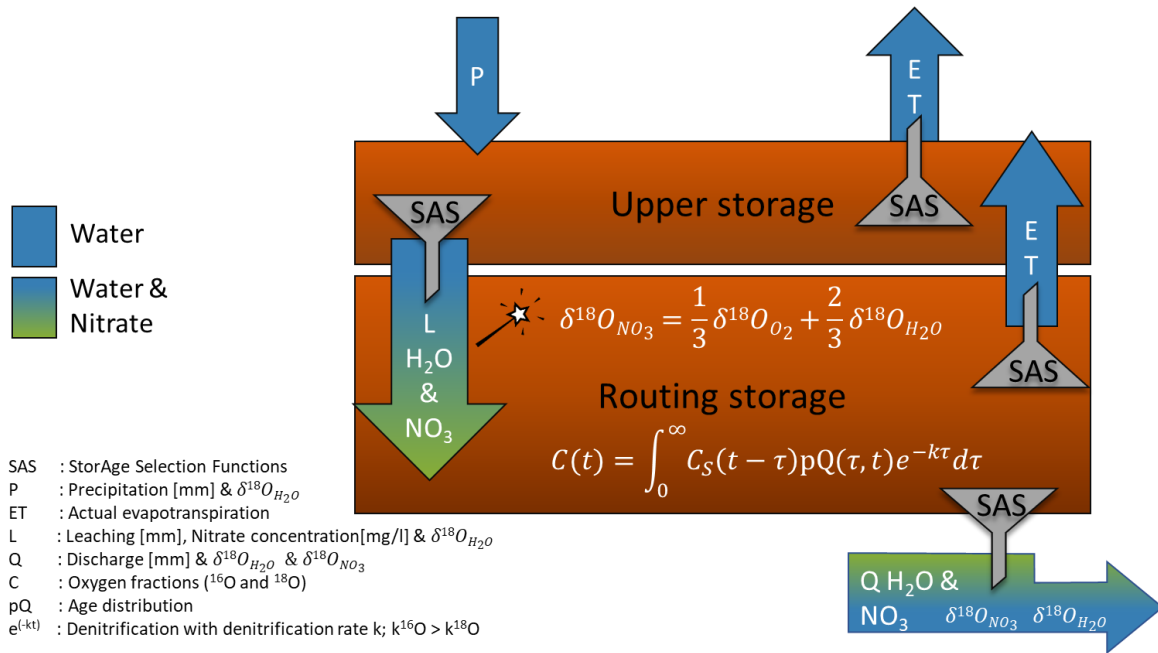


Figure 4: Conceptual nitrate isotope model with two storages and the processes (equations) that influence the isotopic signature of $\delta^{18}O\text{-NO}_3$.

The age distributions and backward transit times of both, water and nitrate, are modelled using storage age selection (SAS) functions. For leaching and discharge the power-law time-variant function (Equ. 7) was used. Since the focus of this study is not on the water age of evapotranspiration and due to the lack of tracer data from evapotranspiration, the time invariant power law function (Equ. 6) was applied to evapotranspiration fluxes of both storages for the completeness of the model. By doing so, the influence of evapotranspiration on discharge is considered in a straightforward way. By this, there are eight parameters to be evaluated for catchment 6 using the fit of modelled vs. observed streamflow isotope data, i.e., $kQ1$ and $kQ2$ for stream water, $kL1$ and $kL2$ for leaching water, k_{ET1} for evapotranspiration from the upper storage, k_{ET2} for evapotranspiration from the routing storage and the initial storage parameter $S1.0$ for the upper storage and the initial storage parameter $S2.0$ for the routing storage. A spin up period repeating the period 2013 to 2016 three times is used to minimize the effect of initial conditions. More details about tran-SAS are provided by Benettin & Bertuzzo (2018).

The tran-SAS model (Benettin & Bertuzzo, 2018) is a numerical model that is used to derive age distributions of water by using tracer concentrations such as isotopic

signatures of water. By simulating transit time distributions to describe the age composition of water and nitrate that has travelled through the routing storage, deeper insights on how the age of nitrate differs from the age of water can be gained, because usually the transit time of water is considered to be the same for solutes such as nitrate, but due to denitrification processes it is assumed that nitrate is younger than water.

To derive water and nitrate transit times, the tran-SAS model has been extended by introducing the upper and routing storage, including nitrification coupled to leaching from the upper to the routing storage, and simulating denitrification in the routing storage affecting nitrate age. The model extension is based on the assumption that nitrate is formed with water leaching from the upper storage; i.e., nitrate has the age zero when entering the routing storage. The simplified assumption that during the forming process of nitrate, the oxygen isotopic signature of the surrounding leaching water is incorporated in the nitrate, there is the ability to track the age of nitrate. This assumption is made on the basis of several studies that reported the incorporation of oxygen isotopic signatures of surrounding water into nitrate during nitrification (Boshers et al., 2019; Casciotti et al., 2011; Granger & Wankel, 2016; Griffiths et al., 2016; Kool et al., 2011). In contrast, the isotopic signature $\delta^{15}\text{N-NO}_3$ is mainly driven by nitrogen isotopic signatures of precursor nitrogen-bearing substrates like inorganic reduced nitrogen and organic nitrogen that are processed during nitrification. Therefore, the nitrogen isotopic signatures are not suitable for revealing the age information of dissolved nitrate. Using equation 9, the isotopic signature of nitrate that has been formed during nitrification can be described as follows (Boshers et al., 2019; Kool et al., 2011):

$$\delta^{18}\text{O}_{\text{NO}_3} = \frac{1}{3}\delta^{18}\text{O}_{\text{O}_2} + \frac{2}{3}\delta^{18}\text{O}_{\text{H}_2\text{O}} \quad (9)$$

With $\delta^{18}\text{O}_{\text{O}_2}$ being the isotopic signature of soil air (parameter between 22 and 29 ‰ according to Mayer et al. (2001)) and $\delta^{18}\text{O}_{\text{H}_2\text{O}}$ being the isotopic signature of leaching water.

The oxygen isotopic signature of soil air is often determined with a value of 23.5 ‰ (Boshers et al., 2019; Griffiths et al., 2016; Kendall et al., 2007, Kool et al., 2011), although the isotopic signature of soil air can vary due to different influences. Kendall et al. (2007) mentioned that the isotopic signature of soil air can be lower due to photosynthesis or higher due to respiration by microbes which is in line with findings

by Mayer et al. (2001), who observed variations of isotopic signature of soil air between 22 and 29 ‰. In this study, for reasons of simplification, the isotopic signature of soil air is set to 23.5 ‰. Initial oxygen nitrate isotope signatures fixed during nitrification may undergo an alteration that could bias the extracted age information. This alteration is related to an isotope fractionation during denitrification or a secondary oxygen isotope exchange of process intermediates (NO_x) with the ambient water (Granger & Wankel, 2016). While the potential impact of denitrification is considered in the model, a secondary exchange of oxygen isotopes is not taken into account because of the high uncertainty related to the reliable numerical prediction of that exchange in combination with multiple environmental and ecological parameters driving the exchange process. Nevertheless, the alteration of oxygen isotopic signatures by secondary isotope exchange is expected to have a minor impact on the nitrate age simulations. Therefore, for the sake of simplification, that process is neglected in the presented model.

In this study, transit time distributions (TTD) are simulated to describe the age composition of discharge and nitrate export at a daily time step (Rinaldo et al. 2015). By this, the TTD gives information about the distribution of transit times for all parcels of water and nitrate moving through the storage system. For the comparison of water and nitrate TTDs, only the routing storage is considered in this analysis, due to the fact that nitrate is only moving through the routing storage. To allow for the model being able to simulate nitrate isotopic compositions of nitrate leaching to the routing storage flowing into the system, the upper storage was implemented. The TTD for water describes how long a water parcel has travelled through the routing storage, while transit times of nitrate describe the transport time through the routing storage with consideration of the denitrification. Based on the simplified assumption that nitrate is formed with water leaching from the upper soil, nitrate has the age zero, when nitrate leaches from the upper storage to the routing storage, where denitrification happens. Denitrification with first order kinetics (Equ. 10) was implemented in the routing storage of the model. The extent of denitrification, described with first order kinetics, is determined by the TTDs of water that transports nitrate through the routing storage. The transport and denitrification for the two isotopic species of nitrate (^{16}O and ^{18}O) are simulated separately. This leads to the following expression for nitrate isotope values in the stream:

$$C(t) = \int_0^{\infty} C_S(t - \tau)pQ(\tau, t)e^{-k\tau}d\tau \quad (10)$$

Where C is the respective concentrations of the two different oxygen isotopes of nitrate (^{18}O , ^{16}O) at the catchment outlet, C_S describes the respective concentrations of ^{18}O and ^{16}O of nitrate in the routing storage per timestep, and pQ represents the transit time distribution of water that transports nitrate through the routing storage. The first order kinetics $e^{-k\tau}$ describes denitrification during transport through the routing storage, where k is the degradation rate constant and τ describes transit time. The resulting oxygen isotopic signature in the stream was calculated using Equ. 1. The nitrate concentration obtained by the nitrate isotope model is calculated by using equation 11:

$$C_{NO_3}(t) = {}^{18}O(t) + {}^{16}O(t) \quad (11)$$

With the respective concentrations of the two different oxygen isotopes of nitrate (^{18}O , ^{16}O) at the catchment outlet for each time step and C_{NO_3} as resulting nitrate concentration in mg/l.

Isotope fractionation during denitrification is determined by the isotope fractionation factor (α) (Equ. 12).

$$\alpha = \frac{k_{18O}}{k_{16O}} \quad (12)$$

The corresponding range of values for the fractionation factor and degradation rate constant of the light oxygen isotope species (k_{16O}) were taken from Granger & Wankel (2016). The range of fractionation factors was given as epsilon values ($\epsilon \approx 1000\ln(\alpha)$). The modified version of tran-SAS model only considers isotope fractionation for oxygen isotopes in nitrate. For further analysis the transit time during the routing storage of both, water and nitrate were extracted as model output.

The model is driven by time series of water and nitrate fluxes and isotopic signatures of precipitation, while oxygen isotope measurements from streamflow are used for calibration.

2.6. Model evaluation

In the following chapters, the evaluation of the water isotope model and the nitrate isotope model has been described. The performance of the water isotope model has been tested against different sampling frequencies, which is described in chapter 2.6.2.

2.6.1. Goodness of fit evaluation

The statistical method generalized likelihood uncertainty estimation (GLUE) (Beven & Binley, 2006, 2014) was applied to evaluate both model performances of 10.000 parameter sets of each catchment. The GLUE approach is a valuable tool to evaluate the parameter uncertainty and equifinality. Multiple sets of parameter values can be evaluated within the limitations that are given for a model (Beven & Binley, 2006, 2014). In this study, the 10% best simulations are selected (Table 2) considering the Kling-Gupta-Efficiency (Gupta et al., 2009) between observed isotopic signatures in stream and simulated isotopic signatures in stream (Equ. 13).

$$KGE = 1 - \sqrt{(r - 1)^2 + \left(\frac{\sigma_{sim}}{\sigma_{obs}} - 1\right)^2 + \left(\frac{\mu_{sim}}{\mu_{obs}} - 1\right)^2} \quad (13)$$

Where $\sigma_{sim/obs}$ is the standard deviation in simulation/observation, $\mu_{sim/obs}$ is the mean of simulation/observation and r is the Pearson correlation between observations and simulations. $KGE=1$ indicates perfect agreement between simulations and observations. The initial condition of the isotopic signature $\delta^{18}O$ in the storage is set to -8 ‰ for both models (and both storages in the nitrate isotope model). The mean of all 10% best simulations according to the highest KGE for water isotopic signatures in stream were selected for further analysis. In Table 2 the parameter ranges for the water isotope model are given for catchments 1 – 5.

Table 2: Water isotope model parameter ranges of the 10% best simulations according to the KGE of the water isotopic signatures in stream.

Catchment	alpha	beta	k	Initial storage	Spin-up (years)
1	0.35-0.65 [0.2-1.9]	0.30-1.89 [0.2-1.9]	0.40-0.99 [0.4-1.0]	1005-1689 [1000-1700]	1-18 [mean: 7]
2	0.48-1.44 [0.2-1.9]	0.30-0.84 [0.2-1.9]	0.40-0.70 [0.4-1.0]	531-992 [500-1000]	2-15 [mean: 7]
3	0.60-0.99 [0.2-1.9]	0.40-1.74 [0.2-1.9]	0.12-0.17 [0.1-1.0]	593-981 [500-1000]	2-12 [mean: 6]
4	0.31-1.10 [0.2-1.9]	0.22-1.85 [0.2-1.9]	0.20-0.98 [0.2-1.0]	706-1295 [700-1300]	1-6 [mean: 3]
5	0.45-0.67 [0.2-1.9]	0.48-1.49 [0.2-1.9]	0.42-0.86 [0.4-1.0]	1853-2799 [1800-2800]	1-6 [mean: 3]

In Table 3 the parameter ranges as well as a short parameter description for the nitrate isotope model in catchment 6 are given.

Table 3: Nitrate isotope model parameter ranges of the 10% best simulations according to the KGE of the water isotopic signatures in stream (amount simulations = 212).

Parameter	Parameter description	Lower boundary	Upper boundary
kL1 [-]	Time-variant power-law function parameter for leaching water	0.01	0.09
kL2 [-]	Time-variant power-law function parameter for leaching water	0.01	0.10
k_ET1 [-]	Time-invariant power-law function parameter for evapotranspiration, upper storage	0.60	0.99
S1.0 [mm]	Initial condition of the water volume in the upper storage	80	190
kQ1 [-]	Time-variant power-law function parameter for discharge	0.10	0.47
kQ2 [-]	Time-variant power-law function parameter for discharge	0.10	0.21
k_ET2 [-]	Time-invariant power-law function parameter for evapotranspiration, routing storage	0.60	0.99
S2.0 [mm]	Initial condition of the water volume in the routing storage	153	499
k_{16o}	Denitrification rate of the light oxygen isotope [day ⁻¹]	0.01	0.10
ϵ	Epsilon as fractionation factor for the isotopic signature [‰]	-5	5

2.6.2. Influence of sampling frequency

The water isotope model has thoroughly been tested of how the model performs with regard to different sampling frequencies and sampling techniques using the observed isotopic signature in stream flow as value to be fitted by the model simulated isotopic signature for the evaluation of the goodness of fit. In monitoring programs, the sampling frequency of water samples is often in ranges of fortnightly up to monthly samples (Birkel et al., 2010; Stockinger et al., 2016; Timbe et al., 2015). Precipitation is mostly taken as composite sample over the whole period, whereas stream flow is usually sampled as grab sample in the specific time step or as composite sample, covering a predefined time span (hours, days, weeks). With the high-frequency water samples that have been taken in this study, an analysis of how the sampling frequency and sampling technique affect the model results can be done. For that purpose, the time series of stream flow samples of each catchment is resampled as grab samples and as composite samples according to the chosen sampling frequency. Here, sampling frequencies of weekly, fortnightly and monthly data sets are evaluated against the daily data sets. To analyse how the model performance also selection of parameter sets is affected by using grab samples versus composite samples from stream flow during the GLUE approach, the composite samples of isotopic signatures in stream water are generated as weighted means over the chosen sampling frequency, considering the discharge volume as weight. The tran-SAS model (Benettin & Bertuzzo, 2018) has been set up with the same input for each sampling frequency to be evaluated, that means precipitation, evapotranspiration, discharge and the isotopic signature in precipitation is given as daily input as described in chapter 2.4, while the stream flow isotopic signature varies depending on the sampling frequency and sampling technique. The models have been evaluated using the same 10.000 parameter combinations gained from the GLUE approach and the KGE (Gupta et al., 2009) as model efficiency parameter (Chapter 2.6.1) to describe the goodness of fit between the observed and simulated isotopic signature in stream. The mean of the 10% best simulations of each model set up has been used for evaluation. The deviation of the model simulation based on the high-frequency stream flow data is used for comparison of the different model set ups.

2.7. Statistical analysis of model results

In the following statistical methods that are used to analyse and evaluate the model results are described. Model results from the water isotope model are analysed with regard to discharge volumes using the discharge sensitivity analysis of young water. An event separation has been conducted for catchments 1 to 5 to analyse the effect of wet and dry spells on water age metrics. The Rayleigh plot analysis is used for the analysis of denitrification indicators in catchment 6 as preparation for the nitrate isotope model.

2.7.1. Discharge sensitivity analysis of young water

To evaluate how water ages are affected by catchment characteristics and the hydrological behaviour during different flow conditions, the discharge sensitivity of young water fractions after von Freyberg et al. (2018a) and further developed by Gallart et al. (2020b) was applied. The discharge sensitivity of young water fractions (Fyw) was presented as valuable tool to investigate the hydrological behavior of different catchments with each other. In the study of von Freyberg et al. (2018a) it was shown that Fyw react sensitive to increasing discharge, while each catchment was affected differently by the discharge. Due to these findings, the Fyw-discharge sensitivity was introduced as indicator to describe catchment specific water age dynamics. This method was developed further by Gallart et al. (2020b), using an exponential equation (Equ. 14) to describe the relationship between Fyw and discharge by fitting the parameters F_0 and S_d of the exponential equation to the estimated Fyw of each catchment.

$$Fyw(Q) = 1 - (1 - F_0) * \exp(-Q * S_d) \quad (14)$$

With F_0 as virtual Fyw for discharge (Q) being zero and S_d (unit of Q^{-1}) as a new discharge sensitivity metric (Gallart et al., 2020b). Gallart et al. (2020b) showed that an exponential equation is necessary to describe the relationship between Fyw and discharge with the consideration that Fyw cannot be above one even when discharge rises infinitely. Nevertheless, for low discharges the curve approximates a linear line (Gallart et al. 2020b). In comparison to that the discharge sensitivity presented by von

Freyberg et al. (2018a) was described by a linear equation which led to F_{yw} above 1 in the case of strong increasing discharge. Still, the discharge sensitivity metric S_d of von Freyberg et al. (2018a) equals the discharge sensitivity metric of Gallart et al. (2020b) as long as F_{yw} is lower than 1. In the studies of von Freyberg et al. (2018a) and Gallart et al. (2020b) F_{yw} were derived from the approach after Kirchner (2016a, 2016b) using the ratio between the amplitudes of sinusoidal curves that were fitted to observed stream flow isotopic signatures and precipitation isotopic signatures. Even though the approach after Kirchner (2016a, 2016b) is a widely used tool to estimate F_{yw} , the daily variation of F_{yw} cannot be described with this method. Therefore, the tran-SAS model was used in this study to compute daily F_{yw} of different water age thresholds (7, 14, 28, 60 and 180 days). The different water age thresholds were implemented to reflect water age distributions during short term events (F_{yw7} – Fraction of water with an age up to 7 days) and to be able to compare general catchment water age distributions with an age up to 60 days (F_{yw60}) with F_{yw} from other studies that are commonly described as water with an age between 60 and 90 days (Kirchner, 2016a, 2016b). For the investigation of the sensitivity of young water release in catchments as a function of discharge, the F_{yw7} and F_{yw60} were used. By using a non-linear analytic Gauss-Newton algorithm to fit Equ. 14 to the F_{yw7} and F_{yw60} obtained from the tran-SAS model, the parameters F_0 and S_d were estimated. The daily data of F_{yw7} and F_{yw60} showed a scatter that was not able to be represented by the exponential equation Equ. 14, therefore the discharge was separated into 10% percentiles to cover different discharge intensities (from low flows to high flows).

2.7.2. Event separation based on discharge

To analyze the differing water age behavior in hydrologically varying periods, the runoff time series is separated into dry and wet spells. Dry spells are defined as periods with low flow conditions, and wet spells as periods with high flow conditions. There are two common approaches to separate discharge time series. The first is a simple threshold approach categorizing periods above the threshold as wet spells, and periods below the threshold as dry spells (Lang et al., 1999; Sikorska et al., 2015). This approach has the disadvantage that parts of the same rainfall-runoff event may belong to dry spells (e.g. start of the rising limb, end or the recession), while other parts may be categorized

as wet spells. For highly seasonal regimes, where seasonal variance in runoff is higher than the variance between rainfall-runoff events and no events, the threshold approach may only be able to classify according to the seasons. A second approach is a classical baseflow filtering approach, where all periods with direct flow components (i.e. rainfall-runoff events) are classified as wet spells (Ladson et al., 2013; Merz et al., 2006). This approach usually tends to lead to very short events. In this study a combination of both approaches is used. In a first step, single rainfall-runoff events were identified following the baseflow separation approach of Lyne and Hollick (1979) using R package hydroEvents (Kaur et al., 2017; Ladson et al., 2013; Tang & Carey, 2017). In a second step, all events with a peak flow in discharge higher than long-term median peak flows were categorized as wet spells, while periods with peak flows under the threshold belong to the category dry spells. By this, each catchment has an individual threshold value for wet spells corresponding to its median peak flow. No event periods were also categorized as dry spells. This approach tends to generate longer contiguous periods of dry and wet spells, while still accounting for single rainfall-runoff events.

Wet spells and dry spells were gained from the time series 2013 to 2021, except for the catchment 4, which covers only the years 2020 to 2021. The relation between water age metrics (median transit time, fractions of different water ages) and catchment characteristics, such as land use share, elevation, slope and some more, of the different catchments were analyzed statistically. To understand how recent precipitation, in particular, affects the stream water age composition, the fraction of water with an age up to 7 days (Fyw7) was investigated in more detail in relation to catchment characteristics.

2.7.3. Rayleigh plot analysis for denitrification indicators

To evaluate the occurrence of microbial activity such as denitrification, the Rayleigh plot can be used. Isotopic enrichment during denitrification can be expressed by a simplified Rayleigh equation (Equ. 15):

$$\delta^{15}N_t = \varepsilon \ln \left(\frac{C_t}{C_{max}} \right) + \delta^{15}N_{C-max} \quad (15)$$

In a strict sense, the application of the Rayleigh equation is valid for closed system conditions only. In open system conditions, as most likely present at the study site,

concentration changes may not only be attributed to biological nitrate degradation but also to flow-related phenomena such as mixing or dilution. Therefore, where ε is the isotopic enrichment factor, C_t expresses the nitrogen isotopic composition and nitrate concentration at any time step and max refers to the highest measured concentration and the isotopic composition determined at that particular timestep.

3. Results and discussion

The following chapters are separated in results and discussion of measured data of water isotopic signatures, following the results and discussion of the water isotope model. Thereafter, the analysis of the discharge sensitivity of young water fractions is presented and discussed. The hydrological events that are categorized as wet and dry spells are further presented and discussed in section 3.5, following the analysis of catchment characteristics with respect to hydrological events. The results of the observed hydrological and nitrate concentration data are presented in chapter 3.7, following the analysis of the model simulations of the nitrate isotope model.

3.1. Monitored water samples

The sampling frequency of measured isotopic signatures differs from sub-daily to monthly data. In Figure 5 the different sampling frequencies for precipitation and discharge are shown. For catchments 1-3 and 5, isotopic signatures of precipitation were available from further studies in a monthly sampling resolution (Lutz et al., 2018; Müller et al., 2018; Wollschläger et al., 2016). The installation of the autosamplers to collect daily and sub-daily water samples was conducted in 2018 in catchment 5 and 2020 in catchments 1-3. In catchment 4, manual samples have been taken in a daily resolution since the end of 2019. Since 2020 some sub-daily sampling campaigns have been conducted in catchments 1-3 and 5 ranging between 4 and 8 hours (Figure 5: green = 4h, light blue = 6h, dark blue = 8h).

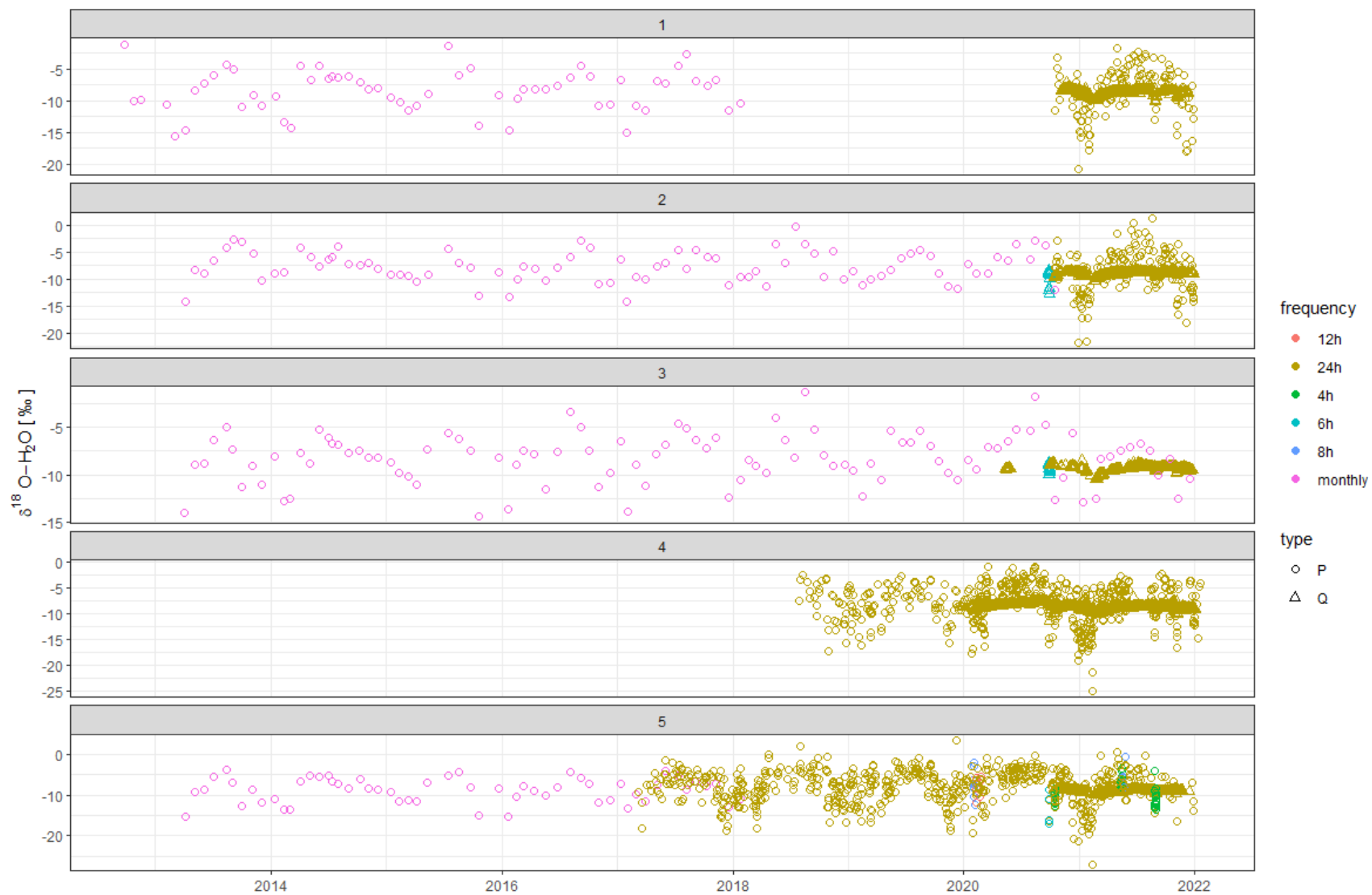


Figure 5: Collection of isotopic signatures of water for both, precipitation and discharge, in catchments 1-5.

3.2. Sampling frequency affects the model simulation

An investigation about the sampling frequency and sampling technique is conducted to get deeper insights about how the model performance is affected by sampling strategies. As found by Birkel et al. (2010) the model set up of a lumped-conceptual flow-tracer model with daily data compared to weekly or fortnightly data is beneficial for the conceptualization and calibration of the model. Therefore, the tran-SAS model has been tested against different sampling frequencies. The tran-SAS model has been set up for catchments 1 to 5 as water isotope model to simulate isotopic signatures in stream flow with fixed input data, but varying observed isotopic signatures in stream flow for the evaluation of model performance. With lower sampling resolutions the Kling-Gupta-Efficiency as goodness of fit parameter between the measured isotopic signature in stream flow and the simulated isotopic signature in stream flow is increasing (Table 4). Considering the increasing KGE value with lowered sampling resolutions can lead to the assumption that the model performance becomes better with lower resolutions of evaluation data which was also found in the study of Birkel et al. (2010). In fact, comparing model simulations based on daily measured isotopic signatures in stream with model simulations based on lower sampling frequencies yield a notable deterioration of the model performance (Figure 6 and Table 5). As described by Timbe et al. (2015), the better simulation statistics for lower resolutions such as monthly data, compared to finer data resolutions are caused by the fact that less data are involved in the evaluation of the model performance.

Table 4: KGE values of the different sampling frequencies and sampling techniques with minimum, maximum and the mean in brackets.

Catchment		1	2	3	4	5
Daily	Grab	0.65 - 0.72 [0.66]	0.48 - 0.53 [0.49]	0.63 - 0.71 [0.65]	0.68 - 0.75 [0.71]	0.71 - 0.79 [0.75]
	Com- posite	0.64 - 0.71 [0.66]	0.53 - 0.66 [0.57]	0.73 - 0.81 [0.76]	0.74 - 0.83 [0.77]	0.71 - 0.79 [0.75]
Weekly	Grab	0.72 - 0.79 [0.76]	0.65 - 0.71 [0.67]	0.73 - 0.81 [0.75]	0.71 - 0.70 [0.74]	0.74 - 0.83 [0.78]
	Com- posite	0.74 - 0.80 [0.77]	0.73 - 0.81 [0.75]	0.74 - 0.83 [0.78]	0.78 - 0.86 [0.81]	0.76 - 0.84 [0.79]
Fort- nightly	Grab	0.68 - 0.76 [0.69]	0.65 - 0.71 [0.67]	0.68 - 0.76 [0.70]	0.75 - 0.84 [0.78]	0.77 - 0.85 [0.80]
	Com- posite	0.75 - 0.82 [0.77]	0.60 - 0.72 [0.66]	0.78 - 0.86 [0.79]	0.77 - 0.86 [0.80]	0.81 - 0.90 [0.85]
Monthly	Grab	0.65 - 0.72 [0.69]	0.68 - 0.74 [0.70]	0.69 - 0.76 [0.72]	0.83 - 0.92 [0.86]	0.76 - 0.85 [0.79]

Focusing on the comparison between daily sampling frequency and the lower resolutions such as fortnightly and monthly samples, the analysis revealed high deviations of fortnightly and monthly sampling frequencies of composite and grab samples in most of the catchments (Table 5). Weekly samplings show more often low deviations from the daily simulation, whereas weekly composite samples are more likely matching the same good parameter combinations as daily grab samples. These findings show that evaluating and calibrating a model based on daily observations is more accurate even though the goodness of fit function is low (Birkel et al., 2010). The scenario that low-frequency calibration data results in similar good parameter sets as high-frequency data is seldom and should be considered as infrequent luck of very precisely selected parameter ranges. In this study, the suitable parameter ranges and parameter sets have been gained from the daily data. For the analysis of the effect of sampling frequencies, these parameter sets have been used to evaluate if lower sampling resolutions are able to capture the same good parameter sets as possible with high-frequency data. As described by Benettin et al. (2020), Gallart et al. (2020a) and Stevenson et al. (2021), the sampling frequency influences the modelling results. Therefore, weekly data can provide information about weekly water age metrics, but

not about higher resolutions such as daily time steps. For the analysis of daily water age metrics, daily input data is needed. As a result, further modelling set ups are carried out based on the high-frequency data, to be able to analyse daily results of the simulations.

Comparing the deviation of grab samples and the deviation of composite samples, results in similar ranges and it depends on the catchment and the parameterization which samples technique is able to capture the parameter sets that are closest to the parameter set derived from daily simulations and observations. For weekly and fortnightly sampling frequencies, composite samples have lower deviations than grab samples. Even though, daily monitoring of isotopic signatures results in the best model behaviour, studies that are restricted to low sampling frequencies because of sampling management and/or costs, should consider to collect composite samples instead of grab samples.

Table 5: Deviation between the simulated isotopic signature in a daily sampling frequency versus the respective sampling frequencies (weekly, fortnightly, monthly), values given as percent bias (%).

Catchment	Weekly		Fortnightly		Monthly	
	grab	composite	grab	composite	grab	composite
1	0.00	0.00	0.80	4.10	4.60	4.10
2	2.80	0.00	4.80	1.80	3.90	0.00
3	0.00	0.00	8.40	0.00	5.70	9.20
4	8.40	8.40	8.40	2.80	1.80	6.50
5	5.10	5.10	8.60	7.40	0.00	8.50

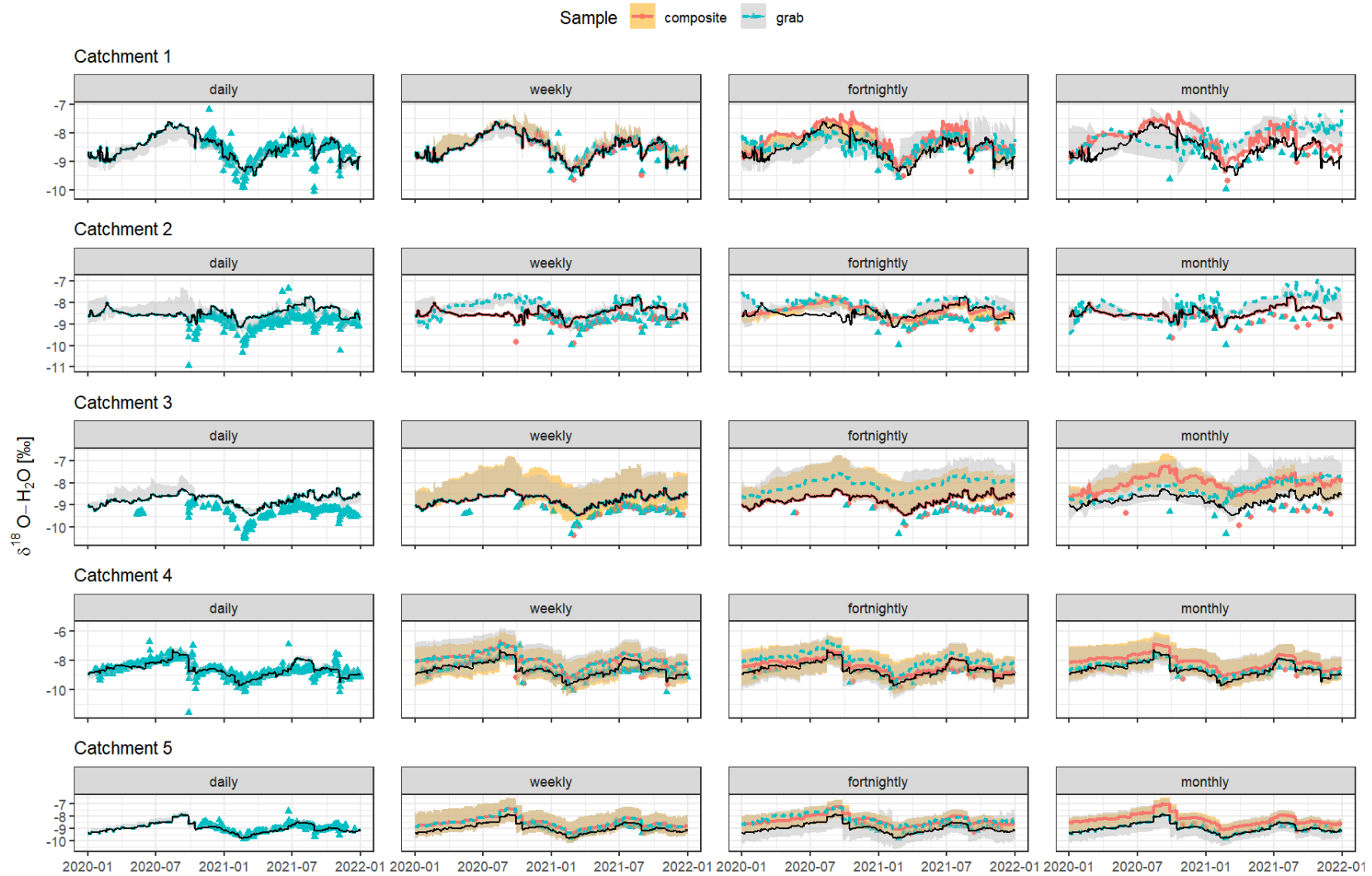


Figure 6: Model results (lines) and observed data (points and triangles) of different sampling frequencies and sampling techniques (composite samples = dots versus grab samples = triangles) in comparison for catchments 1 to 5.

3.3. Water age modelling

The model was able to simulate the overall pattern of measured isotopic signatures with a good to acceptable agreement (Figure 7). Moreover, it showed varying contributions of the fraction of three categories of water ages during the simulation period. Here, the focus is on the fraction of young water up to 7 days (<7 days) highlighting water flow through fast flow paths, the fraction of water up to 180 days and water older than 180 days, representing water that was stored in the catchments and/or travelled along slow flow paths (Figure 7). The fraction of young water up to 7 days (<7 days) is highest in the hilly anthropogenic catchment (catchment 1; mean: 0.065 ± 0.04 or 6.5 %) and lowest in the pristine forested headwater catchment (catchment 3; mean: 0.032 ± 0.03 or 3.2 %), considering the mean of all best simulations and the whole time series. In the forested hilly catchment (catchment 5), the contribution of water older than 180 days (>180 days) is highest compared to the other catchments (mean: 0.75 ± 0.03 or 75 %), which is also reflected by high median transit times (see Figure 10). The hilly anthropogenic and the anthropogenic catchments (catchments 1 and 2, respectively) as well as the agriculturally dominated catchment (catchment 4) have similar proportions of different water ages. The water age contributions of the mountainous agricultural dominated catchment (catchment 4) are in similar ranges as from the hilly anthropogenic (catchment 1) and the anthropogenic (catchment 2) catchments.

The performance of simulated isotopic signature by tran-SAS is shown in Figure 7, in which the black line shows the mean of all best simulations and the red area reflects the variability of all best simulations. For the catchments 1 (hilly, high anthropogenic impact), 4 (mountainous agriculturally dominated), and 5 (forested, hilly), the simulations match the observed values (grey dots in Figure 7), which is reflected by high KGE values ($KGE = 0.65 - 0.79$) and low absolute biases (absolute bias = $-0.09 - 0.09$). The 10% best simulations for the catchment 3 (pristine forested headwater catchment) show KGE values ranging from 0.63 to 0.71 but larger biases (absolute bias = $-0.58 - 0.49$), while for catchment 2 (high anthropogenic impact), the KGE is lower ($KGE = 0.48 - 0.54$) and the bias is visibly higher (absolute bias = $-0.48 - -0.25$). In catchments 3 and 5 the model tends to overestimate isotopic measurements.

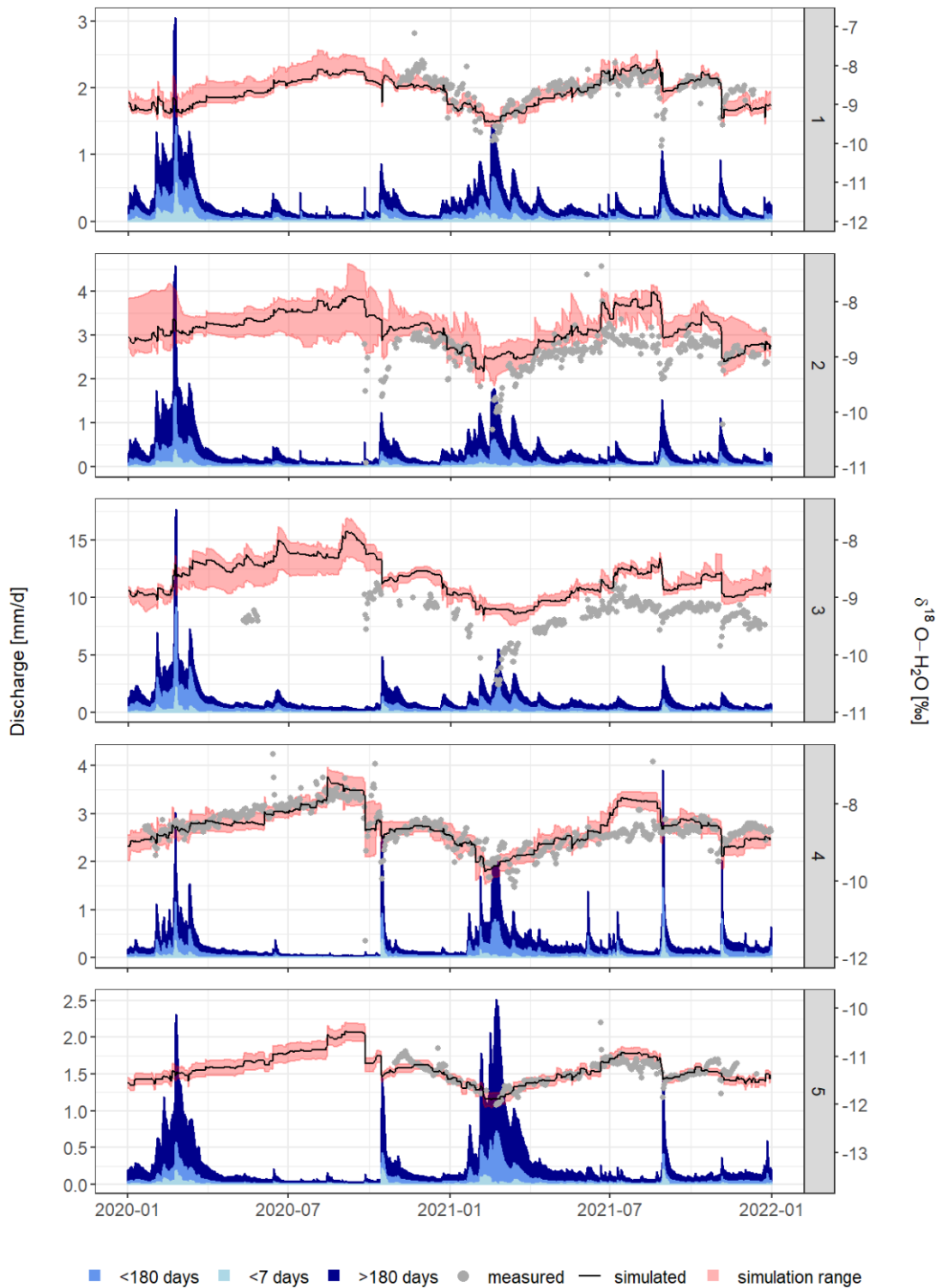


Figure 7: Discharge with the different fractions of water age in light blue (water age up to 7 days), medium blue (water age up to 180 days) and dark blue (water age more than 180 days) for the five investigated catchments; the measured isotopic signature of discharge is shown as grey dots, while the simulated isotopic signature of discharge gained from the tran-SAS model is shown as black line; the range of simulated stream isotopic signature from the 10% best simulations is shown as red shading.

3.4. Sensitivity of young water fractions to discharge

Figures 8 and 9 display the discharge sensitivity according to Equ. 14 as black line in each plot, showing a positive slope for each catchment. The goodness of fit between Equ. 14 and the discharge quartiles is evaluated using the coefficient of determination, which shows general agreement for all catchments (R^2 ranging between 0.65 and 0.85). With increasing discharge percentiles, the F_{yw60} increases as well, but in different intensities for each catchment. S_d as discharge sensitivity metric (Gallart et al., 2020b) is highest in the hilly catchment with high anthropogenic impact (catchment 1; $S_d = 0.067$) and lowest in the hilly forested catchment (catchment 5; $S_d = 0.024$). The discharge sensitivity of the investigated catchments yielded similar ranges as found in von Freyberg et al. (2018a) and Gallart et al. (2020b) (Table 6).

Table 6: Values for F_0 and S_d and their standard deviation obtained from Gauss-Newton fitting algorithm using Equ. 14 for $F_{yw7}(Q)$ (water with an age up to 7 days) and $F_{yw60}(Q)$ (water with an age up to 60 days).

Catchment	Fyw7(Q)		Fyw60(Q)	
	F_0	S_d	F_0	S_d
1	0.043 ± 0.002	0.067 ± 0.005	0.208 ± 0.005	0.069 ± 0.014
2	0.032 ± 0.002	0.036 ± 0.003	0.152 ± 0.006	0.051 ± 0.011
3	0.006 ± 0.001	0.019 ± 0.001	0.092 ± 0.015	0.064 ± 0.010
4	0.034 ± 0.004	0.058 ± 0.011	0.170 ± 0.007	0.087 ± 0.023
5	0.032 ± 0.001	0.028 ± 0.003	0.136 ± 0.002	0.024 ± 0.006

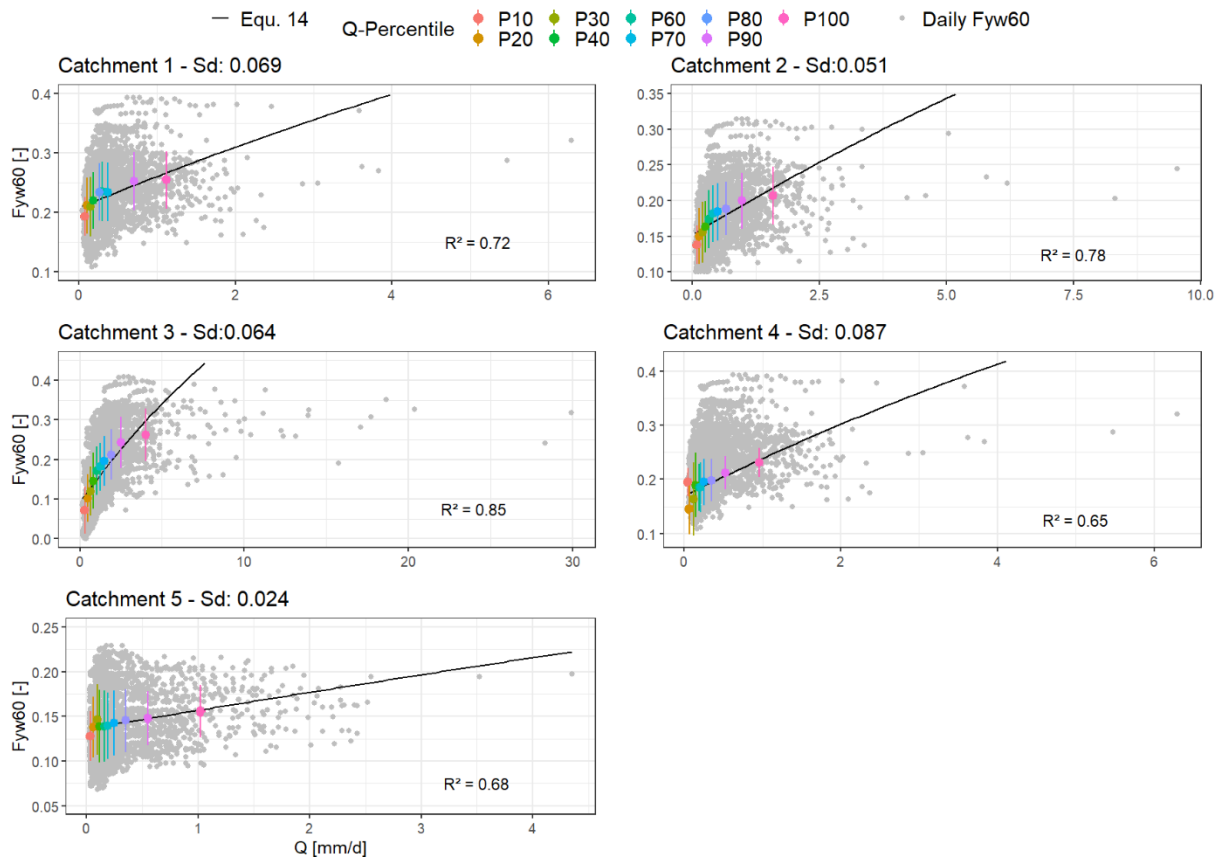


Figure 8: Relationship between discharge and the fraction of water with an age up to 60 days (F_{yw60}) with the median discharge (Q [mm/d]) from each percentile and the mean F_{yw60} as well as its standard deviation from each Q-percentile for the whole time series; F_{yw60} of discharge percentiles (P10-P100) are represented as coloured points with standard deviation, while the black line represents Equ. 14 to describe the discharge sensitivity (S_d) of the F_{yw60} ; the coefficient of determination (R^2) describes the fit of Equ. 14 to the coloured dots.

Considering F_{yw7} (Figure 9), the discharge sensitivity of catchments 1 to 4 is lower compared to the discharge sensitivity of F_{yw60} (Figure 8). In catchment 5, the discharge sensitivity of both water age fractions are in a similar range. For some catchments (i.e., hilly anthropogenic catchment 1 and forested, hilly catchment 5) the difference of the discharge sensitivities of both fractions of water is small, while for other catchments the difference of the discharge sensitivities is large (pristine forested headwater catchment 3). This means that the F_{yw7} is generally less affected by

discharge than Fyw60, and the magnitude of the difference between S_d for Fyw7 and S_d for Fyw60 depends on the catchment. Catchments that were characterized by a hilly landscape showed a small difference of the discharge sensitivities between Fyw7 and Fyw60, while the catchment with the highest discharge showed the largest difference of discharge sensitivities between Fyw7 and Fyw60. Based on these differences in discharge sensitivities, the focus is on further investigating the catchment's characteristics and their relationship to young water (Fyw7 and Fyw60) in a separate chapter (Chapter 3.6).

While Equ. 14 and the discharge sensitivity metric S_d give information about the average behavior of the fractions of different water ages of each catchment, the daily Fyw7 and Fyw60 values (grey dots in Figure 8 and Figure 9) give the opportunity to evaluate their variations with respect to discharge. Most of the catchments show similar patterns: they have discharge sensitivities of Fyw60 which do not differ strongly across catchments, considering the standard deviation (Table 6) (Catchments 1, 2, 3, 4). The anthropogenic catchment (catchment 2) and the pristine forested headwater catchment (catchment 3) show steeper slopes for Fyw60 than for Fyw7, which indicates that Fyw60 is more sensitive to discharge than Fyw7 in these catchments. Catchments with steep slopes of Fyw60 but lower slopes for Fyw7 can be catchments that release water from previous precipitation events (Fyw7) more uniformly, but with increasing discharge young water with an age up to 60 days is released more dominantly. Benettin et al. (2015) found that more young water is released to the stream during storm events, which complements the results of this study of increasing Fyw60 during increasing discharge. The finding that Fyw60 is more sensitive to discharge than Fyw7 in some catchments might result from a varying degree of connectivity of deeper water storages, which causes the contribution of different water fractions to vary over time especially for Fyw60. Water that fell during previous precipitation events is less affected by discharge because its contribution to overall discharge is low compared to that of water with an age up to 60 days. Moreover, surface storages that contain water that infiltrated after recent precipitation events and stayed in the storage for longer time (e.g., up to 60 days) can be flushed out as long as some part of the storage containing that water is connected to the discharging flow path. Hence, various Fyw60 values are obtained (depending on the degree of connectivity) for a larger range of discharge values. In contrast, very young water can only be discharged during high-connectivity conditions and if rainfall is followed by a

runoff event shortly after (e.g., within 7 days). Considering the daily Fyw60 and Fyw7, the catchment 5 (hilly, forested) shows a more distributed pattern of the daily Fyw7 and Fyw60 values than the other catchments. The high day-to-day variability of different young water fractions indicates that this catchment is more affected by climatic conditions such as dry periods, during which the connectivity of water storages and water pathways is low. As a result, more young water (both Fyw7 and Fyw60) is released during high flows after prolonged dry conditions. These findings lead to a further investigation about wet spells with high flow conditions and dry spells with low flows conditions in the following sections.

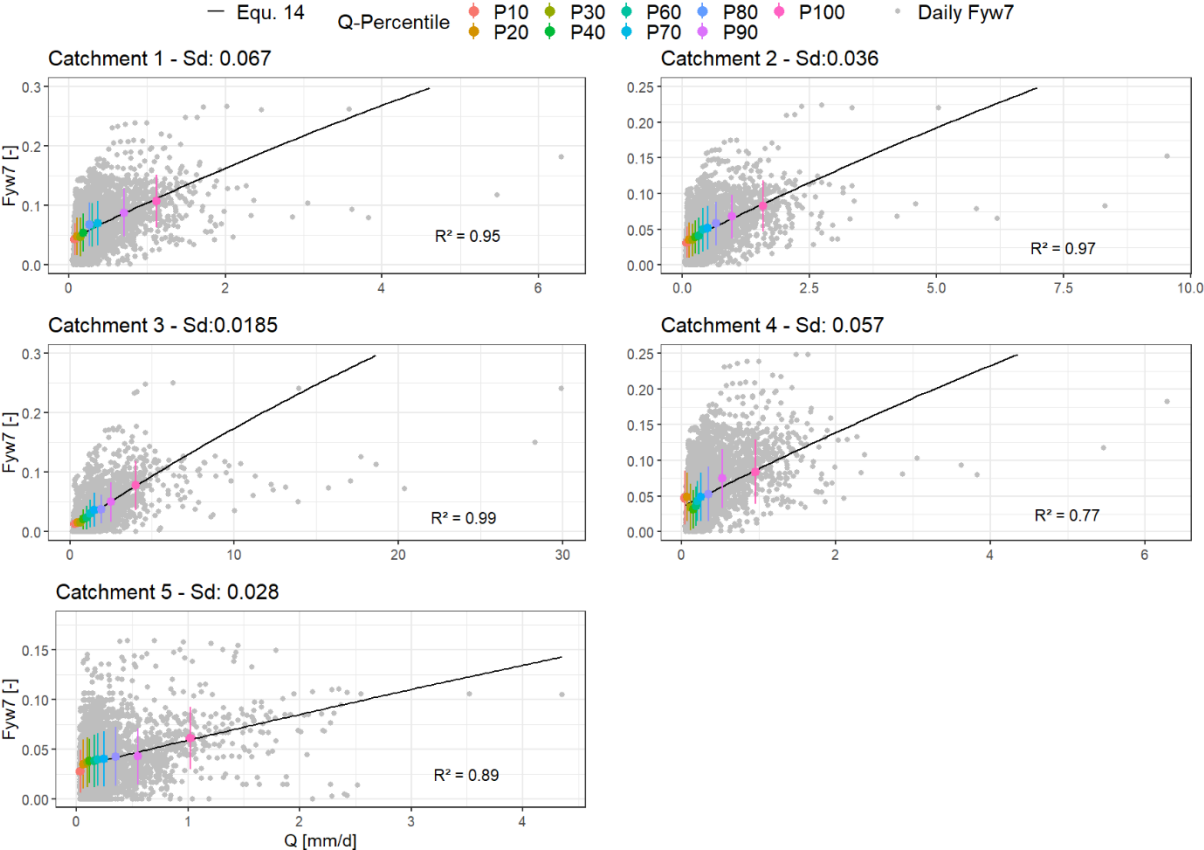


Figure 9: Relationship between discharge and the fraction of water with an age up to 7 days (Fyw7) with the median discharge (Q [mm/d]) from each percentile and the mean Fyw7 as well as its standard deviation from each Q-percentile from the whole time series; Fyw7 of discharge percentiles (P10-P100) are represented as coloured points with standard deviation, while the black line represents Equ. 9 to describe the discharge sensitivity (S_d) of the Fyw7; the coefficient of determination (R^2) describes the fit of Equ. 14 on the coloured dots.

3.5. The effect of hydrologically varying periods on discharge age distributions

The discharge sensitivity analysis showed that both Fyw7 and Fyw60 are sensitive to discharge, albeit to a different extent. To better understand how fractions of different water ages are affected during low flows and high flows and to highlight hydrologically varying periods, the time series was separated into dry and wet spells according to their discharge as described in section 2.7.2. The results of this separation and the differences in the number of wet spells are shown in Table 7 for each catchment.

Table 7: The number of wet spells in total and the mean duration [days] of wet spells during the years for the investigated catchments.

Catchment	1		2		3		4		5	
	Wet Spell	Mean duration	Wet Spell	Mean duration	Wet Spell	Mean duration	Wet Spell	Mean duration	Wet Spell	Mean duration
	No.	days	No.	days	No.	days	No.	days	No.	days
Total	43	-	36	-	28	-	10	-	53	-
Mean	5	74	4	90	3	97	5	65	6	50
2013	2	132	1	152	1	117	-	-	4	60
2014	7	65	7	77	4	103	-	-	11	28
2015	5	56	4	100	3	77	-	-	5	45
2016	5	72	4	72	4	97	-	-	7	39
2017	6	64	6	64	4	95	-	-	6	53
2018	4	80	3	111	2	144	-	-	4	64
2019	4	55	3	85	3	96	-	-	5	31
2020	6	58	5	60	4	71	4	70	3	55
2021	4	84	3	87	3	71	6	60	6	74

The mean median transit times (TT50) of all simulations across the study period varies strongly for the different catchments (Figure 10). Whereas TT50s are the smallest in the hilly anthropogenic catchment (catchment 1) and the pristine forested headwater catchment (catchment 3) with 150 to 450 days, the highest TT50s occur in catchment 5 (forested, hilly) (between 600 and 1000 days). The anthropogenic catchment (catchment 2) and the mountainous agriculturally dominated catchment (catchment 4) are in the middle of the distribution, covering TT50s of between 300 and 600 days. In general, the TT50s are smaller during wet spells compared to dry spells for the catchments of this study, which was also found by studies in other catchments (e.g. Benettin et al., 2015). This illustrates the higher contribution of young water during wet

spells compared to dry spells. The fractions of young water complement this observation by showing a higher Fyw of up to 7 days during wet spells for all the catchments, compared to dry spells and the time series in general. This behavior of more young water holds for all Fyw metrics investigated (i.e., water with an age of up to 14, 28, 60 and 180 days; Figure 10).

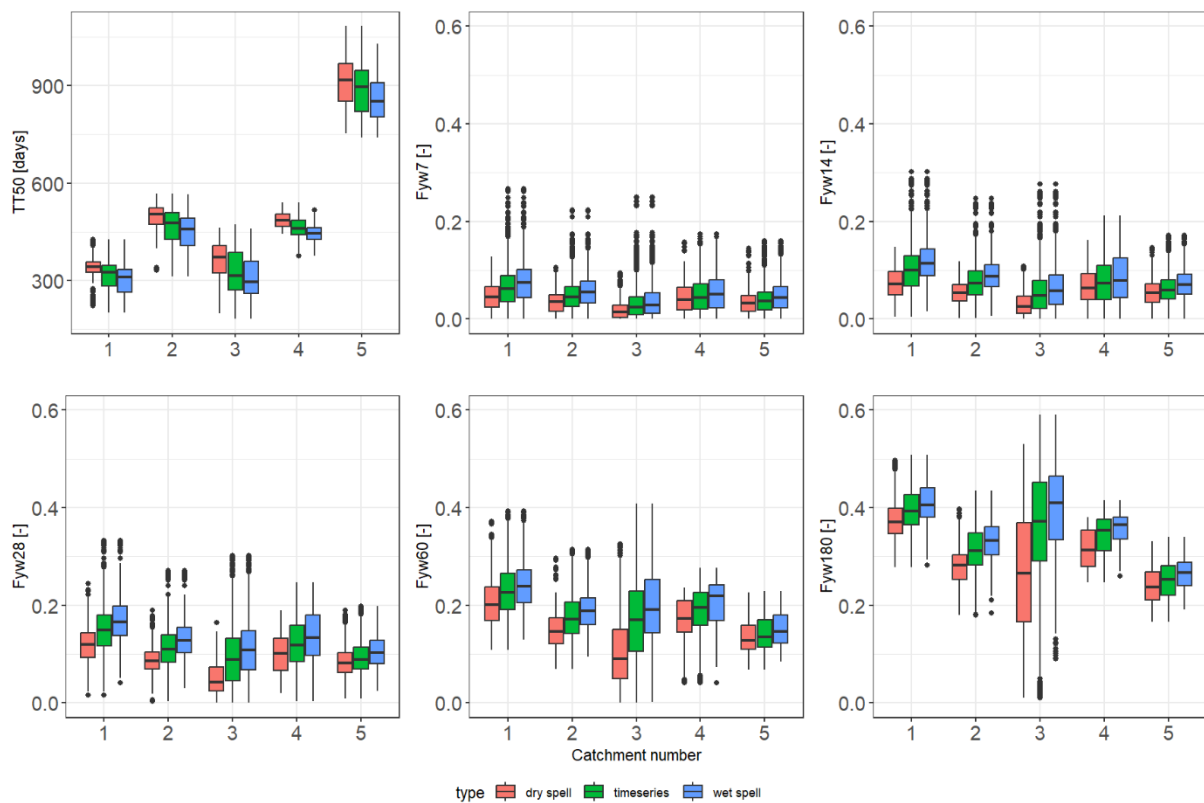


Figure 10: The age metrics ($TT50$ and $Fyw7-180$) for each catchment during dry spells (red), the whole time series (green) and wet spells (blue).

The higher proportion of young water during wet spells as seen in Figure 10 becomes also apparent in the different seasons (Figure 11 and Figure 12). All catchments show significantly higher contributions of young water up to 7 days during wet spells compared to dry spells during all seasons ($p < 0.05$), except for the mountainous agriculturally dominated catchment (catchment 4) where there is no significant difference between spring and autumn. During summer and in some cases during autumn, the relative contribution of Fyw7 to overall discharge is significantly larger than during the other seasons ($p < 0.05$), except for the hilly catchments 2 and 4 where no significant difference can be found between summer and winter periods. Moreover, the

pristine forested headwater catchment (catchment 3) does not show a significant difference between summer and spring. Especially catchment 5 (forested, hilly) shows larger Fyw7 values during summer and autumn with a significant difference ($p < 0.05$) to spring and winter. The mountainous agriculturally dominated catchment (catchment 4), which has the shortest simulation and measurement time series (2020-2021, 2 years), shows a somewhat different pattern with only small differences between the three categories during spring and autumn. In summer and winter, on the contrary, Fyw7 shows the same pattern as in all the other catchments. Considering the time series, Fyw7 is lowest for most of the catchments during spring, while Fyw7 is highest during winter. During summer and autumn, the distribution of Fyw7 is similar across all catchments (see green boxplots in Figure 11).

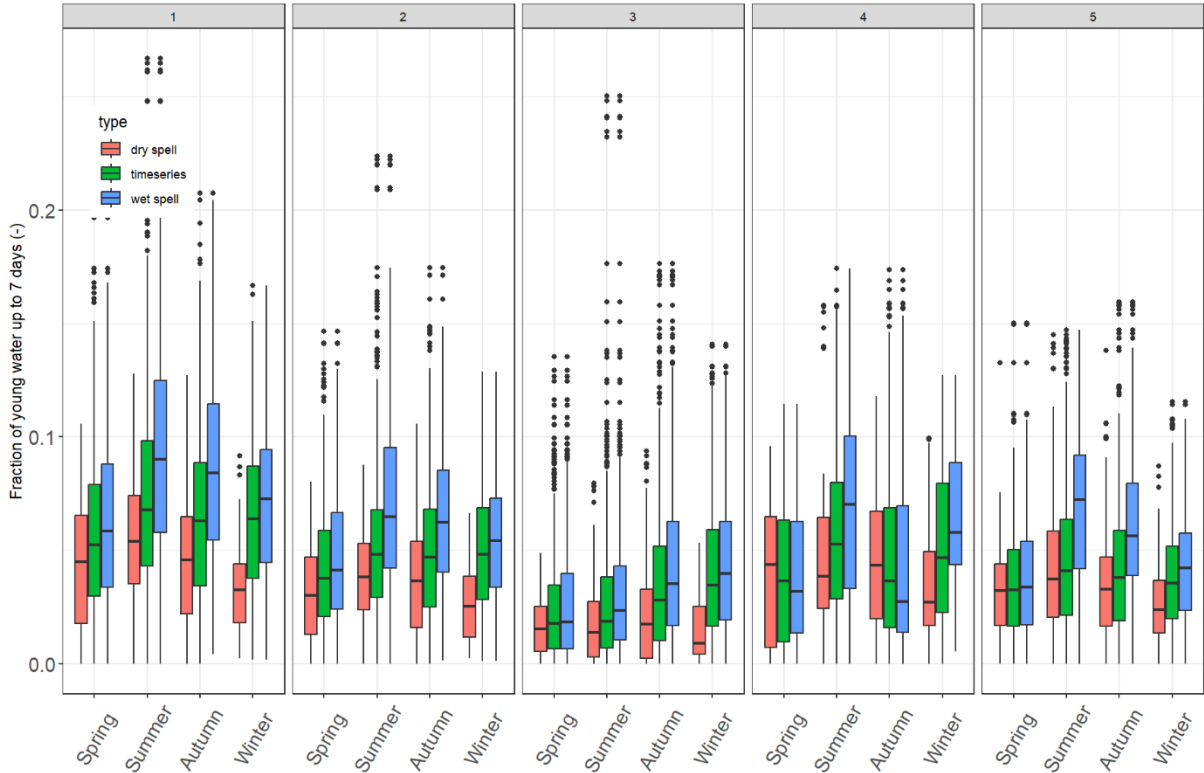


Figure 11: Focusing on the Fyw7 (Fractions of young water up to 7 days), boxplots are plotted for dry spells (red), time series (green) and wet spells (blue) during the seasons (Spring, Summer, Autumn and Winter).

For four out of five catchments, a significant difference ($p < 0.05$) between the seasons is obvious with respect to Fyw60 (Figure 12). The anthropogenic catchment (catchment 2) does not show a significant difference of Fyw60 between the seasons summer and autumn for wet spells, while the mountainous agriculturally dominated catchment (catchment 4) does not show a significant difference of Fyw60 between spring and winter for both wet and dry spells. This implies that catchment 4 has similar sources of water during winter and spring. Likewise, for wet spells in summer, the Fyw60 does not differ significantly from wet spells during spring in the same catchment supporting the assumption that similar water sources are active during these periods. Considering that catchment 4 has the shortest observation period, which started in 2020 after the drought years 2018 and 2019, it is most likely that the seasonal differences in Fyw60 that can be seen in the other catchments become apparent because of the longer observation periods that reveal a broader range of different climatic conditions and a more systematic perspective compared to catchment 4. In the anthropogenic catchment (catchment 2), the difference between Fyw60 of dry spells during spring and autumn is not significant.

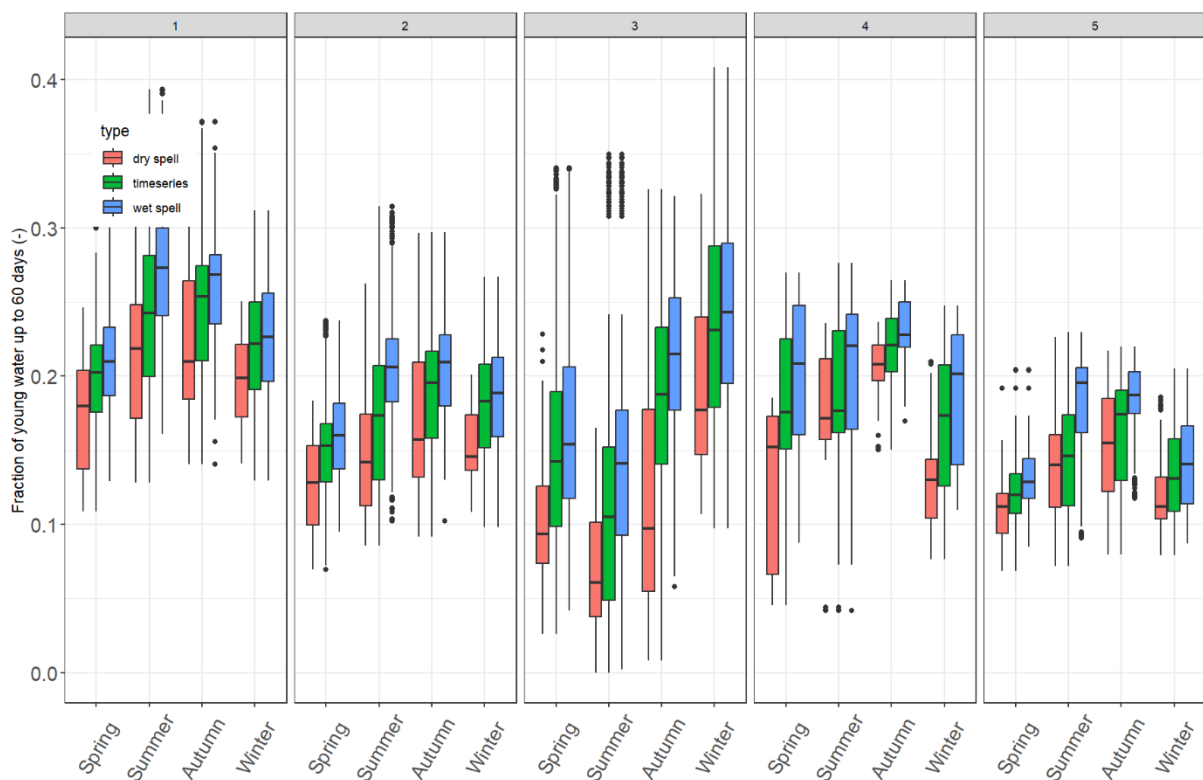


Figure 12: Focusing on the Fyw60 (Fractions of young water up to 60 days), boxplots are plotted for dry spells (red), time series (green) and wet spells (blue) during the seasons (Spring, Summer, Autumn and Winter).

In agreement with a conceptual perspective, the findings of this study match the common expectations that higher contributions of young water (Fyw7 and Fyw60) were found for wet spells than for dry spells. While this behavior was occurring throughout the time series from 2013 to 2021 for all the five catchments that have been investigated, a much higher contribution of Fyw7 during summer high flows was found for catchment 5. In the forested, hilly catchment (catchment 5), Fyw7 was higher compared to the other seasons, which indicates that high discharge during summer is mainly fed by recent precipitation events. These observations are in line with findings from other studies (Brown et al., 1999; Lee et al., 2020). Brown et al. (1999) investigated five summer rain events in seven different catchments with the aim to evaluate the storm runoff components and the effect of catchment size on water sources. Using a two-component hydrograph separation to analyze the contribution of water sources during rain events, they were able to show that there were high event water contributions to stormflow for the most intense event and that during dry periods, event water is a major contributor to stormflow.

3.6. Catchment characteristics influence the discharge age distribution

A comparison of the relationship between different land use types (agriculture, forest, grassland and urban) and Fyw7 revealed trends for agriculture and grassland depending on their relative proportions (Figure 13). With increasing agricultural land use share, the Fyw7 increases significantly ($p < 0.05$, $R^2 = 0.72$; Figure 13) while the Fyw7 increases when the proportion of grassland decreases in catchments ($p > 0.05$, $R^2 = 0.81$; Figure 13). Fyw7 decreases for increasing forest proportion in the investigated catchments ($p > 0.05$, $R^2 = 0.68$; Figure 13). Considering the urban land use share, the pattern and trend are similar to the one of agricultural land use share: here again the Fyw7 increases with increasing urban land use share ($p > 0.05$, $R^2 = 0.84$; Figure 13). For catchment characteristics such as catchment area, slope, gradient, baseflow index, mean elevation and flow path length, significant differences of the Fyw7 across catchments were found (Figure 14), but no trend was found for the different catchment characteristics. For the anthropogenic catchment (catchment 2) and the mountainous agriculturally dominated catchment (catchment 4) the differences of Fyw7 according to their mean elevation, catchment area, gradient, flow path length and baseflow index were not significant.

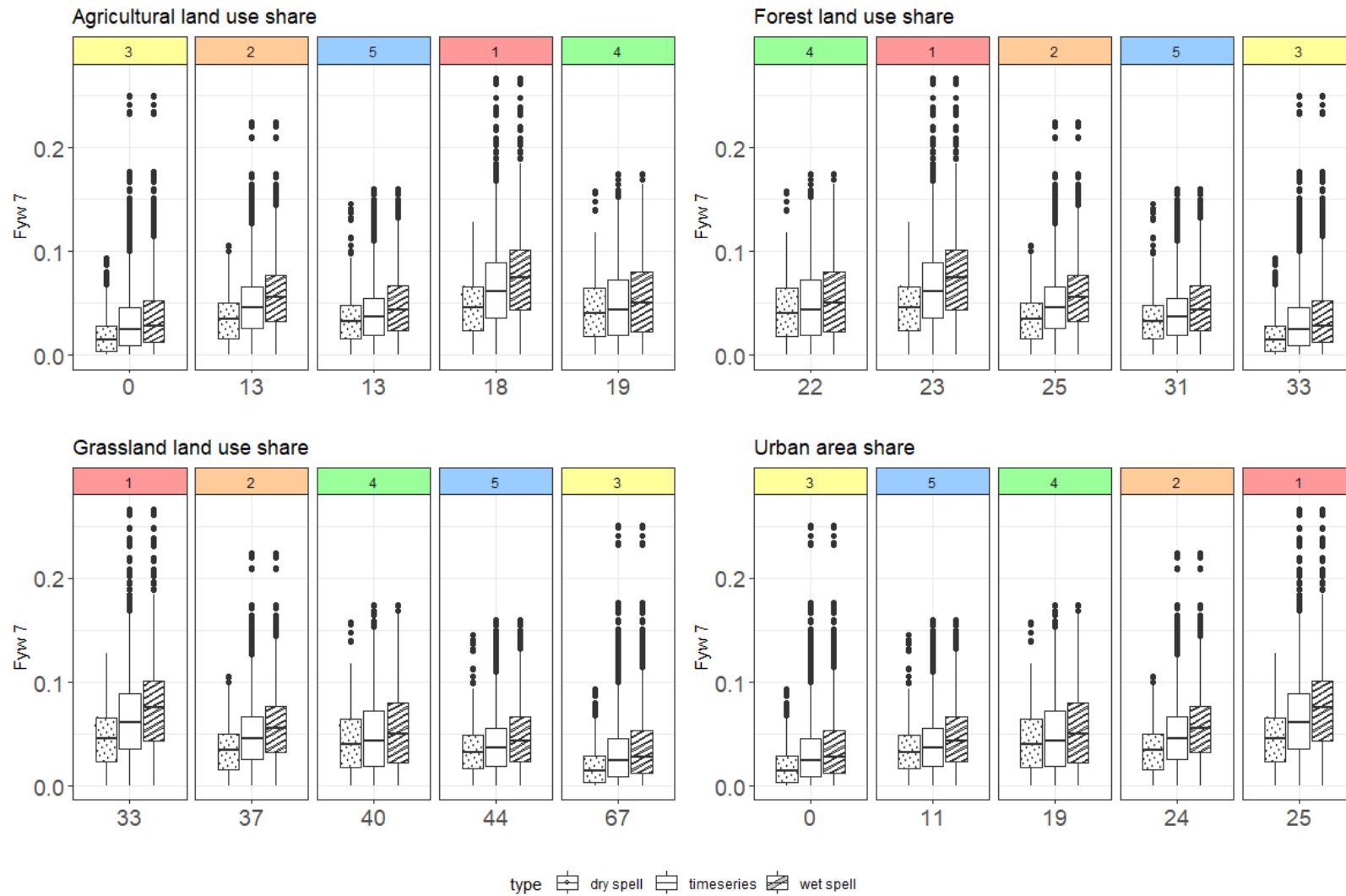


Figure 13: Fyw7 for different catchment characteristics (land use share [%]: agriculture, forest, grassland and urban area) with boxplots representing dry spells (dots), the entire time series (blank) and wet spells (stripes).

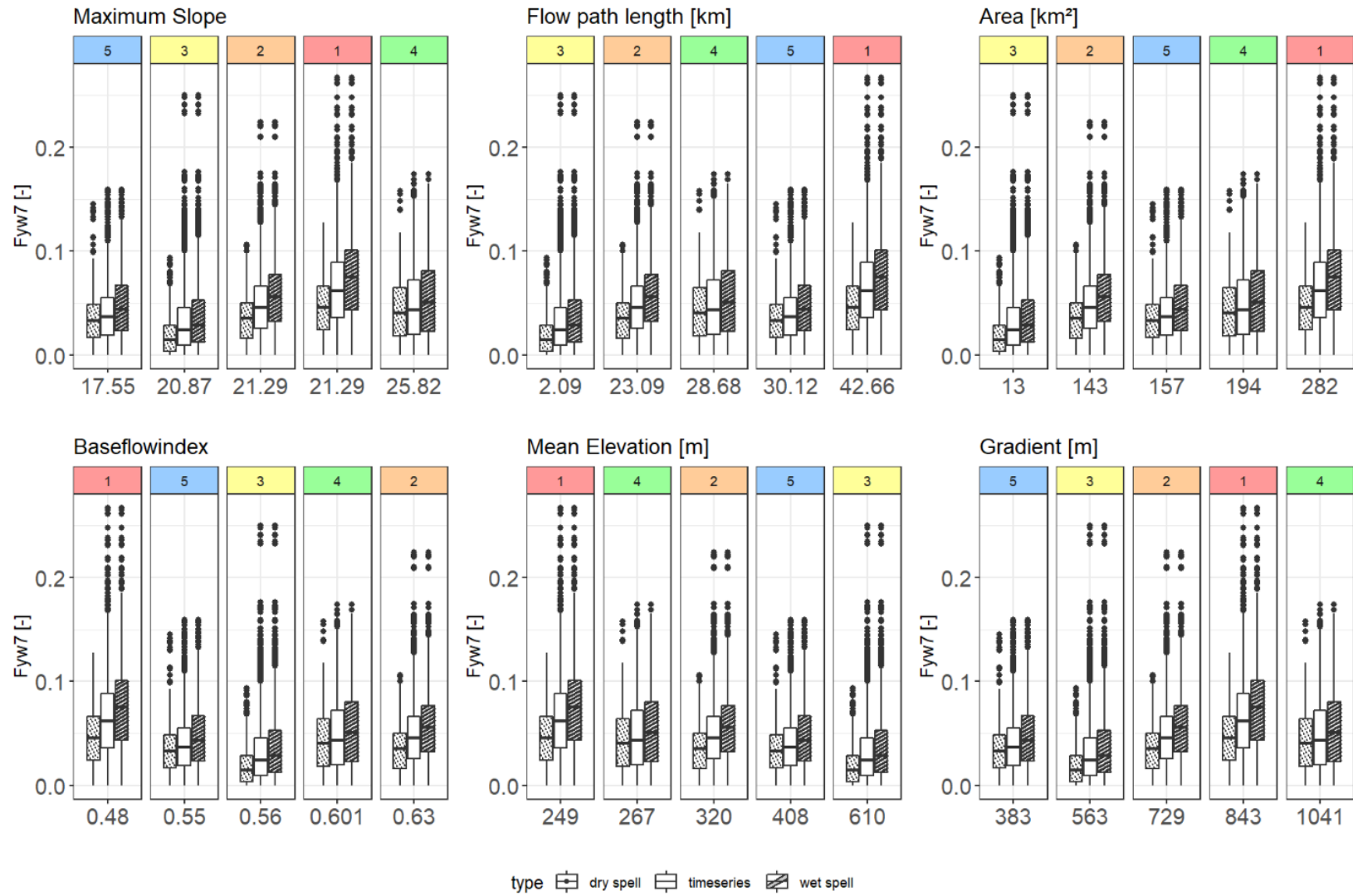


Figure 14: Fyw7 for different catchment characteristics (maximum slope, flow path length, catchment area, baseflow index, mean elevation, gradient) with boxplots representing dry spells (dots), the entire time series (blank) and wet spells (stripes).

For Fyw60, the pattern of increasing fraction of young water with increasing agricultural land use share as well as the increasing fraction of young water with decreasing grassland proportion is less obvious compared to Fyw7 (R^2 : agriculture = 0.33; grassland = 0.6) (Figure 15). This suggests that the release of water from previous rainfall events, such as Fyw7 is more dependent on land use and land cover characteristics than Fyw60. Hence, one can assume that agriculturally dominated catchments are in general more sensitive to short term precipitation events as agriculturally dominated catchments release predominantly young water from recent precipitation rather than from deeper water sources, which is supported by results from Jasechko et al. (2016), who found out that agriculturally dominated catchments release more young water than catchments with other landscape characteristics. Catchments with higher proportions of forest release more old water, which is reflected by the decreasing fractions of young water (Fyw60) with increasing forest share ($R^2 = 0.53$) (Figure 15).

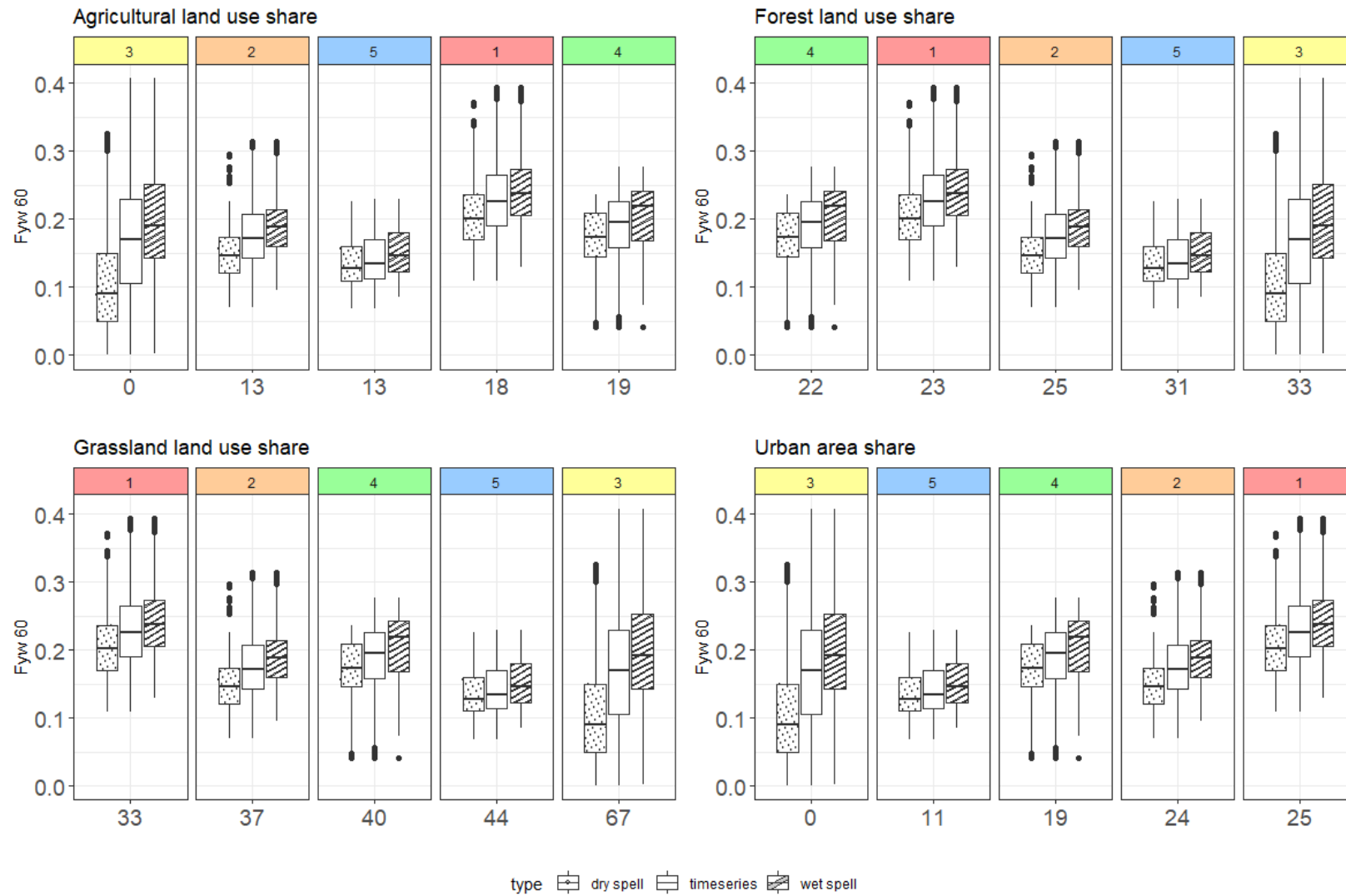


Figure 15: Fyw60 for different catchment characteristics (land use share [%]: agriculture, forest, grassland and urban area) with boxplots representing dry spells (dots), the entire time series (blank) and wet spells (stripes).

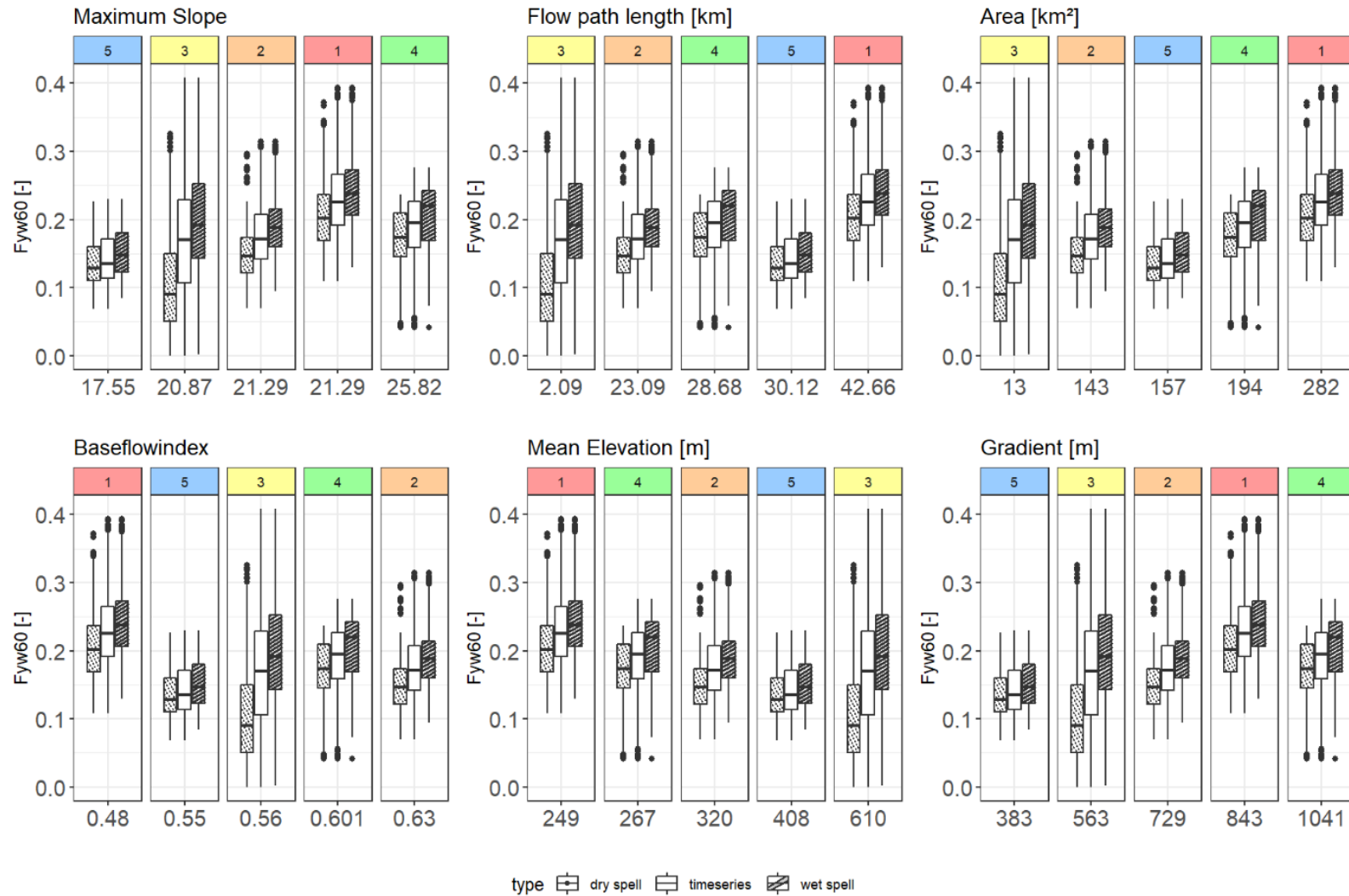


Figure 16: Fyw60 for different catchment characteristics (maximum slope, flow path length, catchment area, baseflow index, mean elevation, gradient) with boxplots representing dry spells (dots), the entire time series (blank) and wet spells (stripes).

The data suggests that there is no direct relation between Fyw7 and the catchment area. This is in line with other studies that did not find a relationship between transit time metrics and catchment area (Brown et al. 1999; Tetzlaff et al. 2009; Lutz et al. 2018; Lee et al. 2020). Lutz et al. (2018) already investigated the relationship between water age metrics and catchment characteristics such as soil types, flow path length, catchment area and other catchment characteristics in the Bode region, where this study is conducted as well. They found out that there is no relationship between the catchment characteristics and the Fyw up to 2-3 months after Kirchner (2016a, 2016b) during the observed time series from 2013 to 2015. In this study, a weak relationship between Fyw60 and land use types such as grassland and agriculture has been found for the five selected catchments, but for other catchment characteristics such as slope, gradient, mean elevation, flow path length and catchment area, there was no relation either (Figure 16).

A positive relation between agricultural land use share and increasing Fyw has also been found by Jasechko et al. (2016), who investigated 254 catchments globally in terms of the contribution of Fyw in stream networks. Agricultural land is different from grassland mainly with respect to soil cultivation and the plant cultures growing on the fields. To maintain a plant-favourable soil environment by directing water from rain events immediately from fields to streams, drainage pipes are built in many cases. By this, the transit time of water through the system is shortened. In other studies, a relation between the drainage density and water age metrics such as mean transit times (MTT) and Fyw up to 2-3 months was found (Soulsby et al. 2010; von Freyberg et al. 2018a; Dimitrova-Petrova et al., 2020). For the catchments investigated in this study, information about the drainage network and explicit crop cultures were not available, but given that the Corine land-use data can give an overview of general landscape structures with shares of land use types such as grassland, agriculture, forest and urban area, it can be concluded that there are general relationships between the land use types and the water age metrics. It is thus possible that the drainage network which is usually implemented on agricultural fields in the region causes the positive relationship between agricultural land use share and the fraction of Fyw7. Since water table management is not mandatory for cultivated grassland used as meadows as well as for grassland that is part of environmental protection areas, the density of artificial drains in such grassland areas is often low or non-existent. By this, grassland areas can hold back more water (from recent precipitation events) before it

is released to the stream network (Zhang & Yang, 2022). Therefore, the decreasing trend of Fyw7 with increasing grassland share in catchments is most likely caused by the buffer capacity of the meadows, mires and environmental protection areas.

Since underlying geology has an influence on the landscape structure as well as elevation, it cannot be ruled out that there might be a co-relationship that governs the visible relationship between the land use and Fyw7. Combining the information from all investigated catchments, no correlation between the contribution of Fyw7 and catchment characteristics such as the slope, elevation or gradient was found. Despite the missing correlation, significant differences of Fyw7 are found for all catchments that are in turn quite diverse with respect to their natural catchment properties like slopes, gradients and mean elevations. To gain more insights into the systematics of the relationship between Fyw7 and catchment characteristics, more detailed information about catchments such as drainage intensity as well as an extended catchment intercomparing study with more investigation areas in different locations from different regions seems necessary.

3.7. Evaluation of observed data in the Meisdorfer Sauerbach catchment

Considering the time series between 2013 and 2020, the precipitation amount in the Sauerbach catchment (catchment 6) was highest in 2014 (579 mm) while the lowest annual amount was recorded in 2018 (417 mm). A general trend towards drier conditions is reflected by both less precipitation and decreased mean annual discharge. Even the rate of evapotranspiration has a decreasing trend but with higher peaks in between. The isotopic signature of $\delta^{18}\text{O}$ of water in stream shows a damped signal compared to the isotopic signature of water in precipitation. Only during event sampling with higher sampling frequencies, higher fluctuations of isotopic signatures are visible in stream water. The isotopic signature in precipitation varies between -1.3 ‰ and 3.4 ‰ for $\delta^{18}\text{O}$ while the isotopic signature in stream water varies between -11.2 ‰ and -6.7 ‰ for $\delta^{18}\text{O}$. Soil moisture and groundwater samples for $\delta^{18}\text{O}\text{-H}_2\text{O}$ varied from -14.9 ‰ to -1.0 ‰ and from -9.2 ‰ to -7.9 ‰, respectively. For instream nitrate, $\delta^{18}\text{O}\text{-NO}_3$ varied between -3.3 ‰ and 33.1 ‰ and $\delta^{15}\text{N}\text{-NO}_3$ varied between 3.5 ‰ and 27.4 ‰ (Figure 17). Measured $\text{NO}_3\text{-N}$ concentrations in stream water varied between 0.25 mg/l and 9.6 mg/l.

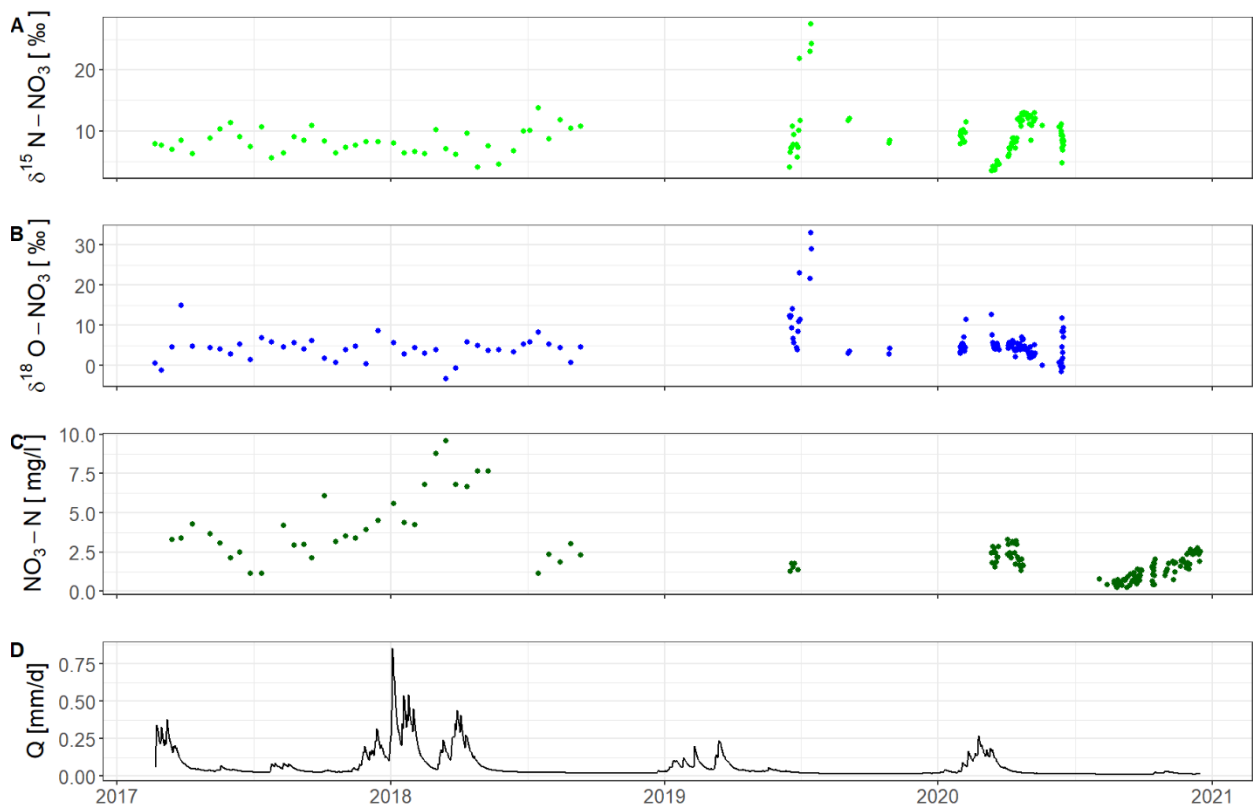


Figure 17: Isotopic signatures of nitrate (A, B) as well as the concentration of $\text{NO}_3\text{-N}$ in stream water (C) and the discharge (Q) [mm/d] (D) for the observation period.

Isotopic signatures of nitrate that were measured fortnightly (2017-2018) show less strong variations compared to the isotopic signatures of nitrate that have been measured sub-daily to daily (since 2019) (Figure 17). In 2019 the highest isotopic signatures of nitrate can be found during the daily sampling scheme. Considering the $\text{NO}_3\text{-N}$ concentrations, the pattern is different. During the fortnightly sampling campaign, $\text{NO}_3\text{-N}$ concentrations rose up to 10 mg/l while during the sub-daily to daily sampling scheme, $\text{NO}_3\text{-N}$ concentrations rose up to 3.5 mg/l. In general, $\text{NO}_3\text{-N}$ concentrations during the high-frequency sampling scheme were lower compared to the low-frequency sampling scheme. With a delay, the $\text{NO}_3\text{-N}$ concentrations increase in response to an increasing discharge, which can be seen at the beginning of 2018 and 2020. The isotopic signatures show a minor change in their composition in response to changing hydrologic conditions: the oxygen isotopes show a more scattered pattern during high flows, while nitrogen isotopes show a decrease in their

isotopic signatures during high flows, which can be seen both at the beginning of 2018 and 2020. These findings indicate that nitrate is flushed out of the storage system due to high flow events. Storage selection functions that are used in numerical models such as the tran-SAS (Benettin & Bertuzzo, 2018) can reflect these varying conditions; therefore, the SAS approach is used for further investigation of nitrate and its age derived from nitrate isotopic compositions. Since nitrate can derive from different nitrogen sources, it is not straightforward to determine the exact nitrogen source. In Figure 18 the possible sources of nitrate in the Meisdorfer Sauerbach catchment according to its isotopic values are shown.

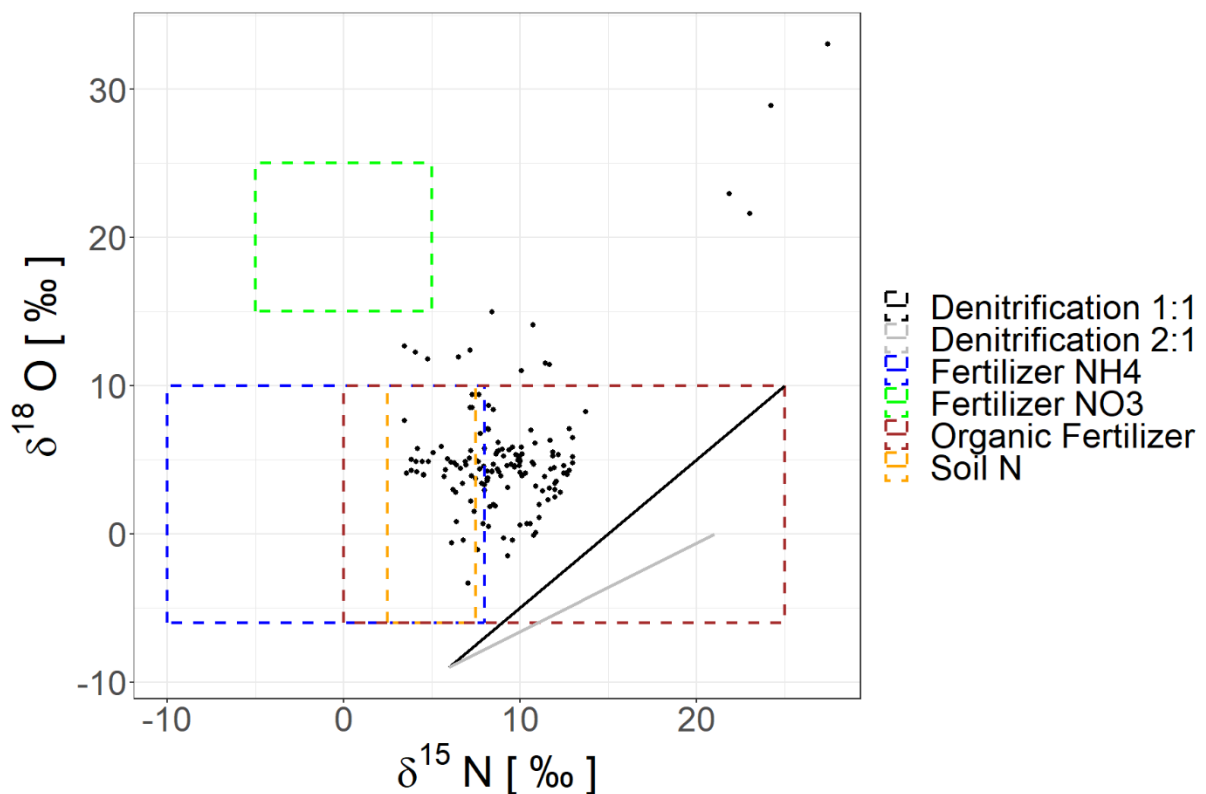


Figure 18: Isotopic signatures of nitrate in stream water in the Meisdorfer Sauerbach catchment, indicating different possible nitrate sources.

In the Meisdorfer Sauerbach catchment, the relation between both isotopic signatures ($\delta^{15}\text{N}$ and $\delta^{18}\text{O}$ of nitrate) show possible sources mainly from fertilizer such as organic fertilizer and ammonium fertilizer as well as nitrate formed in the soil zone (Figure 18), with boundaries of the isotopic signatures of the sources taken from Kendall et al. (2007) and adapted to the precipitation isotopic signature that have been measured in the catchment 6. Secondary processes, that influence the isotopic signature of nitrate are assumed to occur considering the measured isotopic signatures that do not plot within the given ranges of the possible sources. There is no clear sign of denitrification evident in the isotopic measurements. Nevertheless, denitrification cannot be excluded, since some gaps in the measured time series due to a lack of sample water are present (Figure 17). To further investigate whether the dataset points towards the occurrence of denitrification, monthly distributions of isotopic signatures of nitrate are compared with the monthly distributions of measured nitrate concentrations (Figure 19).

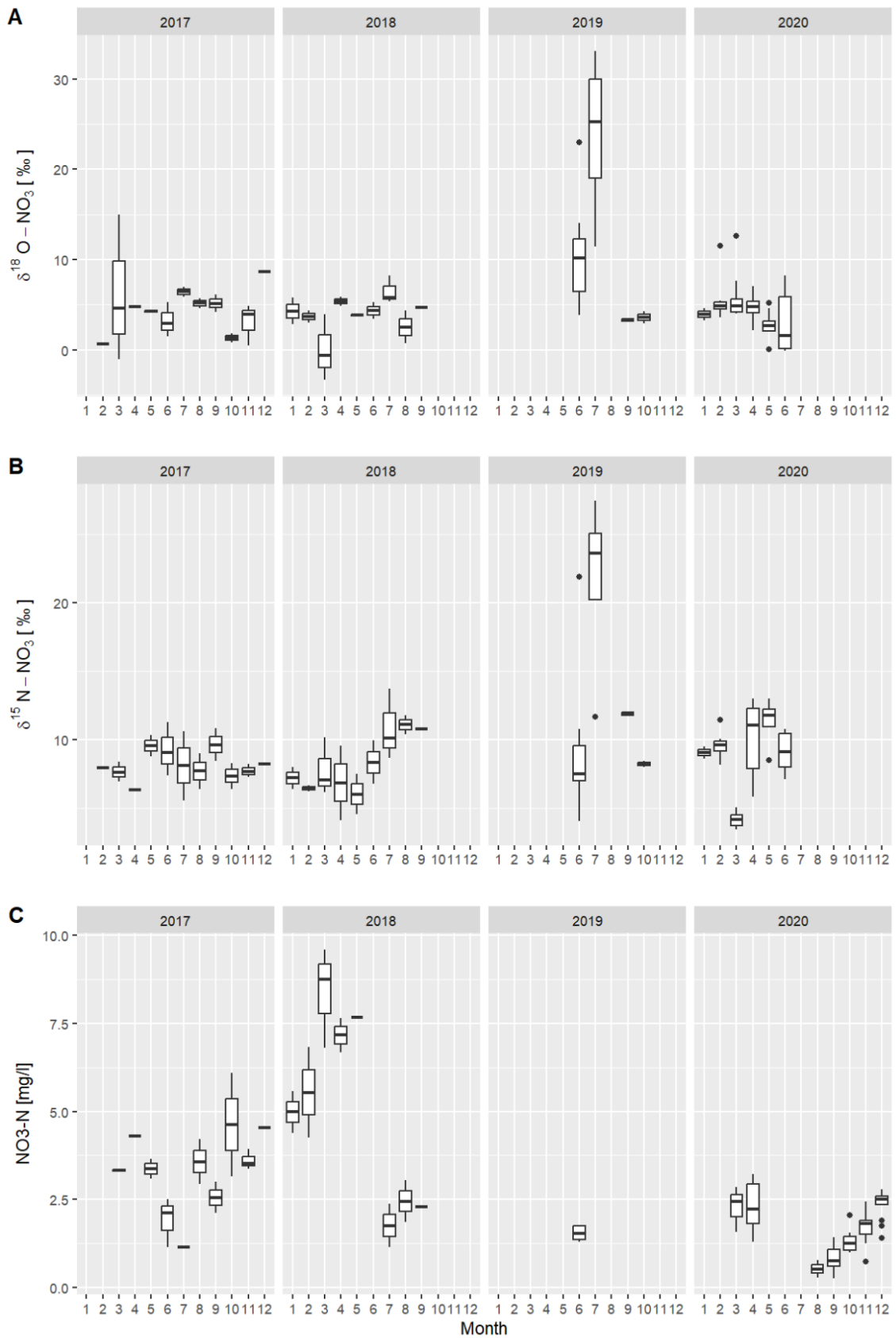


Figure 19: Monthly distribution of the isotopic signature (panel A) $\delta^{18}\text{O-NO}_3$, (panel B) $\delta^{15}\text{N-NO}_3$ and (panel C) nitrate-N concentration during the years 2017-2020.

The monthly distribution of $\delta^{18}\text{O}\text{-NO}_3$ in comparison to the nitrate-N concentration shows increasing isotopic signatures for decreasing nitrate-N concentrations (Figure 19). Even though this relationship is not strong (Pearson correlation: -0.12), the behavior is visible for instance in 2019. The highest variability of oxygen isotopic signatures was found in the summer of 2019, where low nitrate-N concentrations under 10 mg/l were observed. At the beginning of 2018, the nitrate-N concentrations increased, and the most depleted oxygen isotopic signatures coincide with the highest nitrate-N concentrations. The observed pattern points towards processes that occur in the catchment. After fertilizer application, microorganisms in the soil zone consume the infiltrated substances of the fertilizer application and nitrify them to nitrate. The isotopic signature of the nitrified nitrate, which can be taken up by plants as well as flushed out of the system due to high flow periods, is dominated by the soil oxygen isotope signature and therefore shows more decreased oxygen isotopic signatures. In summer, with higher temperatures, nitrate consuming processes such as denitrification occur under moist conditions (Kendall et al., 2007; Kaneko & Poulson, 2013; Granger & Wankel, 2016). Depleted nitrate-N concentrations during summer months with increasing oxygen isotopic signatures are indicators for denitrification that occurred in the soil zone under high temperatures and high soil moisture. The measured samples in the Meisdorfer Sauerbach show only short-term periods; therefore, a continuous time series analysis is not possible. Considering the measured samples, some indications (variations of isotopic signatures; fractionation) of microbial processes can be observed such as nitrification and denitrification, even though these processes likely occur irregularly and cannot be confirmed by the dual isotope plot or the relation between nitrate concentrations and isotopic signatures of $\delta^{15}\text{N}$.

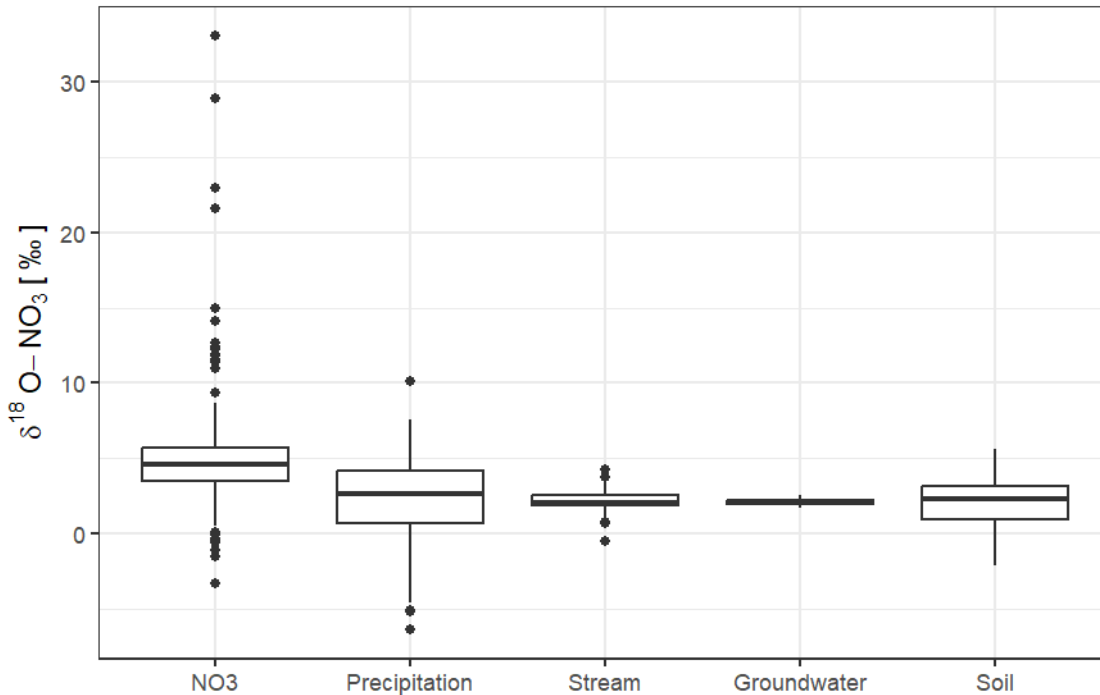


Figure 20: Comparison of the measured range of $\delta^{18}\text{O-NO}_3$ in stream water with calculated ranges of $\delta^{18}\text{O-NO}_3$ based on the $\delta^{18}\text{O-H}_2\text{O}$ ranges observed in different compartments using Equ. 9.

By using Equ. 9 with the isotopic signature of 23.5 ‰ for $\delta^{18}\text{O-O}_2$ and the $\delta^{18}\text{O-H}_2\text{O}$ isotopic signatures of precipitation, groundwater, soil moisture and stream water result in hypothetical $\delta^{18}\text{O-NO}_3$ values that reflect the compartment in which nitrification has occurred. Interestingly, Figure 20 illustrates that the actually observed range of $\delta^{18}\text{O-NO}_3$ is larger than the calculated ranges for the different compartments. Moreover, while the calculated means are very close to each other (2 - 3 ‰), the mean of the observed oxygen isotopic range in nitrate is significantly higher (4.5 ‰). The most obvious reason for the differences between calculated and observed ranges is a secondary biogeochemical impact on the oxygen isotopic composition of the nitrate pool that to some extent disturbs the original isotopic signature fixed during nitrification. A negative deviation from the calculated range could be associated with oxygen isotope exchange of reaction intermediates (primarily nitrite) with the ambient water. This scenario is especially likely for temporally or locally variable biogeochemical conditions favouring both the reductive pathway of nitrate reduction and the oxidative pathway of nitrite oxidation (Granger and Wankel, 2016). A positive deviation of

observed $\delta^{18}\text{O}-\text{NO}_3$ from computed $\delta^{18}\text{O}-\text{NO}_3$ is most likely caused by the impact of denitrification. The overall impact of denitrification on the catchment scale can be evaluated by integrated data analysis as shown below (Kendall et al., 2007). Considering all measured isotope signatures of nitrate and nitrate concentrations throughout the observation period, the integrated analysis with a Rayleigh plot and an isotope cross-plot (Figure 21) clearly suggests a minor impact of denitrification at the catchment scale. Fitting the Rayleigh equation to the observed data only yields an apparent, field-based enrichment factor that is normally smaller than the intrinsic enrichment factor that would be observed under closed system conditions (Druhan & Maher, 2017). Despite this uncertainty, the obtained value of -2.7‰ cannot be considered as indicative for straightforward denitrification (Knöller et al., 2011). Even though a minor number of samples undoubtedly show the impact of denitrification with elevated isotope values and low concentrations (Figure 21a), the overall nitrate isotope-concentration pattern is controlled by dilution and other flow-related processes as well as by the isotopic nitrate source variability (Benettin et al., 2020; Lutz et al., 2020). Accordingly, the dual isotope plot (Figure 21b) does not show a strong positive correlation between nitrogen and oxygen isotope signatures expressed by a so-called denitrification line with a slope between 0.5 and 1.

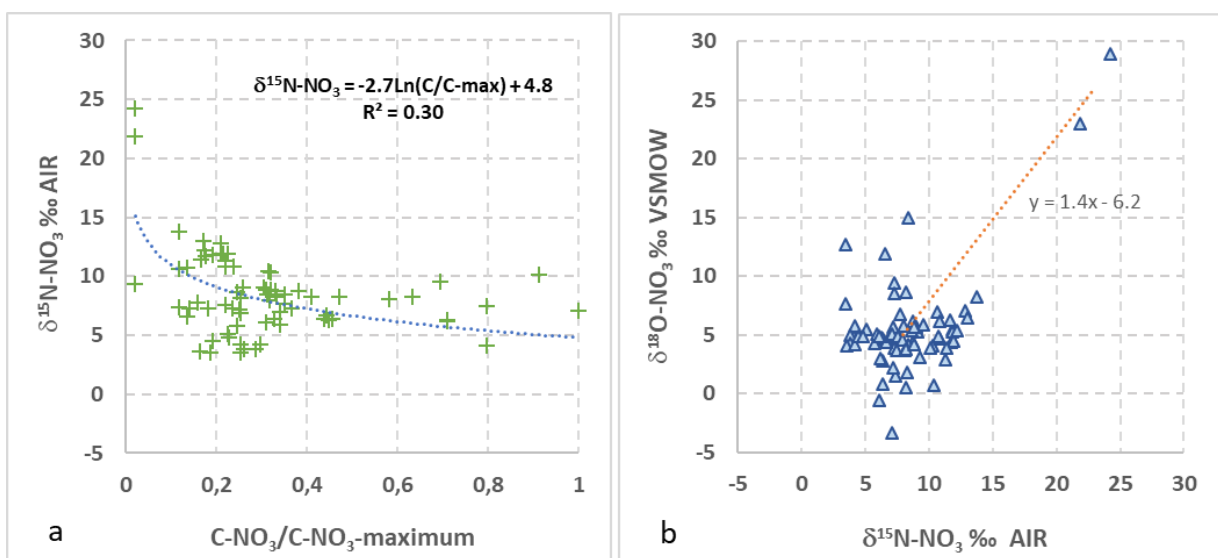


Figure 21: a. Relationship between nitrate concentrations (normalized to the highest measured concentration) and b. dual isotope plot showing the correlation between measured nitrogen and oxygen isotope signatures.

3.8. Simulation results of the modified tran-SAS

The following chapters present the results of the nitrate isotope model, separated into two chapters, the first chapter discusses the simulation results of water isotopic signatures and water ages, while the second chapter discusses the simulation results of the nitrate isotopic signatures and nitrate ages in combination with the water ages.

3.8.1. Water isotopic signatures and water age distributions in discharge

In general, the simulated isotopic signature of stream water using the tran-SAS model mirrors the behavior of measured isotopic signature in stream water with a KGE of 0.48 (Figure 22). Except for short-term strong fluctuations of the isotopic signatures in stream for instance in 2019 and at the end of 2020, the model performs behavioural and is able to capture the general variation of isotopic signatures during the years.

For the comparison of transit times of both water and nitrate (Figure 24), the transit times of the routing storage are considered only. Transit times of water are lower during high flow conditions and higher during low flow conditions. Discharge during winter and spring of 2018, 2019 and 2020 becomes lower and by this the proportion of old water becomes higher, which is reflected by increasing median transit times. Water of different ages contributes to stream water with variable proportions over time. During the entire observation period between 2017 and 2020, the wettest conditions were observed in 2017. The highest proportion of young water was found during a peak flow at the beginning of 2018, after the wet year 2017. The following years 2019 and 2020 were influenced by dry climate conditions with lowered discharge and increasing transit times of water. This implies that the higher proportion of older ages in stream flow during the dry year 2018 compared to the wet year 2017 is most likely related to higher relative contribution of older (ground-)water to the streamflow in that period and less young water from recent precipitation events, since less precipitation fell during the dry year 2018. The following years 2019 and 2020 are affected by drought conditions and overall less precipitation, causing higher old water contributions during summertime. It is most likely that the replenishment of water storages took a few months after the drought in 2018. A similar behavior was reported by Smith et al. (2020) who analyzed the effect of the drought in 2018 on ecohydrological fluxes in Central Germany. According to their findings, the replenishment of the water storages took 6 to 8 months

depending on the vegetation canopy. The impact of the drought can easily be followed by the discharge time series. Lowered discharge in subsequent years after 2018 reflect that the catchment has not yet recovered from the drought impact, as similarly found by Kleine et al. (2020).

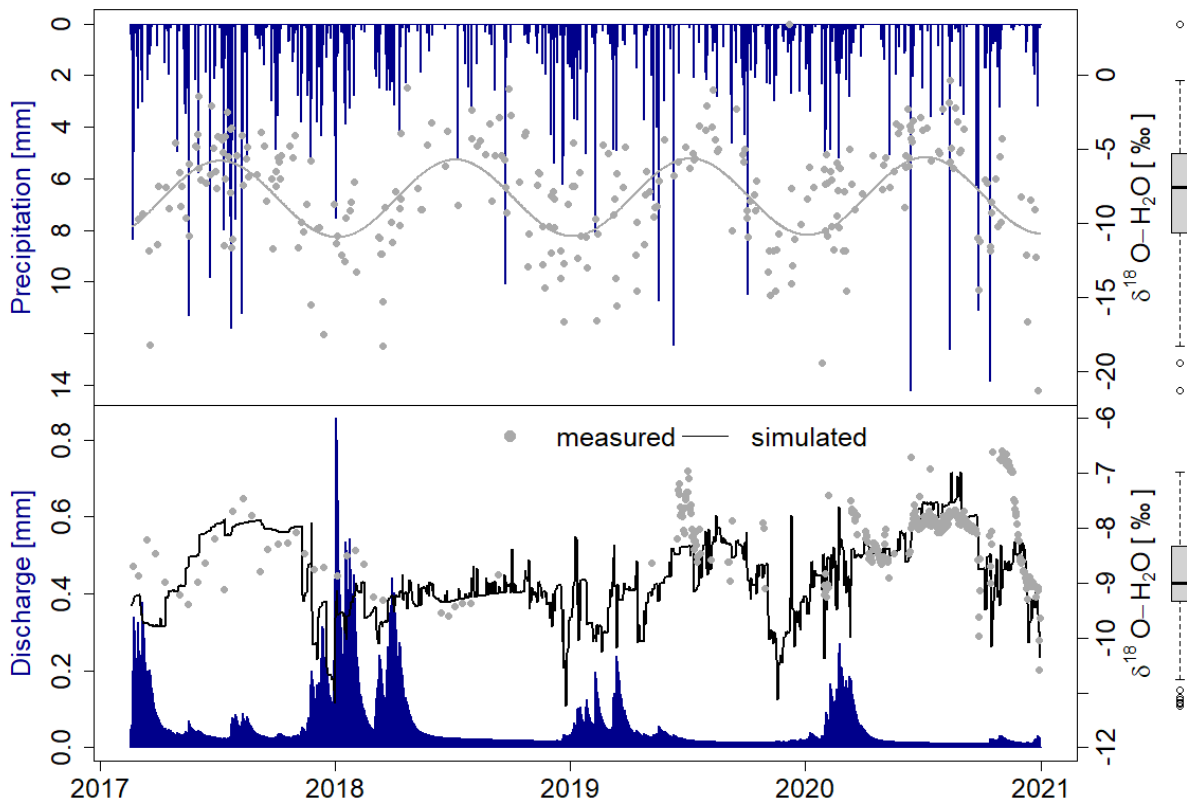


Figure 22: Precipitation [mm] (blue) and isotopic signature of $\delta^{18}\text{O}-\text{H}_2\text{O}$ in precipitation (grey: dots = measured, line = sinusoidal fitting line to precipitation isotopic signature) on top and discharge [mm] boxplots on the right side of the graph show the distribution of isotopic signature in precipitation (top) and streamflow (bottom).

3.8.2. Nitrate isotopic signatures and TTDs gained from the nitrate isotope model

The measured nitrate oxygen isotopic signature $\delta^{18}\text{O}-\text{NO}_3$ in stream water samples shows a considerable scatter (Figure 18 and Figure 21). Considering a range of literature values for isotope fractionation of denitrification parameters and degradation rates as proposed by Granger & Wankel (2016), a simulated scattering of oxygen isotopic signatures is obtained and shown in grey in Figure 23. Most of the measured

values plot within that simulated range. Instead of applying variable fractionation parameters, a simple model approach with constant degradation rates and constant fractionation factors during the time series was used which is able to reflect the range of measured isotopic signatures. It is obvious though that biogeochemical processes in soil and stream water are more complex and that $\delta^{18}\text{O}\text{-NO}_3$ is not only determined by nitrification and denitrification. A significant share of nitrate with an oxygen isotopic signature not related to nitrification in any way can be introduced into the catchment by direct input through inorganic fertilization using nitrate salts. That share can account for up to 20-30% of the total fertilization in arable land (Boshers et al., 2019). Moreover, as already discussed in section 3.7 based on the evaluation of the observed data, intermediates of redox reactions in the unsaturated and saturated zones involving nitrogen transformations such as hydroxylamine or nitrite have the capability of quickly exchanging oxygen isotopes with the ambient water and thereby introducing an uncertainty on the prediction of $\delta^{18}\text{O}\text{-NO}_3$ formed during nitrification according to equation 2 (Buchwald & Casciotti, 2010; Casciotti et al., 2011; Boshers et al., 2019). Kool et al. (2011) state that the isotopic signature $\delta^{18}\text{O}\text{-NO}_3$ may be completely controlled by $\delta^{18}\text{O}\text{-H}_2\text{O}$, due to the above-mentioned isotope exchange during biogeochemical processes in the reactive zones. This potential exchange of $\delta^{18}\text{O}$ and any water flow related mixing phenomena of nitrate from different sources is not considered in the simple model, due to the fact that other mixing phenomena of nitrate are not measurable with the data provided. Moreover, the isotopic signature of surrounding soil air has an influence on the nitrified nitrate. In this study, it is assumed that the proportion of oxygen from water and soil air are the same in soils as observed in laboratory cultures and that, therefore, the incorporation of oxygen from soil air or water during nitrification is not associated with isotope fractionation (Kendall et al., 2007). Besides, it is assumed that the isotopic signature $\delta^{18}\text{O}$ of water used by microbes is the same as the isotopic signature of water in the soil storage and that the isotopic signature $\delta^{18}\text{O}$ of soil air used by microbes is the same as the atmospheric isotopic signature (Kendall et al., 2007). However, under natural conditions in aquatic systems, other processes can influence the $\delta^{18}\text{O}$ of dissolved oxygen of soil air, e.g., the diffusion of atmospheric oxygen of air in the subsurface as well as photosynthesis which lowers the $\delta^{18}\text{O}$ of soil air, and respiration by microbes which leads to higher $\delta^{18}\text{O}$ values of soil air due to isotopic fractionation (Kendall et al., 2007; Boshers et al., 2019). In general, the observed $\delta^{18}\text{O}$ of nitrate can show an offset compared to $\delta^{18}\text{O}$

of nitrate computed with the simple equation 2, due to the implemented oxygen isotopic signature of soil air which undergoes respiration (Kendall, 1998; Kendall et al., 2007). Besides, in addition to the common autotrophic nitrification pathway, nitrate formation can occur to some extent via heterotrophic aerobic ammonia oxidation (Mayer et al., 2001). Moreover, the proportion of oxygen from surrounding water and soil air can change to a minor degree during nitrification (Aravena et al., 1993; Kool et al., 2011). It is still unresolved how these different mechanisms affect the isotopic signature of nitrate during nitrification reactions and to what extent, they can therefore not be adequately mirrored with simple equations such as equation 2 (Kendall et al., 2007). Instead the applied equation gives a possible range of nitrate isotopic signatures that could occur under the previously mentioned restrictions.

During wet periods, younger nitrate is dominant, which is released from the upper subsurface storages. In the Meisdorfer Sauerbach catchment, transit times of water up to 300 days with lowest transit times (50 days) during high flows were found. Hence, water with such short transit times easily transports soluble nitrate directly to the stream (Figure 24). Considering such short contact times between water-borne nitrate and biofilms on the mineral matrix hosting denitrifying microbial communities, it can be concluded that the impact of denitrification during the transport process at the catchment scale is relatively low. This assumption is clearly supported by an integrated analysis of observed field data (Figure 21). Therefore, a low denitrification rate constant was chosen during the calibration process.

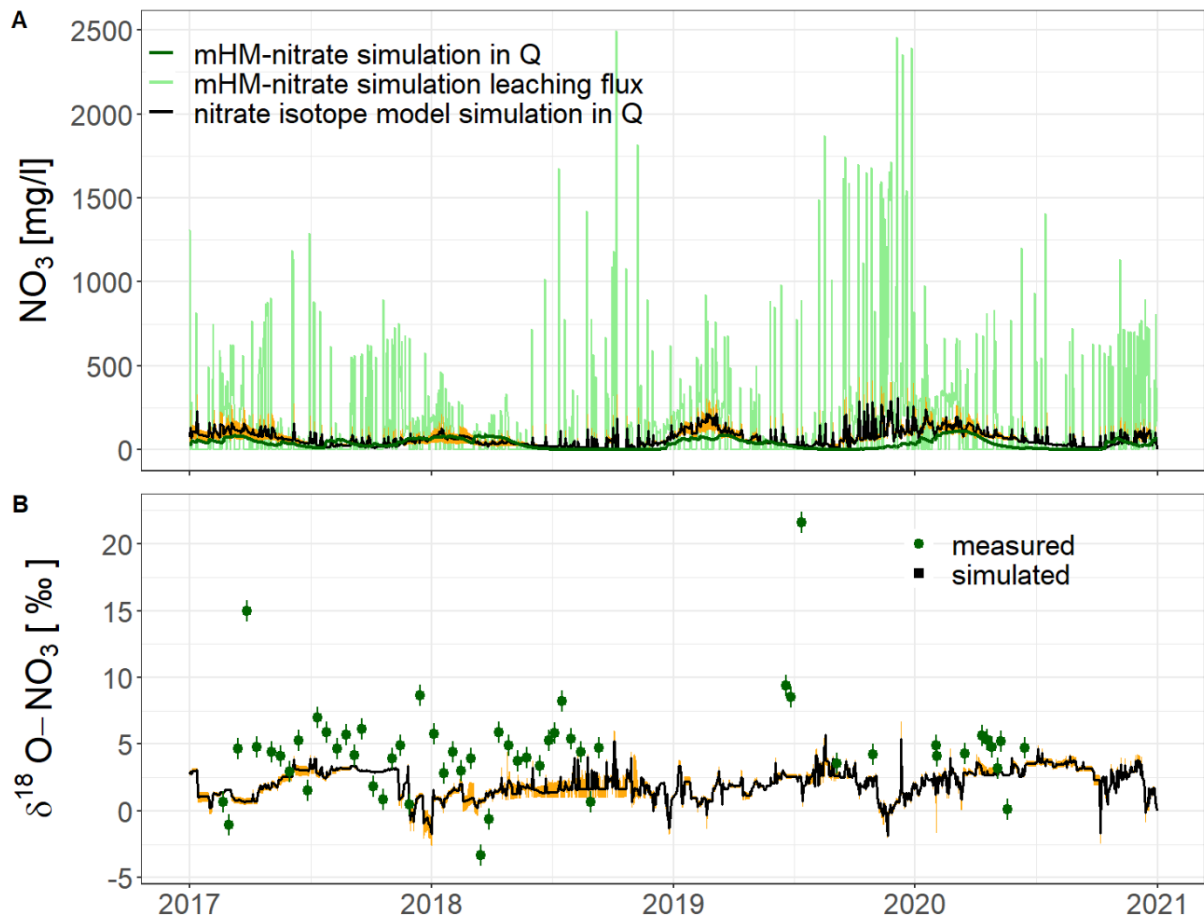


Figure 23: Panel A with the simulated nitrate concentrations [mg/l] of the mHM model of discharge in dark green and as leaching flux in light green. The black line in panel A shows the nitrate concentrations obtained from the nitrate isotope model. Panel B shows the isotopic signature of $\delta^{18}\text{O}-\text{NO}_3^-$ in stream: green dots= measured with measuring error 0.8 ‰, black line= simulated, orange area= 10% best simulation according to a small bias.

Once mobilized, the transport of nitrate within the catchment is expected to be closely linked to the transport pathways of water (Maher, 2010, 2011). Therefore, the TTDs of nitrate should display a similar behavior like the TTDs of water. Considering the median transit times in the lower storage (TT50) as shown in Figure 25, nitrate has lower TT50s than water throughout the entire observation period, but both lines reflect the same seasonal behavior. The offset shown is caused by denitrification in the lower storage, as nitrate associated with short transit times contributes significantly more to the overall

nitrate transit time because of its higher concentration compared to nitrate associated with large water transit times, which has been mostly denitrified before reaching the catchment outlet.

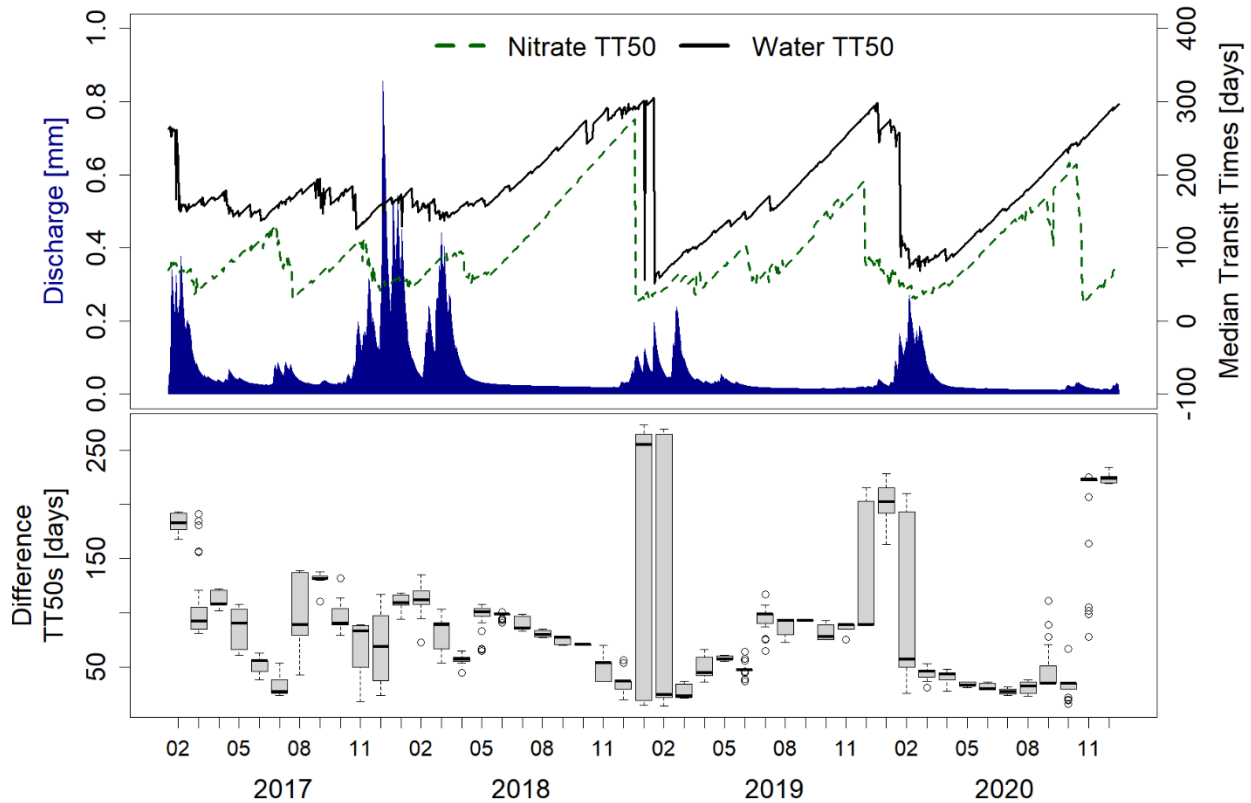


Figure 24: Top panel: Median Transit Times (TT50) of water (black, solid line) and nitrate (green, dashed line) through the lower storage, and discharge bottom panel: monthly boxplots of difference between TT50 of water and of nitrate.

Nevertheless, the offset between TT50 of water and TT50 of nitrate is not constant but shows a significant temporal variability. While the differences between TT50 of water and TT50 of nitrate are highest during periods with high discharge during winter time, lowest differences are observed during dry periods such as summertime (Figure 24). The offset between TT50 of water and TT50 of nitrate at the beginning of periods with high discharge (i.e., earlier lower TT50 of nitrate than TT50 of water in December 2018 and December 2019) is most likely caused by more old water contributions from deeper water sources such as groundwater that are active at the beginning of a high flow event before the young water from precipitation is dominating the runoff process. The first

flush after drier period carries larger amounts of young nitrate that underwent less denitrification compared to older water contributing to runoff that carries less amount of nitrate because of the denitrification that happened. Water transit times are known to decrease during increasing discharge (Benettin et al., 2015; Soulsby et al., 2015). The nitrate concentrations are diluted with young nitrate that infiltrates in deeper storages and therefore the transit time of nitrate is lower than the water transit times.

Considering the low offset between both transit times during summertime in 2018, 2019 and 2020, compared to the wintertime of the years, one can assume that denitrification is lowered during these times. Even though high temperatures are occurring during summer, the wetness of soils is lowered because of the prolonged drought conditions since 2018 (Kleine et al., 2020). During the year 2017 much more variability of nitrate transit times can be seen (Figure 24). With the observed isotope data, it was not possible to demonstrate significant denitrification due to missing data. Nevertheless, the nitrate concentrations indicated that denitrification happened to a limited extent (Figure 19). This is complemented by the relation between the transit time and nitrate concentration (Figure 25): The lowered nitrate concentrations with higher transit times are an indicator for processes that degrade the solute nitrate along its transport path through the catchment.

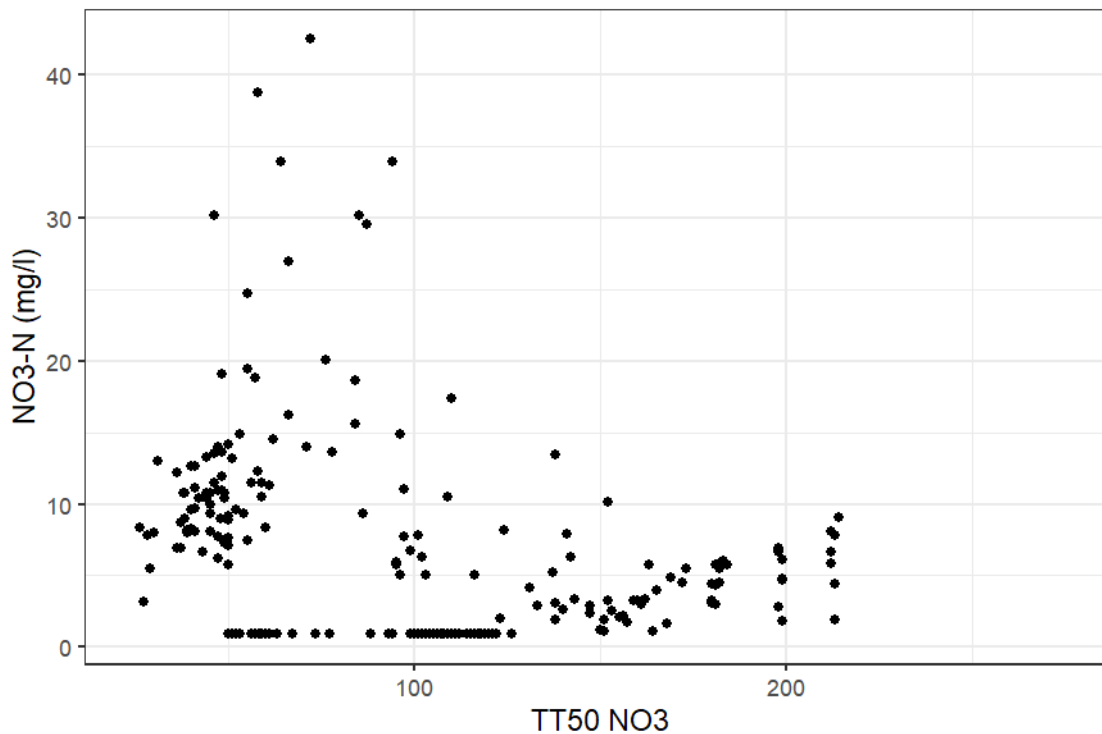


Figure 25: Relation between the measured nitrate concentration in stream water and the simulated median transit time of nitrate.

Considering the underlying geology with low to moderate groundwater connectivity, significant nitrate contributions to the stream from deeper aquifers hosting older groundwater do not seem very likely in the study catchment. These results are in line with the findings of Jasechko et al. (2016) who point out that soluble contaminant inputs can be transmitted from watersheds to streams during short time scales, which are in the range of young water fractions (~2 months), and especially in flat agriculturally dominated catchments where a higher proportion of young water is present, a faster release of solutes is possible. Especially for farmers it is relevant to improve the understanding of the processes in the catchments with the aim to prevent ecological habitats such as water bodies from high nitrate loads that cause eutrophication and are in general harmful to the ecosystem.

In general, the computation of water and nitrate transit times does not only have scientific, but also practical implications, as a relevant goal for farmers is to increase the efficiency of fertilizer application on agricultural fields so that nutrients are available for the crops as long as possible without being flushed out during precipitation events.

Knowing how fast nitrate is released to the stream, farmers can improve their management practices, e.g., by reducing the amount of nitrate fertilizers that are applied several times per year, but also by considering that even when it is allowed to apply fertilizer (e.g., until the end of October in Germany), the weather forecast and discharge intensity has to be considered more strongly with the aim to avoid fertilizer application before and during precipitation intense periods.

3.8.3. Potential impact of conceptual simplifications on the nitrate isotope model performance

The deliberately chosen parsimonious modelling approach provided valuable insights into the transit time dynamics of water and nitrate in the investigated catchment 6. Nevertheless, this relatively simple concept might be associated with higher uncertainties with respect to the model output.

One issue that might have some impact on the model performance is the data collection strategy proving the data sets implemented in the model. For technical reasons, stream water samples were collected as grab samples at specific times of the day. Birkel et al. (2010) analyzed the effect of different sampling strategies such as composite samples versus grab samples and how model performances of different model types are affected by samples taken in different timesteps. They report a decreasing model performance related to lowered sampling frequencies. Moreover, especially for catchments that release water predominantly from shallow subsurface storages, the influence of composite samples in lowered sampling frequencies causes less accurate model performances (Birkel et al., 2010). The findings of Birkel et al. (2010) have been shown in this study as well, where model simulations of the original tran-SAS model (Benettin & Bertuzzo, 2018) using grab samples for model evaluation were compared with composite samples for the model evaluation, which revealed higher deviations for composite samples as well as higher deviations for lower sampling frequencies. The fact that the Meisdorfer Sauerbach catchment releases predominantly water from the shallow subsurface during the investigated time series as well as the low sampling frequency from 2013 to 2017 may be responsible for the relatively low Kling-Gupta-Efficiency of 0.48 for stream water isotopic signatures.

Regarding the modifications made for the nitrate isotopic signatures in tran-SAS, the model concept was deliberately simple. The calculation of the oxygen isotopic signature of nitrate generated during nitrification is based on a straightforward implementation of $\delta^{18}\text{O}$ of water and $\delta^{18}\text{O}$ of soil air according to equation 9. For calculating $\delta^{18}\text{O}\text{-NO}_3$, the simplified assumption that water oxygen is incorporated from the leaching flux leaving the upper storage is applied. Compared to the $\delta^{18}\text{O}\text{-H}_2\text{O}$ of the precipitation input function, the leaching flux shows a damped signal with a lower variability of the simulated $\delta^{18}\text{O}\text{-H}_2\text{O}$ values. Under natural conditions, however, some of the nitrate will be formed with water that has not reached the same level of isotope signal dampening as expected for the leaching flux. As a consequence, the overall variability of the observed $\delta^{18}\text{O}\text{-NO}_3$ could be slightly higher compared to the computed $\delta^{18}\text{O}\text{-NO}_3$. By assuming that denitrification is the only process affecting the isotopic signatures of nitrate after initial nitrification, a further simplification for the model concept was applied.

The main goal of this study part was to describe the age of nitrate compared to the age of water using median transit times as age metric gained from a high-frequency isotope dataset. Despite the simplifications and related uncertainties described above, the approach provides a novel tool that is fully in line with the intention of this study to provide information on the differences or similarities of the age metrics of water and nitrate in a mixed land-use headwater catchment.

4. Conclusion

In this study an elaborate high-frequency water isotope monitoring program of stream flow and precipitation was conducted in six contrasting catchments in the Harz mountains and the adjacent northern lowlands, Germany, aiming to investigate sampling frequency, sampling technique and their influence on transit time model results, the relation between age metrics (fractions of different water ages, transit times) and catchment characteristics (discharge, landscape structure metrics) with special focus on hydrological varying periods and last but not least the age of nitrate in relation to the age of water was investigated. Water age metrics are obtained by the tran-SAS model (Benettin & Bertuzzo, 2018) with daily input data. Nitrate age metrics are obtained by a modified version of the tran-SAS model.

The analysis of sampling frequencies revealed higher uncertainties for lower sampling resolutions even though a higher Kling-Gupta-Efficiency as metric to evaluate the model performance was found. With daily data the model simulation showed lower KGE values, but the model was able to mirror better the daily variations of isotopic signatures in stream. These findings are highly relevant for further research, because most of the studies rely on low sampling resolutions such as monthly and fortnightly data. Knowing that the uncertainty increases with lower sampling resolutions is an important result for result evaluation and monitoring set ups that aim to collect data for the establishment of catchment models. The techniques of sampling such as grab samples and composite samples showed differences in modelling results according to the sampling frequency, which highlight that monitoring set ups that are restricted to low sampling frequencies, such as weekly and fortnightly samples, due to the management planning, costs and analysis should collect composite samples to better reflect the isotopic signatures in stream.

Daily sampling frequencies allow to investigate more precisely the daily variation of hydrological processes. Moreover, more knowledge can be gained from daily data during events such as wet and dry spells. This study analyzed the discharge sensitivity of two fractions of young water: the young water fraction with an age up to 60 days (Fyw60) and water that stems from recent precipitation events with an age up to 7 days (Fyw7). Discharge sensitivities of water parcels with an age of up to 7 and 60 days were obtained using the approach after Gallart et al. (2020b), revealing the highest sensitivity for a hilly anthropogenic catchment. With increasing share of grassland,

Fyw7 decreases, which indicates that landscape structures affect the hydrological conditions of streams. Probably, higher amounts of grassland as well as more grassland patches between agricultural fields could decrease the release of young water by holding back young water proportions and supporting the infiltration to deeper storages. This might create a positive side effect with respect to control of anthropogenic pollution by facilitating longer transit times and, as a consequence, an enhanced pollutant degradation potential. However, especially in Central and Western Europe, climate change impacts will result in more frequent rainfall events after prolonged dry conditions leading to a scenario with more dominant release of young water increasing the pollution risk of the streams. The assumption of such a scenario is supported by the findings of this study with respect to increasing amounts of young water, both Fyw60 and Fyw7, from summer to autumn. This behavior might result from the catchment storage drying out during prolonged dry spells resulting in less connectivity of water storages and due to that less mixing between water sources in the subsurface. Considering their large potential variability on a regional or even global scale, the hydro-climatic properties of the investigated catchments were in a quite narrow range. To some extent, this hampers the recognition of the systematic relationships between catchment characteristics and fractions of young water. Significant additional knowledge can be expected if the selected catchments reflect a much broader range of catchment characteristics and hydro-climatic properties acknowledging though that such an approach would be associated with enormous logistical challenges. However, one of the valuable contributions of this study is that it could serve as a blueprint for further investigations aiming at the recognition of hydrological processes and the age distribution of stream water during varying hydrological periods in a more global context. Upcoming studies should in particular pay attention to the differing tendency of catchments to release water from previous precipitation events and water that is categorized as young water with an age around 2-3 months as this young water share carries a high pollution risk by anthropogenic contaminants.

Understanding how catchments react during differing hydrological conditions and the implementation of this understanding into land management actions is crucial for controlling nutrient losses and pollution risks of streams and other water bodies. As shown by this study, high-frequency isotope monitoring programs in concert with the application of appropriate transit time models can significantly contribute to this

understanding. These findings are important information for future landscape structure changes. Knowing that more young water from recent precipitation events is released from agriculturally dominated catchments is an inevitable information for farmers, who apply nutrients and pesticides on their fields to support and prevent crops.

Based on time series observed between 2017 and 2020 for one selected catchment, the transit time distributions of water and nitrate are investigated using their oxygen isotopic signatures ($\delta^{18}\text{O}$) as a characteristic fingerprint in concert with a simple model. The numerical model tran-SAS (Benettin & Bertuzzo, 2018) was modified by introducing a second storage and by applying simple biogeochemical equations to describe nitrification and denitrification as well as associated isotopic signatures and isotope fractionations. The study was conducted in a 11.5 km² headwater catchment in the Northern lowland of the Harz mountains, Central Germany.

Generally, nitrate transit times behave in the same way as water transit times, but with an apparent offset between median transit times of water and nitrate, which was highest at the beginning of high discharge periods due to higher contributions of water from water storages that contain old water such as groundwater storages with less nitrate, while smaller contribution of young water flushes nitrate pools in the soil layers into the rivers. Due to biogeochemical processes such as denitrification, the apparent transit time of nitrate can be lower than that of water, because the old nitrate has been degraded and, therefore, contributes less to the overall nitrate transit time. Hence, predominantly young nitrate is released to the stream. This information is highly relevant for understanding processes that control nitrate export from agricultural fields to surface water ecosystems that are stressed by the impact of high nitrate loads. Moreover, this knowledge may be used to enhance farming practices with the aim to increase the efficiency of fertilizer application on agricultural fields. For instance, to be sure that the loss of nutrients from fertilizer application is lowered, a buffer time before and after wet periods such as high precipitation events that cause the discharge to rise, could be considered for the planning of fertilizer application.

These findings are characteristic for a mixed land use headwater catchment under significant hydrological and ecological stress associated with increasing drought conditions due to climate change. However, these assumptions cannot necessarily be transferred to other catchments displaying largely different hydro-meteorological, topographic and/or land use boundary conditions. Therefore, a broader investigation

involving catchments of various characteristics is advisable in order to provide a more general view on the link between such catchment characteristics and transit times of water and nitrate.

Generally, these findings regarding the varying offset between water and nitrate transit times underline the importance of analyses of solute transport and transformation in the light of projected more frequent hydrological extremes (droughts and floods) under future climate conditions

References

- Aravena, R., Evans, M. L., & Cherry, J. A. (2005). Stable Isotopes of Oxygen and Nitrogen in Source Identification of Nitrate from Septic Systems. *Groundwater*, 31(2), 180-186. <https://doi.org/10.1111/j.1745-6584.1993.tb01809.x>
- Asadollahi, M., Stumpp, C., Rinaldo, A., & Benettin, P. (2020). Transport and Water Age Dynamics in Soils: A Comparative Study of Spatially Integrated and Spatially Explicit Models. *Water Resources Research*, 56(3). <https://doi.org/10.1029/2019wr025539>
- Benettin, P., Bailey, S. W., Campbell, J. L., Green, M. B., Rinaldo, A., Likens, G. E., McGuire, K. J., & Botter, G. (2015). Linking water age and solute dynamics in streamflow at the Hubbard Brook Experimental Forest, NH, USA. *Water Resources Research*, 51(11), 9256-9272. <https://doi.org/10.1002/2015wr017552>
- Benettin, P., Bailey, S. W., Rinaldo, A., Likens, G. E., McGuire, K. J., & Botter, G. (2017). Young runoff fractions control streamwater age and solute concentration dynamics. *Hydrological Processes*, 31(16), 2982-2986. <https://doi.org/10.1002/hyp.11243>
- Benettin, P., & Bertuzzo, E. (2018). tran-SAS v1.0: a numerical model to compute catchment-scale hydrologic transport using StorAge Selection functions. *Geoscientific Model Development*, 11(4), 1627-1639. <https://doi.org/10.5194/gmd-11-1627-2018>
- Benettin, P., Fovet, O., & Li, L. (2020). Nitrate removal and young stream water fractions at the catchment scale. *Hydrological Processes*, 34(12), 2725-2738. <https://doi.org/10.1002/hyp.13781>
- Benettin, P., Rodriguez, N. B., Sprenger, M., Kim, M., Klaus, J., Harman, C. J., van der Velde, Y., Hrachowitz, M., Botter, G., McGuire, K. J., Kirchner, J. W., Rinaldo, A., & McDonnell, J. J. (2022). Transit Time Estimation in Catchments: Recent Developments and Future Directions. *Water Resources Research*, 58(11). <https://doi.org/10.1029/2022wr033096>
- Beven, K., & Binley, A. (2006). The future of distributed models: Model calibration and uncertainty prediction. *Hydrological Processes*, 6(3), 279-298. <https://doi.org/10.1002/hyp.3360060305>
- Beven, K., & Binley, A. (2014). GLUE: 20 years on. *Hydrological Processes*, 28(24), 5897-5918. <https://doi.org/10.1002/hyp.10082>
- BGR. (2020). Bodenübersichtskarte. Bundesanstalt für Geowissenschaften und Rohstoffe.
- BGR. (2020). Hydrogeologische Übersichtskarte. Bundesanstalt für Geowissenschaften und Rohstoffe.
- Bijay, S., & Craswell, E. (2021). Fertilizers and nitrate pollution of surface and ground water: an increasingly pervasive global problem. *SN Applied Sciences*, 3(4). <https://doi.org/10.1007/s42452-021-04521-8>
- Birkel, C., Dunn, S. M., Tetzlaff, D., & Soulsby, C. (2010). Assessing the value of high-resolution isotope tracer data in the stepwise development of a lumped conceptual rainfall-runoff model. *Hydrological Processes*, 24(16), 2335-2348. <https://doi.org/10.1002/hyp.7763>
- Boeing, F., Rakovec, O., Kumar, R., Samaniego, L., Schrön, M., Hildebrandt, A., Rebmann, C., Thober, S., Müller, S., Zacharias, S., Bogena, H., Schneider, K., Kiese, R., Attinger, S., & Marx, A. (2022). High-resolution drought simulations and comparison to soil moisture observations in Germany. *Hydrology and Earth System Sciences*, 26(19), 5137-5161. <https://doi.org/10.5194/hess-26-5137-2022>

- Borriero, A., Kumar, R., Nguyen, T. V., Fleckenstein, J. H., & Lutz, S. R. (2023). Uncertainty in water transit time estimation with StorAge Selection functions and tracer data interpolation. *Hydrology and Earth System Sciences*, 27(15), 2989-3004. <https://doi.org/10.5194/hess-27-2989-2023>
- Boshers, D. S., Granger, J., Tobias, C. R., Böhlke, J. K., & Smith, R. L. (2019). Constraining the Oxygen Isotopic Composition of Nitrate Produced by Nitrification. *Environmental Science & Technology*, 53(3), 1206-1216. <https://doi.org/10.1021/acs.est.8b03386>
- Brown, V. A., McDonnell, J. J., Burns, D. A., & Kendall, C. (1999). The role of event water, a rapid shallow flow component, and catchment size in summer stormflow. *Journal of Hydrology*.
- Buchwald, C., & Casciotti, K. L. (2010). Oxygen isotopic fractionation and exchange during bacterial nitrite oxidation. *Limnology and Oceanography*, 55(3), 1064-1074. <https://doi.org/10.4319/lo.2010.55.3.1064>
- Casciotti, K. L., Buchwald, C., Santoro, A. E., & Frame, C. (2011). Assessment of nitrogen and oxygen isotopic fractionation during nitrification and its expression in the marine environment. *Methods Enzymol*, 486, 253-280. <https://doi.org/10.1016/B978-0-12-381294-0.00011-0>
- Casciotti, K. L., & Ward, B. B. (2001). Dissimilatory nitrite reductase genes from autotrophic ammonia-oxidizing bacteria. *Appl Environ Microbiol*, 67(5), 2213-2221. <https://doi.org/10.1128/AEM.67.5.2213-2221.2001>
- Dimitrova-Petrova, K., Geris, J., Wilkinson, M. E., Lilly, A., & Soulsby, C. (2020). Using isotopes to understand the evolution of water ages in disturbed mixed land-use catchments. *Hydrological Processes*, 34(4), 972-990. <https://doi.org/10.1002/hyp.13627>
- Drever, M. C., Hrachowitz, M., & Auger-Méthé, M. (2017). Migration as flow: using hydrological concepts to estimate the residence time of migrating birds from the daily counts. *Methods in Ecology and Evolution*, 8(9), 1146-1157. <https://doi.org/10.1111/2041-210x.12727>
- Druhan, J. L., & Maher, K. (2017). The influence of mixing on stable isotope ratios in porous media: A revised Rayleigh model. *Water Resources Research*, 53(2), 1101-1124. <https://doi.org/10.1002/2016wr019666>
- Dupas, R., Ehrhardt, S., Musolff, A., Fovet, O., & Durand, P. (2020). Long-term nitrogen retention and transit time distribution in agricultural catchments in western France. *Environmental Research Letters*, 15(11). <https://doi.org/10.1088/1748-9326/abbe47>
- DWD (2017): Abteilung Hydrometeorologie: REGNIE (REGionalisierte NIEederschläge): Verfahrensbeschreibung & Nutzeranleitung, DWD internal report, Offenbach 2017.
- Ehrhardt, S., Ebeling, P., Dupas, R., Kumar, R., Fleckenstein, J. H., & Musolff, A. (2021). Nitrate Transport and Retention in Western European Catchments Are Shaped by Hydroclimate and Subsurface Properties. *Water Resources Research*, 57(10). <https://doi.org/10.1029/2020wr029469>
- Gallart, F., Valiente, M. a., Llorens, P., Cayuela, C., Sprenger, M., & Latron, J. r. m. (2020a). Investigating young water fractions in a small Mediterranean mountain catchment: both precipitation forcing and sampling frequency matter. <https://doi.org/10.22541/au.157979613.39458719>
- Gallart, F., von Freyberg, J., Valiente, M., Kirchner, J. W., Llorens, P., & Latron, J. (2020b). Technical note: An improved discharge sensitivity metric for young water fractions. *Hydrology and Earth System Sciences*, 24(3), 1101-1107. <https://doi.org/10.5194/hess-24-1101-2020>

- Galloway, J. N., DENTENER, F. J., CAPONE, D. G., BOYER, E. W., HOWARTH, R. W., SEITZINGER, S. P., ASNER, G. P., CLEVELAND, C. C., GREEN, P. A., HOLLAND, E. A., KARL, D. M., MICHAELS, A. F., PORTER, J. H., TOWNSEND, A. R., & VÖRÖSMARTY, C. J. (2004). Nitrogen cycles: past, present, and future.
- GeoBasis-DE / BKG. (2013). Elevation data 200m resolution. Bundesamt für Kartographie und Geodäsie.
- GeoBasis-DE / BKG. (2018). Land-use data. Bundesamt für Kartographie und Geodäsie.
- Giani, G., Tarasova, L., Woods, R. A., & Rico-Ramirez, M. A. (2022). An Objective Time-Series-Analysis Method for Rainfall-Runoff Event Identification. *Water Resources Research*, *58*(2). <https://doi.org/10.1029/2021wr031283>
- Granger, J., & Wankel, S. D. (2016). Isotopic overprinting of nitrification on denitrification as a ubiquitous and unifying feature of environmental nitrogen cycling. *Proc Natl Acad Sci U S A*, *113*(42), E6391-E6400. <https://doi.org/10.1073/pnas.1601383113>
- Griffiths, N. A., Jackson, C. R., McDonnell, J. J., Klaus, J., Du, E., & Bitew, M. M. (2016). Dual nitrate isotopes clarify the role of biological processing and hydrologic flow paths on nitrogen cycling in subtropical low-gradient watersheds. *Journal of Geophysical Research: Biogeosciences*, *121*(2), 422-437. <https://doi.org/10.1002/2015jg003189>
- Gupta, H. V., Kling, H., Yilmaz, K. K., & Martinez, G. F. (2009). Decomposition of the mean squared error and NSE performance criteria: Implications for improving hydrological modelling. *Journal of Hydrology*, *377*(1-2), 80-91. <https://doi.org/10.1016/j.jhydrol.2009.08.003>
- Harman, C. J. (2015). Time-variable transit time distributions and transport: Theory and application to storage-dependent transport of chloride in a watershed. *Water Resources Research*, *51*(1), 1-30. <https://doi.org/10.1002/2014wr015707>
- Hrachowitz, M., Benettin, P., van Breukelen, B. M., Fovet, O., Howden, N. J. K., Ruiz, L., van der Velde, Y., & Wade, A. J. (2016). Transit times-the link between hydrology and water quality at the catchment scale. *Wiley Interdisciplinary Reviews: Water*, *3*(5), 629-657. <https://doi.org/10.1002/wat2.1155>
- Hrachowitz, M., Soulsby, C., Tetzlaff, D., Dawson, J. J. C., & Malcolm, I. A. (2009). Regionalization of transit time estimates in montane catchments by integrating landscape controls. *Water Resources Research*, *45*(5). <https://doi.org/10.1029/2008wr007496>
- Jasechko, S., Kirchner, J. W., Welker, J. M., & McDonnell, J. J. (2016). Substantial proportion of global streamflow less than three months old. *Nature Geoscience*, *9*(2), 126-129. <https://doi.org/10.1038/ngeo2636>
- Jutebring Sterte, E., Lidman, F., Lindborg, E., Sjöberg, Y., & Laudon, H. (2021). How catchment characteristics influence hydrological pathways and travel times in a boreal landscape. *Hydrology and Earth System Sciences*, *25*(4), 2133-2158. <https://doi.org/10.5194/hess-25-2133-2021>
- Kaur, S., Horne, A., Stewardson, M. J., Nathan, R., Costa, A. M., Szemis, J. M., & Webb, J. A. (2017). Challenges for determining frequency of high flow spells for varying thresholds in environmental flows programmes. *Journal of Ecohydraulics*, *2*(1), 28-37. <https://doi.org/10.1080/24705357.2016.1276418>
- Kendall, C., Elliott, E. M., & Wankel, S. D. (2007). Tracing anthropogenic inputs of nitrogen to ecosystems, Chapter 12, In: R.H. Michener and K. Lajtha (Eds.). *Stable Isotopes in Ecology and Environmental Science*.

- Kim, M., Pangle, L. A., Cardoso, C., Lora, M., Volkmann, T. H. M., Wang, Y., Harman, C. J., & Troch, P. A. (2016). Transit time distributions and StorAge Selection functions in a sloping soil lysimeter with time-varying flow paths: Direct observation of internal and external transport variability. *Water Resources Research*, 52(9), 7105-7129. <https://doi.org/10.1002/2016wr018620>
- Kim, M., & Troch, P. A. (2020). Transit Time Distributions Estimation Exploiting Flow-Weighted Time: Theory and Proof-of-Concept. *Water Resources Research*, 56(12). <https://doi.org/10.1029/2020wr027186>
- Kirchner, J. (2018). Quantifying new water fractions and transit time distributions using ensemble hydrograph separation: theory and benchmark tests. *Hydrol Earth Syst Sci*. <https://doi.org/10.5194/hess-2018-429>
- Kirchner, J. W. (2016a). Aggregation in environmental systems – Part 1: Seasonal tracer cycles quantify young water fractions, but not mean transit times, in spatially heterogeneous catchments. *Hydrology and Earth System Sciences*, 20(1), 279-297. <https://doi.org/10.5194/hess-20-279-2016>
- Kirchner, J. W. (2016b). Aggregation in environmental systems – Part 2: Catchment mean transit times and young water fractions under hydrologic nonstationarity. *Hydrology and Earth System Sciences*, 20(1), 299-328. <https://doi.org/10.5194/hess-20-299-2016>
- Kirschke, S., Häger, A., Kirschke, D., & Völker, J. (2019). Agricultural Nitrogen Pollution of Freshwater in Germany. The Governance of Sustaining a Complex Problem. *Water*, 11(12). <https://doi.org/10.3390/w11122450>
- Kleine, L., Tetzlaff, D., Smith, A., Wang, H., & Soulsby, C. (2020). Using water stable isotopes to understand evaporation, moisture stress, and re-wetting in catchment forest and grassland soils of the summer drought of 2018. *Hydrology and Earth System Sciences*, 24(7), 3737-3752. <https://doi.org/10.5194/hess-24-3737-2020>
- Knapp, J. L. A., Neal, C., Schlumpf, A., Neal, M., & Kirchner, J. W. (2019). New water fractions and transit time distributions at Plynlimon, Wales, estimated from stable water isotopes in precipitation and streamflow. *Hydrol Earth Syst Sci*. <https://doi.org/10.5194/hess-2019-290>
- Knöller, K., Vogt, C., Haupt, M., Feisthauer, S., & Richnow, H.-H. (2010). Experimental investigation of nitrogen and oxygen isotope fractionation in nitrate and nitrite during denitrification. *Biogeochemistry*, 103(1-3), 371-384. <https://doi.org/10.1007/s10533-010-9483-9>
- Kool, D. M., Wrage, N., Oenema, O., Van Kessel, C., & Van Groenigen, J. W. (2011). Oxygen exchange with water alters the oxygen isotopic signature of nitrate in soil ecosystems. *Soil Biology and Biochemistry*, 43(6), 1180-1185. <https://doi.org/10.1016/j.soilbio.2011.02.006>
- Kumar, R., Samaniego, L., & Attinger, S. (2013). Implications of distributed hydrologic model parameterization on water fluxes at multiple scales and locations. *Water Resources Research*.
- Kuppel, S., Tetzlaff, D., Maneta, M. P., & Soulsby, C. (2018). $\delta^{18}\text{O}$ -iso 1.0: water isotopes and age tracking in a process-based, distributed ecohydrological model. *Geoscientific Model Development*, 11(7), 3045-3069. <https://doi.org/10.5194/gmd-11-3045-2018>
- Ladson, A. R., Brown, R., Neal, B., & Nathan, R. (2013). A standard approach to baseflow separation using the Lyne and Hollick filter. *Australian Journal of Water Resources*, 17(1). <https://doi.org/10.7158/w12-028.2013.17.1>

- Lang, M., Ouarda, T. B. M. J., & Bobée, B. (1999). Towards operational guidelines for over-threshold modeling. *Journal of Hydrology*.
- Lee, J.-Y., Shih, Y.-T., Lan, C.-Y., Lee, T.-Y., Peng, T.-R., Lee, C.-T., & Huang, J.-C. (2020). Rainstorm Magnitude Likely Regulates Event Water Fraction and Its Transit Time in Mesoscale Mountainous Catchments: Implication for Modelling Parameterization. *Water*, 12(4). <https://doi.org/10.3390/w12041169>
- Li, L., Sullivan, P. L., Benettin, P., Cirpka, O. A., Bishop, K., Brantley, S. L., Knapp, J. L. A., Meerveld, I., Rinaldo, A., Seibert, J., Wen, H., & Kirchner, J. W. (2020). Toward catchment hydro-biogeochemical theories. *WIREs Water*, 8(1). <https://doi.org/10.1002/wat2.1495>
- Lindström, G., Arheimer, B., Strömqvist, J., Rosberg, J., & Pers, C. (2010). Development and testing of the HYPE (Hydrological Predictions for the Environment) water quality model for different spatial scales. *Hydrology Research*, 41(3-4), 295-319. <https://doi.org/10.2166/nh.2010.007>
- Lutz, S. R., Krieg, R., Müller, C., Zink, M., Knöller, K., Samaniego, L., & Merz, R. (2018). Spatial Patterns of Water Age: Using Young Water Fractions to Improve the Characterization of Transit Times in Contrasting Catchments. *Water Resources Research*, 54(7), 4767-4784. <https://doi.org/10.1029/2017wr022216>
- Lutz, S. R., Trauth, N., Musolff, A., Van Breukelen, B. M., Knöller, K., & Fleckenstein, J. H. (2020). How Important is Denitrification in Riparian Zones? Combining End-Member Mixing and Isotope Modeling to Quantify Nitrate Removal from Riparian Groundwater. *Water Resources Research*, 56(1). <https://doi.org/10.1029/2019wr025528>
- Lyne, V., & Hollick, M. (1979). Stochastic Time-Variable Rainfall Runoff Modelling. *Institute of Engineers Australia National Conference*.
- Maher, K. (2010). The dependence of chemical weathering rates on fluid residence time. *Earth and Planetary Science Letters*, 294(1-2), 101-110. <https://doi.org/10.1016/j.epsl.2010.03.010>
- Maher, K. (2011). The role of fluid residence time and topographic scales in determining chemical fluxes from landscapes. *Earth and Planetary Science Letters*, 312(1-2), 48-58. <https://doi.org/10.1016/j.epsl.2011.09.040>
- Mariotti, A., GERMON, J. C., HUBERT, P., KAISER, P., LETOLLE, R., TARDIEUX, A., & TARDIEUX, P. (1981). EXPERIMENTAL DETERMINATION OF NITROGEN KINETIC ISOTOPE FRACTIONATION: SOME PRINCIPLES; ILLUSTRATION FOR THE DENITRIFICATION AND NITRIFICATION PROCESSES. *Plant and Soil*.
- Mayer, B., BOLLWERK, S. M., MANSFELDT, T., HÜTTER, B., & VEIZER, J. (2001). The oxygen isotope composition of nitrate generated by nitrification in acid forest floors. *Geochimica et Cosmochimica Acta*.
- Merz, R., Blöschl, G., & Parajka, J. (2006). Spatio-temporal variability of event runoff coefficients. *Journal of Hydrology*, 331(3-4), 591-604. <https://doi.org/10.1016/j.jhydrol.2006.06.008>
- Michelsen, N., Laube, G., Friesen, J., Weise, S. M., Bait Said, A. B. A., & Müller, T. (2019). Technical note: A microcontroller-based automatic rain sampler for stable isotope studies. *Hydrology and Earth System Sciences*, 23(6), 2637-2645. <https://doi.org/10.5194/hess-23-2637-2019>

- Molénat, J., & Gascuel-Oudou, C. (2002). Modelling flow and nitrate transport in groundwater for the prediction of water travel times and of consequences of land use evolution on water quality. *Hydrological Processes*, 16(2), 479-492. <https://doi.org/10.1002/hyp.328>
- Mueller, C., Krieg, R., Merz, R., & Knoller, K. (2016). Regional nitrogen dynamics in the TERENO Bode River catchment, Germany, as constrained by stable isotope patterns. *Isotopes Environ Health Stud*, 52(1-2), 61-74. <https://doi.org/10.1080/10256016.2015.1019489>
- Müller, C., Musolff, A., Strachauer, U., Brauns, M., Tarasova, L., Merz, R., & Knöller, K. (2018). Tomography of anthropogenic nitrate contribution along a mesoscale river. *Science of The Total Environment*, 615, 773-783. <https://doi.org/10.1016/j.scitotenv.2017.09.297>
- Nguyen, T. V., Kumar, R., Lutz, S. R., Musolff, A., Yang, J., & Fleckenstein, J. H. (2021). Modeling Nitrate Export From a Mesoscale Catchment Using StorAge Selection Functions. *Water Resources Research*, 57(2). <https://doi.org/10.1029/2020wr028490>
- Nguyen, T. V., Kumar, R., Musolff, A., Lutz, S. R., Sarrazin, F., Attinger, S., & Fleckenstein, J. H. (2022). Disparate Seasonal Nitrate Export From Nested Heterogeneous Subcatchments Revealed With StorAge Selection Functions. *Water Resources Research*, 58(3). <https://doi.org/10.1029/2021wr030797>
- Rinaldo, A., Benettin, P., Harman, C. J., Hrachowitz, M., McGuire, K. J., van der Velde, Y., Bertuzzo, E., & Botter, G. (2015). Storage selection functions: A coherent framework for quantifying how catchments store and release water and solutes. *Water Resources Research*, 51(6), 4840-4847. <https://doi.org/10.1002/2015wr017273>
- Samaniego, L., Kumar, R., & Attinger, S. (2010). Multiscale parameter regionalization of a grid-based hydrologic model at the mesoscale. *Water Resour Research*.
- Sebilo, M., Mayer, B., Nicolardot, B., Pinay, G., & Mariotti, A. (2013). Long-term fate of nitrate fertilizer in agricultural soils. *Proc Natl Acad Sci U S A*, 110(45), 18185-18189. <https://doi.org/10.1073/pnas.1305372110>
- Seeger, S., & Weiler, M. (2014). Reevaluation of transit time distributions, mean transit times and their relation to catchment topography. *Hydrology and Earth System Sciences*, 18(12), 4751-4771. <https://doi.org/10.5194/hess-18-4751-2014>
- Sigman, D. M., Casciotti, K. L., Andreani, M., Barford, C., Galanter, M., & Böhlke, J. K. (2001). A Bacterial Method for the Nitrogen Isotopic Analysis of Nitrate in Seawater and Freshwater. *Anal. Chem*.
- Sikorska, A. E., Viviroli, D., & Seibert, J. (2015). Flood-type classification in mountainous catchments using crisp and fuzzy decision trees. *Water Resources Research*, 51(10), 7959-7976. <https://doi.org/10.1002/2015wr017326>
- Smith, A., Tetzlaff, D., Kleine, L., Maneta, M. P., & Soulsby, C. (2020). Isotope-aided modelling of ecohydrologic fluxes and water ages under mixed land use in Central Europe: The 2018 drought and its recovery. *Hydrological Processes*, 34(16), 3406-3425. <https://doi.org/10.1002/hyp.13838>
- Soulsby, C., Birkel, C., Geris, J., Dick, J., Tunaley, C., & Tetzlaff, D. (2015). Stream water age distributions controlled by storage dynamics and nonlinear hydrologic connectivity: Modeling with high-resolution isotope data. *Water Resour Res*, 51(9), 7759-7776. <https://doi.org/10.1002/2015WR017888>
- Soulsby, C., Tetzlaff, D., Rodgers, P., Dunn, S., & Waldron, S. (2006). Runoff processes, stream water residence times and controlling landscape characteristics in a

- mesoscale catchment: An initial evaluation. *Journal of Hydrology*, 325(1-4), 197-221. <https://doi.org/10.1016/j.jhydrol.2005.10.024>
- Stevenson, J. L., Birkel, C., Neill, A. J., Tetzlaff, D., & Soulsby, C. (2021). Effects of streamflow isotope sampling strategies on the calibration of a tracer-aided rainfall-runoff model. *Hydrological Processes*, 35(6). <https://doi.org/10.1002/hyp.14223>
- Stockinger, M. P., Bogena, H. R., Lücke, A., Diekkrüger, B., Cornelissen, T., & Vereecken, H. (2016). Tracer sampling frequency influences estimates of young water fraction and streamwater transit time distribution. *Journal of Hydrology*, 541, 952-964. <https://doi.org/10.1016/j.jhydrol.2016.08.007>
- Tang, W., & Carey, S. K. (2017). HydRun: A MATLAB toolbox for rainfall-runoff analysis. *Hydrological Processes*, 31(15), 2670-2682. <https://doi.org/10.1002/hyp.11185>
- Tetzlaff, D., Seibert, J., & Soulsby, C. (2009). Inter-catchment comparison to assess the influence of topography and soils on catchment transit times in a geomorphic province; the Cairngorm mountains, Scotland. *Hydrological Processes*, 23(13), 1874-1886. <https://doi.org/10.1002/hyp.7318>
- Timbe, E., Windhorst, D., Celleri, R., Timbe, L., Crespo, P., Frede, H. G., Feyen, J., & Breuer, L. (2015). Sampling frequency trade-offs in the assessment of mean transit times of tropical montane catchment waters under semi-steady-state conditions. *Hydrology and Earth System Sciences*, 19(3), 1153-1168. <https://doi.org/10.5194/hess-19-1153-2015>
- van der Velde, Y., de Rooij, G. H., Rozemeijer, J. C., van Geer, F. C., & Broers, H. P. (2010). Nitrate response of a lowland catchment: On the relation between stream concentration and travel time distribution dynamics. *Water Resources Research*, 46(11). <https://doi.org/10.1029/2010wr009105>
- van der Velde, Y., Torfs, P. J. J. F., van der Zee, S. E. A. T. M., & Uijlenhoet, R. (2012). Quantifying catchment-scale mixing and its effect on time-varying travel time distributions. *Water Resources Research*, 48(6). <https://doi.org/10.1029/2011wr011310>
- von Freyberg, J., Allen, S. T., Seeger, S., Weiler, M., & Kirchner, J. W. (2018). Sensitivity of young water fractions to hydro-climatic forcing and landscape properties across 22 Swiss catchments. *Hydrology and Earth System Sciences*, 22(7), 3841-3861. <https://doi.org/10.5194/hess-22-3841-2018>
- Wang, S., He, X., Kang, S., Hong, X., Fu, H., Xue, Y., Feng, Z., & Guo, H. (2023). Assessment of streamwater age using water stable isotopes in a headwater catchment of the central Tibetan Plateau. *Journal of Hydrology*, 618. <https://doi.org/10.1016/j.jhydrol.2023.129175>
- Wilusz, D. C., Harman, C. J., & Ball, W. P. (2017). Sensitivity of Catchment Transit Times to Rainfall Variability Under Present and Future Climates. *Water Resources Research*, 53(12), 10231-10256. <https://doi.org/10.1002/2017wr020894>
- Winter, C., Lutz, S. R., Musolff, A., Kumar, R., Weber, M., & Fleckenstein, J. H. (2021). Disentangling the Impact of Catchment Heterogeneity on Nitrate Export Dynamics From Event to Long-Term Time Scales. *Water Resources Research*, 57(1). <https://doi.org/10.1029/2020wr027992>

- Wollschläger, U., Attinger, S., Borchardt, D., Brauns, M., Cuntz, M., Dietrich, P., Fleckenstein, J. H., Friese, K., Friesen, J., Harpke, A., Hildebrandt, A., Jäckel, G., Kamjunke, N., Knöller, K., Kögler, S., Kolditz, O., Krieg, R., Kumar, R., Lausch, A., . . . Zacharias, S. (2016). The Bode hydrological observatory: a platform for integrated, interdisciplinary hydro-ecological research within the TERENO Harz/Central German Lowland Observatory. *Environmental Earth Sciences*, 76(1). <https://doi.org/10.1007/s12665-016-6327-5>
- Xia, C., Zuecco, G., Chen, K., Liu, L., Zhang, Z., & Luo, J. (2023). The estimation of young water fraction based on isotopic signals: challenges and recommendations. *Frontiers in Ecology and Evolution*, 11. <https://doi.org/10.3389/fevo.2023.1114259>
- Yang, X., & Rode, M. (2020). A Fully Distributed Catchment Nitrate Model - mHM-Nitrate v2.0. Zenodo. doi:<https://doi.org/10.5281/zenodo.3891629>
- Yang, X., Jomaa, S., Zink, M., Fleckenstein, J. H., Borchardt, D., & Rode, M. (2018). A New Fully Distributed Model of Nitrate Transport and Removal at Catchment Scale. *Water Resources Research*. doi:<https://doi.org/10.1029/2017WR022380>
- Yang, X., Tetzlaff, D., Soulsby, C., Smith, A., & Borchardt, D. (2021). Catchment Functioning Under Prolonged Drought Stress: Tracer-Aided Ecohydrological Modeling in an Intensively Managed Agricultural Catchment. *Water Resources Research*, 57(3). <https://doi.org/10.1029/2020wr029094>
- Zhang, L., & Yang, F. (2022). Spatio-Temporal Dynamics of Water Conservation Service of Ecosystems in the Zhejiang Greater Bay Area and Its Impact Factors Analysis. *Sustainability*, 14(16). <https://doi.org/10.3390/su141610392>
- Zink, M., Kumar, R., Cuntz, M., & Samaniego, L. (2017). A high-resolution dataset of water fluxes and states for Germany accounting for parametric uncertainty. *Hydrology and Earth System Sciences*, 21(3), 1769-1790. <https://doi.org/10.5194/hess-21-1769-2017>

List of publications related to this thesis

The following manuscripts are submitted in a modified version to the Journals.

Radtke, C.F.; Lutz, S.R.; Mueller, C.; Merz, R.; Kumar, R.; Knoeller, K. (Under Review in Water Resources Research) Fractions of Different Young Water Ages are Sensitive to Discharge and Land Use – an Integrated Analysis of Water Age Metrics under Varying Hydrological Conditions for Contrasting Sub-Catchments in Central Germany

Radtke, C.F.; Yang, X.; Mueller, C.; Rouhiainen, J.; Merz, R.; Lutz, S.R.; Benettin, P.; Wie, H.; Knoeller, K. (submitted to Science of the Total Environment) Nitrate and Water Isotopes as Tools to resolve Nitrate Transit Times in a Mixed Land Use Catchment

The data that has been used in this thesis is available on the CD and in the Nextcloud folder of the Helmholtz-Centre of Environmental Research at the following link:
<https://nc.ufz.de/s/i3gezjz9sEoRGPZ> Password: DissRadtke2024!

Curriculum vitae

Personal Profile

Name Christina Franziska Radtke
Gender Female

Work Experience

Technical University of Braunschweig, Leichtweiß-Institute for Hydraulic Engineering and Water Resources, Department of Hydrology and River Basin Management since February 2024

Helmholtz-Centre for Environmental Research GmbH – UFZ
PhD-Student at the Department Catchment Hydrology
PhD-Topic: “Deciphering Catchment’s Transit Time Dynamics using Event Isotope Signatures”
April 2020 – December 2023

Education

Master’s degree for agricultural science with focus on environmental science
May 2020

Bachelor’s degree for agricultural science September 2018
With focus on environmental science since April 2016
At Christian-Albrechts University of Kiel since October 2014

Activities

May 2022 Research stay at University of Freiburg, Germany
Mentor: Prof. Dr. Markus Weiler
Objective: Teaching

May – August 2018 Internship at State Agency of Agriculture, Environment and Rural Areas Schleswig-Holstein, Germany
Department of river water ecology

Skills

Microsoft Office, - Excel, - Word, -Outlook
Geo-information systems: QGIS, ArcGIS
HOBOWare
Fowlink 5.1
Programming languages: R, Matlab
PC-ORD

German driver's license class B

Written and spoken English-, French- and Danish skills

Publications

Journal (peer reviewed)

Radtke, C. F., Yang, X., Müller, C., Rouhiainen, J., Merz, R., Lutz, S.R., Benettin, P., Wei, H., Knöller, K. (submitted to Sci. Total Environ.) Nitrate and Water Isotopes as Tools to Resolve Nitrate Travel Times in a Mixed Land Use Catchment

Radtke, C.F., Lutz, S.R., Mueller, C., Merz, R., Kumar, R., Knoeller, K. (under Review in WRR) Fractions of Different Young Water Ages are Sensitive to Discharge and Land Use – an Integrated Analysis of Water Age Metrics under Varying Hydrological Conditions for Contrasting Sub-Catchments in Central Germany

Conference contributions

Oral presentations

2023

Radtke, C.F., Yang, X., Müller, C., Rouhiainen, J., Merz, R., Lutz, S.R., Benettin, P., Wei, H., Knöller, K. (25.04.2023) Altersverteilungen des Wassers mittels hochfrequenter Isotopensignaturen, German Isotope Network

Radtke, C.F., Yang, X., Müller, C., Rouhiainen, J., Merz, R., Lutz, S.R., Benettin, P., Wei, H., Knöller, K. (2023) An integrated analysis of water age metrics for contrasting sub-catchments in the Harz mountains, Central Germany, IP Summer Workshop UFZ, DYNAMO Cohort

2022

Radtke, C.F., Yang, X., Müller, C., Rouhiainen, J., Merz, R., Lutz, S.R., Benettin, P., Wei, H., Knöller, K. (2022) Nitrat- und Wasserisotopen als Instrument zur Entschlüsselung der Verweilzeiten von Nitrat in einem heterogenen Einzugsgebiet, Tag der Hydrologie

Radtke, C.F., Lutz, S.R., Mueller, C., Rouhiainen, J., Merz, R., Yang, X., Kumar, R., Benettin, P., and Knoeller, K.: Nitrate and Water Isotopes as Tools to Resolve Nitrate Travel Times in a Mixed Land Use Catchment, EGU General Assembly 2022, Vienna, Austria, 23–27 May 2022, EGU22-662, <https://doi.org/10.5194/egusphere-egu22-662>, 2022.

Radtke, C.F., Lutz, S.R., Mueller, C., Rouhiainen, J., Merz, R., Yang, X., Kumar, R., Benettin, P., and Knoeller, K. (15.06.2022) Nitrate and Water Isotopes as Tools to Resolve Nitrate Travel Times in a Mixed Land Use Catchment, HIGRADE Conference

Eidesstattliche Erklärung / *Declaration under Oath*

Ich erkläre an Eides statt, dass ich die Arbeit selbstständig und ohne fremde Hilfe verfasst, keine anderen als die von mir angegebenen Quellen und Hilfsmittel benutzt und die den benutzten Werken wörtlich oder inhaltlich entnommenen Stellen als solche kenntlich gemacht habe.

I declare under penalty of perjury that this thesis is my own work entirely and has been written without any help from other people. I used only the sources mentioned and included all the citations correctly both in word or content.

Datum / Date

Unterschrift des Antragstellers / *Signature of the applicant*

Erklärung über bestehende Vorstrafen und anhängige Ermittlungsverfahren / Declaration concerning Criminal Record and Pending Investigations

Hiermit erkläre ich, dass ich weder vorbestraft bin noch dass gegen mich Ermittlungsverfahren anhängig sind.

I hereby declare that I have no criminal record and that no preliminary investigations are pending against me.

Datum / Date

Unterschrift des Antragstellers / *Signature of the applicant*